

**A REVIEW AND ANALYSIS OF DATING  
TECHNIQUES FOR NEOGENE AND QUATERNARY  
VOLCANIC ROCKS**

*Prepared for*

**Nuclear Regulatory Commission  
Contract NRC-02-88-005**

*Prepared by*

**Brittain E. Hill  
Bret W. Leslie  
Charles B. Connor**

**Center for Nuclear Waste Regulatory Analyses  
San Antonio, Texas**

**September 1993**

## ABSTRACT

The large uncertainties in many of the published dates for volcanic rocks in the Yucca Mountain region (YMR) strongly affect probability and consequence models of volcanism, especially models focusing on Quaternary volcanism. Dating techniques for post-10 Ma basaltic rocks in the YMR have inherent limitations and uncertainties, which are rarely discussed in detail. Dates produced from the most widely available techniques have uncertainties that generally increase with decreasing age of the rock. Independent evaluation of most published dates is difficult due to a lack of information on analytical techniques, sample characteristics, and sources of error. Neogene basaltic volcanoes in the YMR have reported dates that generally reflect the precision and accuracy of the analytical technique, although the number of samples dated for each volcanic center only ranges from one to three. Dates for Quaternary volcanoes in the YMR have relatively large reported uncertainties and yield averages with large errors when reported uncertainty is propagated through statistical calculations. Using available data, estimates of the average ages of the Quaternary YMR volcanoes are  $1.2 \pm 0.4$  Ma for Crater Flat,  $0.3 \pm 0.2$  Ma for Sleeping Butte, and  $0.1 \pm 0.05$  Ma for Lathrop Wells. These dates generally do not represent the best dates possible with currently available geochronological techniques. Uncertainty in the age of Lathrop Wells is relatively small and does not affect current probability models significantly. However, the relatively large uncertainties in the ages of Crater Flat volcanoes strongly affect probability models.

# CONTENTS

Section		Page
1	INTRODUCTION . . . . .	1-1
1.1	REGULATORY BASIS . . . . .	1-2
1.2	TECHNICAL BACKGROUND . . . . .	1-3
1.2.1	Common Terms . . . . .	1-3
1.2.2	Differences Between Precision and Accuracy . . . . .	1-4
1.2.3	Common Statistical Problems in Geochronology . . . . .	1-4
2	RADIOMETRIC DATING METHODS . . . . .	2-1
2.1	GENERAL PRINCIPLES . . . . .	2-1
2.2	POTASSIUM/ARGON ( $^{40}\text{K}/^{40}\text{Ar}$ ) METHOD . . . . .	2-1
2.2.1	Analytical Methods . . . . .	2-2
2.2.2	Sources of Error . . . . .	2-3
2.2.3	Material Dated . . . . .	2-5
2.2.4	Application to the Yucca Mountain Region . . . . .	2-5
2.2.4.1	Quaternary Basaltic Volcanoes . . . . .	2-5
2.2.4.2	Neogene Basaltic Volcanoes . . . . .	2-12
2.3	ARGON/ARGON ( $^{40}\text{Ar}/^{39}\text{Ar}$ ) METHOD . . . . .	2-14
2.3.1	Analytical Methods . . . . .	2-14
2.3.2	Sources of Error . . . . .	2-17
2.3.3	Material Dated . . . . .	2-19
2.3.4	Application to the Yucca Mountain Region . . . . .	2-20
2.4	URANIUM-SERIES METHODS . . . . .	2-20
2.4.1	Analytical Methods . . . . .	2-29
2.4.2	Sources of Error . . . . .	2-29
2.4.3	Material Dated . . . . .	2-30
2.4.4	Application to the Yucca Mountain Region . . . . .	2-31
2.5	CARBON-14 ( $^{14}\text{C}$ ) METHOD . . . . .	2-32
2.5.1	Analytical Methods . . . . .	2-33
2.5.2	Sources of Error . . . . .	2-34
2.5.3	Material Dated . . . . .	2-35
2.5.4	Application to the Yucca Mountain Region . . . . .	2-35
3	RADIATION INTERACTION METHODS . . . . .	3-1
3.1	GENERAL PRINCIPLES . . . . .	3-1
3.2	THERMOLUMINESCENCE METHOD . . . . .	3-2
3.2.1	Analytical Methods . . . . .	3-2
3.2.2	Sources of Error . . . . .	3-5
3.2.3	Material Dated . . . . .	3-6
3.2.4	Application to the Yucca Mountain Region . . . . .	3-6
3.3	COSMOGENIC NUCLIDES METHODS . . . . .	3-7
3.3.1	Analytical Methods . . . . .	3-8
3.3.2	Sources of Error . . . . .	3-10
3.3.3	Material Dated . . . . .	3-11

## CONTENTS (Cont'd)

Section		Page
3.3.4	Application to the Yucca Mountain Region . . . . .	3-11
3.4	FISSION-TRACK DATING . . . . .	3-13
3.4.1	Analytical Methods . . . . .	3-13
3.4.2	Sources of Error . . . . .	3-15
3.4.3	Material Dated . . . . .	3-15
3.4.4	Application to the Yucca Mountain Region . . . . .	3-15
4	INDIRECT DATING METHODS . . . . .	4-1
4.1	GENERAL PRINCIPLES . . . . .	4-1
4.2	PALEOMAGNETIC DATING . . . . .	4-1
4.2.1	Analytical Methods . . . . .	4-3
4.2.2	Sources of Error . . . . .	4-5
4.2.3	Material Dated . . . . .	4-5
4.2.4	Application to the Yucca Mountain Region . . . . .	4-5
4.3	GEOMORPHIC DATING . . . . .	4-8
4.3.1	Analytical Methods . . . . .	4-9
4.3.2	Sources of Error . . . . .	4-9
4.3.3	Material Dated . . . . .	4-11
4.3.4	Application to the Yucca Mountain Region . . . . .	4-11
4.4	MISCELLANEOUS DATING TECHNIQUES . . . . .	4-12
4.4.1	Soil Development . . . . .	4-12
4.4.2	Tephrastratigraphy . . . . .	4-13
4.4.3	Cation-ratio . . . . .	4-13
5	EFFECTS OF AGE UNCERTAINTY ON PROBABILITY MODELS . . . . .	5-1
5.1	INTRODUCTION . . . . .	5-1
5.2	EFFECT OF AGE UNCERTAINTY ON AVERAGE RECURRENCE RATE ESTIMATES . . . . .	5-1
5.3	EFFECT ON WEIBULL-POISSON MODELS . . . . .	5-3
5.4	EFFECT ON SPATIALLY AND TEMPORALLY NONHOMOGENEOUS POISSON MODELS . . . . .	5-6
5.5	SUMMARY OF EFFECTS ON PROBABILITY MODELS . . . . .	5-9
6	CONCLUSIONS . . . . .	6-1
7	REFERENCES . . . . .	7-1

## FIGURES

Figure	Page
1-1	$^{40}\text{Ar}/^{39}\text{Ar}$ dates for Lathrop Wells from Turrin and Champion (1991) . . . . . 1-8
2-1	Locations and average ages of Neogene and Quaternary post-caldera basaltic volcanoes in the Yucca Mountain area, modified from Crowe (1990) . . . . . 2-9
2-2	K-Ar dates for Lathrop Wells from Sinnock and Easterling (1983) . . . . . 2-10
2-3	K-Ar dates for Red Cone from Sinnock and Easterling (1983) . . . . . 2-11
2-4	K-Ar dates for two Neogene Crater Flat volcanoes from Sinnock and Easterling (1983) . . . . . 2-15
2-5	(A) Example of a $^{40}\text{Ar}/^{39}\text{Ar}$ incremental heating date, modified from Fleck et al. (1977). (B) Example of an isochron plot, modified from McDougall and Harrison (1988). (C) Example of an inverse isochron plot, modified from McDougall and Harrison (1988) . . . . . 2-18
2-6	$^{40}\text{Ar}/^{39}\text{Ar}$ data for Lathrop Wells from Turrin and Champion (1991). . . . . 2-23
2-7	The large errors associated with $^{40}\text{Ar}/^{39}\text{Ar}$ dates for Lathrop Wells by Turrin and Champion (1991) obscure the population distribution of the data; both log-normal and normal distributions can be fit to these data . . . . . 2-24
2-8	$^{230}\text{Th}/^{232}\text{Th}$ - $^{238}\text{U}/^{232}\text{Th}$ isochron diagram showing the schematic evolution of an initially isotopically homogenous crystallizing magma . . . . . 2-27
2-9	Variation of $^{234}\text{U}/^{238}\text{U}$ and $^{230}\text{Th}/^{234}\text{U}$ ratios with time in a closed system free of initial $^{230}\text{Th}$ . . . . . 2-28
3-1	Mean lifetime of electron traps as a function of glow-peak and sample storage temperatures, modified from Aitken (1967) . . . . . 3-3
3-2	(A) Additive dose method for determining the accumulated radiation dose of a sample, modified from Aitken (1978). (B) Partial and Total Bleach methods of TL dating, modified from Geyh and Schleicher (1990) . . . . . 3-4
4-1	Late Cenozoic paleomagnetic polarity timescale from Mankinen and Dalrymple (1979), modified to include new age determinations by Spell and McDougall (1992) . . . . . 4-2
4-2	General geologic map of Lathrop Wells (Crowe et al., 1988) modified to show unit designations of Crowe et al. (1993), Champion (1991)(italics), and Turrin et al. (1991)(italics), and to indicate true north. Unit $Q_{s1}$ , of Champion (1991) is equivalent to unit $Q_{s2a}$ of Crowe et al. (1988). . . . . 4-7
4-3	(A) Cinder cone morphology parameters from Porter (1972) and Dohrenwend et al. (1986) (B) Geomorphic parameters for Cima cinder cones (Dohrenwend et al., 1986) . . . . . 4-10
5-1	The probability of a new volcano forming within the YMR during the next 10,000 to 50,000 yr is strongly dependent on the expected recurrence rate . . . . . 5-2
5-2	Recurrence rate for the formation of new volcanoes in the YMR is estimated using a number of near-neighbor nonhomogeneous Poisson models . . . . . 5-8

## FIGURES (Cont'd)

Figure		Page
5-3	Estimated probability of disruption of the candidate HLW repository varies with the number of near neighbors used in nonhomogeneous Poisson models and because of uncertainty in the ages of Quaternary YMR cinder cones . . . . .	5-10
5-4	The probability of disruption is not strongly affected by uncertainty in the age of Lathrop Wells, unless four or fewer near-neighbor volcanoes are considered . . . . .	5-11

## TABLES

Table	Page
1-1	$^{40}\text{Ar}/^{39}\text{Ar}$ dates for Lathrop Wells unit Ql <sub>5</sub> . . . . . 1-6
2-1	K/Ar dates for Quaternary volcanic rocks in the YMR . . . . . 2-6
2-2	K/Ar dates for Neogene basaltic rocks in the YMR . . . . . 2-16
2-3	$^{40}\text{Ar}/^{39}\text{Ar}$ dates for Lathrop Wells, Nevada, from Turrin and Champion (1991) . . . . . 2-21
3-1	Selected cosmogenic isotopes production reactions in terrestrial rocks . . . . . 3-8
3-2	$^3\text{He}$ dates for units from the Lathrop Wells complex, from Poths and Crowe (1992), and Crowe et al. (1993) unit designations from Crowe et al. (1993) . . . . . 3-12
3-3	$^{36}\text{Cl}$ exposure age dates for units of the Lathrop Wells center (Zreda et al., 1993). Unit designations from Turrin et al. (1991) and Crowe et al. (1993) in braces . . . . . 3-14
5-1	Dependence of the Weibull-Poisson model of recurrence rate of volcano formation on age . . . . . 5-5

## ACKNOWLEDGMENTS

Discussions with Mr. Stephen R. Young, Dr. Gerry L. Stirewalt, and Dr. James F. Luhr helped to define and clarify numerous aspects of this report. The quality of this report was improved from technical reviews by Drs. H. Lawrence McKague and Wesley C. Patrick, and an editorial review by Mr. James W. Pryor. We also thank Ms. Cathy Garcia and Ms. Joyce Foegelle for their valuable technical assistance in the preparation of this report.

This report was prepared to document work performed by the Center for Nuclear Waste Regulatory Analyses (CNWRA) for the U.S. Nuclear Regulatory Commission (NRC) under Contract No. NRC-02-88-005. The activities reported here were performed on behalf of the NRC Office of Nuclear Regulatory Research, Division of Regulatory Applications. This report is an independent product of the CNWRA and does not necessarily reflect the views or regulatory position of the NRC.

# 1 INTRODUCTION

The candidate Yucca Mountain high-level nuclear waste repository site is located in an area that has experienced intermittent volcanic activity since about 16 Ma. Early eruptions, which consisted of voluminous outpourings of rhyolite from shallow crustal magma chambers, buried the Yucca Mountain region (YMR) under several kilometers of ash-flow tuff (e.g., Byers et al., 1976, 1989). Since about 10 Ma, volcanism in the YMR has consisted of relatively small eruptions of basalt, which have formed numerous cinder cones (Crowe et al., 1983; Smith et al., 1990). Based on the past history of volcanism, preliminary studies have shown that the probability of an eruption at or near the candidate repository site during the next 10,000 yr is between  $5 \times 10^{-5}$  and  $1 \times 10^{-3}$  (Ho et al., 1991; Crowe et al., 1992a; Connor and Hill, 1993).

All probability studies to date rely upon the accurate determination of the ages of previous eruptions. In addition, some studies (Ho et al., 1991; Connor and Hill, 1993) recognize that Quaternary volcanoes (i.e., < 1.6 Ma; Palmer, 1983), which occur relatively close to the proposed repository site, present a greater potential risk of repository disruption than older Neogene (i.e., 1.6 - 23.7 Ma) volcanoes. Quantification of that risk is thus critically dependent on the precision and accuracy of the Quaternary ages used to develop probability models. However, geochronologic studies to date have failed to present well-constrained ages for Quaternary and Neogene basaltic volcanoes in the YMR (e.g., Trapp and Justus, 1992; this study).

Basaltic rocks between about 300,000 and 50,000 yr old are difficult to date by conventional geochronologic methods such as K/Ar. Previous attempts to date the Lathrop Wells volcanic center, the youngest volcano in the YMR, by conventional techniques reflect this difficulty (e.g., Sinnock and Easterling, 1983; Turrin and Champion, 1991). Recent work at Lathrop Wells has focussed on relatively new dating techniques, such as cosmogenic  $^3\text{He}$  (Poths and Crowe, 1992), or U-Th disequilibrium (Crowe et al., 1992b). Although these techniques have the potential to date 0.3 to 0.05-Ma basalt, the precision and accuracy of these dates are not sufficiently consistent to derive robust ages for mapped Lathrop Wells units (Crowe et al., 1988; 1992b). In addition, dates for older Quaternary and Neogene basalts have large enough analytical errors to significantly affect probability models (Connor and Hill, 1993). Although the uncertainty in these dates is occasionally incorporated into probability models, most models fail to rigorously propagate age uncertainties through probability calculations.

In addition to providing the necessary data for probability studies, the timing and duration of igneous activity need to be well constrained in order to construct accurate models for the potential consequences of volcanism on repository performance. For example, the determination that a cinder cone forming eruption should be considered a single spatial and temporal event will result in a consequence model that places a single thermal and mechanical load onto the proposed repository. If, however, a cinder cone forming eruption occurs in multiple phases, each separated by thousands of years of inactivity, then consequence models will need to consider multiple thermal and mass loads on the repository if a new volcanic center is established in or near the proposed repository block. The geochronologic methods currently used in volcanology may not have sufficient resolution to place an absolute age on the duration of a hiatus between such eruptions. If such temporal constraints are not possible, conservative consequence models will need to account for the possibility of multiple eruptions that occur over irresolvable periods of time.

This report was prepared as part of the Volcanic Systems of the Basin and Range research project at the Center for Nuclear Waste Regulatory Analyses (CNWRA) to provide a critical review of rock dating techniques for young basaltic volcanic systems. It is designed to present a summary of the techniques and assumptions used for modern geochronologic studies and to provide information on the limitations and uncertainties associated with these methods. The techniques reviewed are those that have been applied, or have the potential to be applied, to young basaltic rocks in the YMR. Application of these techniques to structural geology or tectonic studies in the YMR will be discussed as part of Task 5 of the Tectonic Processes of the Central Basin and Range Region research project.

## **1.1 REGULATORY BASIS**

The performance of the site, the waste package, and the repository during the next 10,000 yr must be evaluated in order to meet U.S. Environmental Protection Agency (EPA) standards for release of radioactivity (40 CFR Part 191; 10 CFR Part 60). System performance objectives for the geological repository, as described in 10 CFR 60.112, require that post-closure releases of radionuclides conform to EPA standards during anticipated events and in the occurrence of unlikely or unusual events such as volcanism. Features of the site that may affect repository performance must be discussed and evaluated in the Safety Analysis Report of the license application [10 CFR 60.21(c)(1)]. As part of the licensing process, the U.S. Nuclear Regulatory Commission (NRC) must evaluate the validity of U.S. Department of Energy (DOE) estimates of the probable release of radionuclides from the repository into the accessible environment.

Based on siting criteria presented in 10 CFR 60.122, evidence of igneous activity since the start of the Quaternary must be included as a potentially adverse condition if it is characteristic of the controlled area or if it could affect HLW isolation within the repository [10 CFR 60.122(c)(15)]. Researchers within the Yucca Mountain project clearly agree that Quaternary igneous activity exists for the study area. Adverse effects on repository performance due to changes in regional groundwater flow as a result of volcanic activity [10 CFR 60.122(c)(3)] also must be considered. Because Quaternary volcanism exists in the region, 10 CFR 60.122(a)(2)(i)-(iii) indicate the criteria necessary to demonstrate that volcanism will not impact repository performance significantly. These criteria are: (i) volcanism has been adequately investigated, (ii) volcanism has been investigated using analytical methods with appropriate sensitivities and assumptions that will not underestimate risks and effects, and (iii) the effects of volcanism are shown by investigation and analysis not to significantly affect waste isolation, are compensated for by favorable site or performance characteristics, or can be mitigated. Clearly, geochronologic studies will need to be performed and evaluated in order to meet the requirements of 10 CFR 60.122.

Insight gained through geochronology studies also will be used to support the following sections of the NRC License Application Review Plan (LARP): (i) evidence of igneous activity since the start of the Quaternary as a potentially adverse condition, Section 3.2.1.9; (ii) impact of volcanism on groundwater movement, Section 3.2.2.7; and (iii) assessment of compliance with the requirement for cumulative releases of radioactive materials, Section 6.1. Research on volcanism is ongoing at the CNWRA to develop these three sections of the LARP for the purpose of providing the NRC with the methodology and acceptance criteria to determine DOE compliance with 10 CFR Part 60 requirements. Compliance Determination Strategies (CDSs) and Compliance Determination Methods (CDMs) for these LARP sections are currently under development. However, the CDS (3.2.1.9) associated with evidence of Quaternary volcanism includes Type 5 Key Technical Uncertainties (KTUs), indicating that

independent research by NRC may be required to evaluate volcanism and that volcanism poses a high risk of noncompliance with 40 CFR Part 191 and 10 CFR 60.112. Developing an understanding on the precision, accuracy, and limitations of geochronological methods is thus critical to the evaluation of LARP (Sections 3.2.1.9, 3.2.2.7, and 6.1).

To date, three KTUs related to igneous activity have been identified as part of CDS 3.2.1.9, evidence of Quaternary igneous activity. These KTUs are:

- Low resolution of exploration techniques to detect and evaluate igneous features (Type 4)
- Inability to sample igneous features (Type 5)
- Development and use of conceptual tectonic models as related to igneous activity (Type 5)

Evaluation of these KTUs will require detailed safety review supported by analyses (Type 4) and detailed safety review supported by independent tests, analyses, and other investigations (Type 5). Geochronological data will be used extensively in these analyses, and this report will provide needed guidance for their use.

## 1.2 TECHNICAL BACKGROUND

### 1.2.1 Common Terms

A date is not an age, nor are these terms synonymous. As a noun, *date* refers to a specific point of time, which implies a degree of accuracy that is seldom present in geochronology. *Date* used as a verb simply refers to the process of analysis (e.g., Colman et al., 1987). Literally any rock can be dated, and can yield a date that has relatively low analytical error. The *age* of a unit, however, refers to some interval of time measured back from the present, and can only be determined after the validity of the date is examined in view of the available geologic information. The most important determination is that the measured date accurately reflects the age of the event under consideration. For volcanic rocks, the age of an eruption is usually the primary goal of geochronology. However, not all samples from a volcano will accurately preserve the age of eruption, even though any of these samples can be dated. The apparent eruption age can be corrupted through postemplacement alteration, complete or partial ingestion of xenoliths or xenocrysts, or by simply dating a flow not associated with the volcano under investigation. Thus, an age can only be assigned to a dated unit after suitable petrographic, geochemical, and stratigraphic tests have been applied.

The abbreviation Ma essentially refers to an age of millions of years ago. When a discrete period of millions of years is being described, the abbreviation m.y. is used (Colman et al., 1987). For example, deposition in a basin began at about 23 Ma and lasted for at least 5 m.y. In a similar manner, ka is used to denote ages of thousands of years and k.y. for periods of thousands of years. A special case is used in reference to <sup>14</sup>C ages, which are generally expressed as years before present (yr B.P.), with the year 1950 A.D. being the present (Stuiver and Polach, 1977).

### 1.2.2 Differences Between Precision and Accuracy

Precision and accuracy are two terms that are often used synonymously, but incorrectly, in geochronology discussions. Simply defined, precision generally refers to the analytical error associated with a date, but accuracy indicates how well a date represents the true age of the unit. For example, a Quaternary soil may have three dates of  $10.9 \pm 0.2$ ,  $11.1 \pm 0.2$ , and  $11.0 \pm 0.2$  ka. These dates are relatively precise because they have reported errors of about 2 percent and are indistinguishable based on reported analytical error. However, if the age of the dated unit is 20 ka, the high-precision data are essentially useless because they do not accurately indicate the true age of the unit. The accuracy of a date must be determined before a meaningful age can be assigned to a unit. Accuracy is, however, a very difficult parameter to determine. In dating volcanic rocks, several tests are available to estimate accuracy:

- Multiple dates of the same unit by different analytical techniques is the most robust test of accuracy, provided that the techniques used are appropriate for the age under investigation. A common test is to date the rock through conventional K-Ar and incremental  $^{40}\text{Ar}/^{39}\text{Ar}$  methods (e.g., McDougall and Harrison, 1988). If dates produced through these two techniques are indistinguishable within analytical error for the same unit, a reasonable test for accuracy has been performed.
- The dating method should be appropriate for the age of the material under consideration. Precision as well as accuracy are commonly poor near the lower application limits of most geochronologic techniques. For example, the conventional K-Ar method has a lower age limit of around 200 ka using standard analytical procedures. A K-Ar date for a 50-ka basalt may be reported as  $200 \pm 100$  ka. Although this date has relatively low precision, the range of uncertainty does not encompass the age of the rock due to inaccurate measurement of small amounts of radiogenic Ar in the sample. Conventional K-Ar dating is thus an inappropriate technique for 50-ka basalt.
- An accurate date should fit within the regional or local stratigraphy. Although many volcanic fields lack robust stratigraphic controls, pyroclastic, pluvial, and fluvial deposits can often provide some measure of stratigraphic position.
- Indirect methods, such as geomorphic development or paleomagnetic orientation, also can provide general tests of date accuracy. For example, a Nevada basalt with a date of  $0.85 \pm 0.05$  Ma should have a paleomagnetic direction that is reversed from the present magnetic field direction, using the widely accepted magnetic polarity time scale of Mankinen and Dalrymple (1979). A normal magnetic polarity for this sample indicates that the age of the rock is  $< 0.78$  Ma or  $> 0.90$  Ma (Spell and McDougall, 1992), and that the date does not accurately reflect the age of the basalt.

### 1.2.3 Common Statistical Problems in Geochronology

Every date has an associated uncertainty. However, this uncertainty generally reflects the analytical precision of the date and only rarely incorporates an estimate of the uncertainty in the age. A general assumption is that the uncertainty is reported at a 1-sigma confidence interval, which effectively states that the date has a 68-percent probability of being within the reported range of error. The uncertainty reported with a date should thus be viewed as a minimum estimate of error. Calculations that

use dates must preserve the associated uncertainty and necessarily result in a value that also has an uncertainty, if the result is to be significant.

Dates reported by Turrin and Champion (1991) provide a useful example of how uncertainty can be propagated through statistical calculations. These data are used as an example because Turrin and Champion report sufficient analytical data to independently determine some aspects of analytical uncertainty, and these dates were produced at the internationally recognized Berkeley geochronology lab. A mean of  $170 \pm 114$  ka is reported by Turrin and Champion (1991) for eight  $^{40}\text{Ar}/^{39}\text{Ar}$  dates from Lathrop Wells lava Q1<sub>5</sub> (Table 1-1). However, the reported uncertainty only represents 1 standard deviation of the absolute date population and does not reflect the large analytical errors (average of 284 percent) associated with these data. Using general rules for calculations involving numbers  $X_i$  with associated uncertainties ( $x$ ) (e.g., Wang et al., 1975), propagation of reported errors through the calculation of a mean requires

$$\bar{X} \pm \bar{x} = \frac{\sum X_i}{n} \pm \frac{\sqrt{\sum x_i^2}}{n} \quad (1-1)$$

when  $\bar{X}$  = Average of  $n$  samples  
 $\bar{x}$  = Uncertainty in the average

and results in a mean of  $170 \pm 121$  ka. Note that the 121 ka uncertainty does not indicate 68 percent of the dates fall within 121 ka of the mean, only that the mean has an uncertainty of 121 ka. Calculation of the standard deviation for this date population requires

$$Sdev = \sqrt{\frac{\sum (X_i \pm x_i - \bar{X} \pm \bar{x})^2}{n}} \quad (1-2)$$

resulting in 1 standard deviation of  $106 \pm 161$  ka. Thus, 68 percent of these dates fall within the range of  $170 \pm 388$  (i.e.,  $121 + 106 + 161$ ) ka. Although this range is large, it accurately reflects a data set of eight samples that have an average reported analytical error of 284 percent. Raw (i.e., nonaveraged) data must be presented in order to adequately evaluate the precision of a series of dates, because reported averages and associated uncertainties in many radiometric dating reports (e.g., Turrin and Champion, 1991) do not necessarily reflect the large precision errors associated with the data.

Another statistical technique commonly used in geochronology involves calculation of a weighted mean for a series of dates (e.g., Taylor, 1990). Dates with large analytical errors ( $\sigma_i$ ) are given relatively little weight in the mean, but dates with small analytical errors are weighed more extensively in the mean. A weighted mean can be calculated as

Table 1-1.  $^{40}\text{Ar}/^{39}\text{Ar}$  dates for Lathrop Wells unit Q1<sub>5</sub> from Turrin and Champion (1991). Col Average and Std Dev refer to the simple averages and standard deviations of the data columns. The weighted mean is calculated by weighing the individual dates with the inverse of the associated error squared [Eq. (1-3)]. Average date and Std Dev refer to statistics calculated by propagation of analytical error [Eqs. (1-1 and 1-2)] and are combined to give an approximate age of  $0.170 \pm 0.388$  Ma (i.e.,  $0.2 \pm 0.4$  Ma) for this unit. Note that the 228-percent error associated with the approximate age is comparable to the average reported error of 284 percent for these dates.

Sample	Date (Ma)	$\pm 1\sigma$ Error (Ma)	$^{40}\text{Ar}_{\text{rad}}$ (%)	Error (%)
1555-1	0.168	0.318	0.6	189
1555-2	-0.020	0.263	-0.1	1315
1555-3	0.368	0.644	0.7	175
1555-4	0.164	0.089	0.9	54
1555-10	0.112	0.090	0.6	80
1555-11	0.107	0.155	0.4	145
1555-12	0.235	0.521	0.4	222
1555-13	0.228	0.200	1.2	88
Col Average	0.170	0.285	0.6	284
Col Std Dev	0.106	0.084	0.4	
Weighted mean	0.138	0.054		39
Average Date	0.170	0.121		
Avg Std Dev	0.106	0.161		
Approximate Age	0.170	0.388		228

$$\bar{X} \pm \bar{x} = \frac{\sum X_i w_i}{\sum w_i} \pm \sqrt{\frac{1}{\sum w_i}} \quad (1-3)$$

where  $w_i = \frac{1}{\sigma_i^2}$

However, a basic assumption in calculating a weighted mean is that analytical error has a normal distribution (i.e., gaussian) about the mean (e.g., Geyh and Schleicher, 1990). This assumption often cannot be made for dates that are determined near the limits of resolution for the technique. In such instances, analytical error will generally have a log-normal instead of a gaussian distribution about the mean. For example,  $^{40}\text{Ar}/^{39}\text{Ar}$  dates by Turrin and Champion (1991) have a roughly log-normal distribution to analytical error (Figure 1-1). This distribution reflects the roughly 100–150-ka lower age limit to this dating technique for rocks such as Lathrop Wells, which have  $\text{K}/\text{Ca} < 1$  (cf. Dalrymple and Lanphere, 1971; McDougall and Harrison, 1988). Application of a weighted mean to these data will incorrectly skew the mean towards older dates, which have lower analytical error (Figure 1-1). Using Eq. (1-3), a weighted mean for the eight Lathrop Wells dates in Table 1-1 is  $0.138 \pm 0.054$  Ma (Turrin et al., 1991). Note that this calculation takes a series of dates that have an average error of 284 percent and produces a weighted mean with only 39-percent error. Clearly, a weighted mean does not accurately reflect the analytical uncertainty associated with these dates.

Another common statistical test used in geochronology is to determine if two dates or ages are significantly distinct. At a 95-percent confidence interval, two ages are distinct if the apparent difference in the ages exceeds a Critical Value (Dalrymple and Lanphere, 1969)

$$\text{C.V.} = 1.960 \left( \frac{\sigma_1^2}{n_1} + \frac{\sigma_2^2}{n_2} \right)^{1/2} \quad (1-4)$$

where:  $\sigma$  = standard deviations of ages  
 $n$  = number of measurements made on the units

Thus, in order to distinguish age differences of 100 ka between roughly 1-Ma units, a dating technique with 10-percent error must be used and seven samples from each unit must be dated. If one sample from each unit is dated, only age differences in excess of 270 ka can be determined at a 95-percent confidence level.

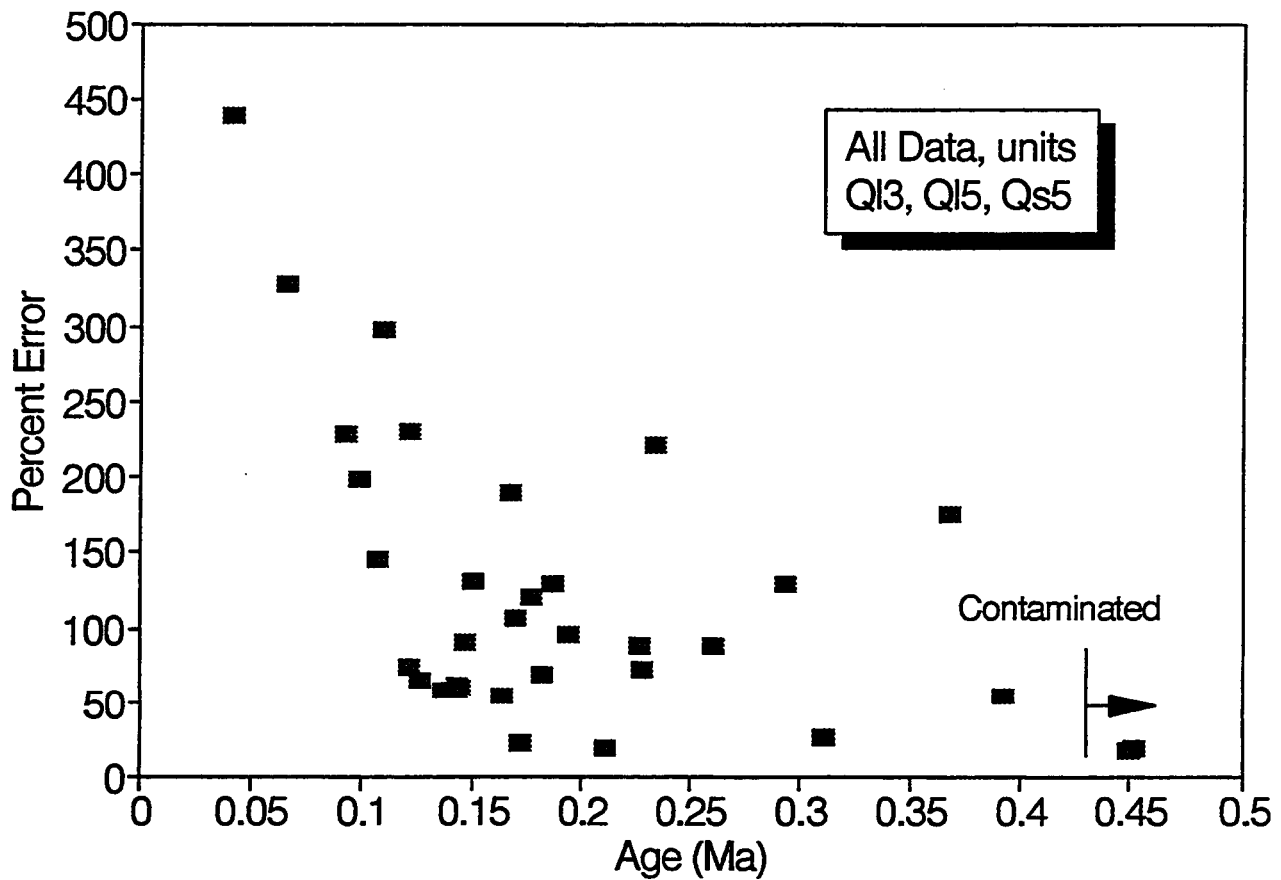


Figure 1-1.  $^{40}\text{Ar}/^{39}\text{Ar}$  dates for Lathrop Wells from Turrin and Champion (1991). The large amount of error associated with young dates follows an approximately log-normal distribution, which reflects the difficulty in dating low-K basalt near the detection limits of the technique. Error is not normally distributed about the mean, and thus a weighted average does not accurately represent these data.

## 2 RADIOMETRIC DATING METHODS

### 2.1 GENERAL PRINCIPLES

Most absolute dating methods for volcanic rocks are based on the production of decay products from naturally occurring radioactive elements. For Neogene and Quaternary (i.e., young) volcanic rocks, the most important isotopic systems are K/Ar and U/Th. Other isotopic systems, such as Rb/Sr and Sm/Nd (e.g., Geyh and Schleicher, 1990), are used to date significantly older rocks and will not be discussed in this report.

The application of any radiometric dating technique requires that specific assumptions can be made about the rocks being analyzed.

- The parent nuclide decays at a rate that is well known, and is not affected by variations in pressure or temperature. For the radioactive isotopes of K, U, and Th, this assumption is valid for all conditions on Earth.
- The ratio between the radioactive isotope and the stable isotope in nature remains constant. This assumption is valid for the systems and times under consideration in this report.
- All of the radiogenic daughter present in the sample was produced by *in situ* decay of the radioactive parent. Although this assumption is generally valid, it is possible for some volcanic rocks to inherit radiogenic daughter products prior to crystallization.
- The isotopic system has remained closed (i.e., no gain or loss of atoms except through radioactive decay) since the unit was formed. This assumption can be violated by young volcanic rocks, and closed-system behavior should be rigorously tested through petrographic and geochemical analyses before a unit is dated.

The youthful appearance of a volcanic rock is not a sufficient basis to assume that no element mobility has occurred. For example, basaltic glass has poor Ar retentivity when hydrated (Kaneoka, 1972). Neogene K/Ar dates from basaltic glass with only 1 weight percent H<sub>2</sub>O may be 50-percent younger than dates from nonhydrated glass (Kaneoka, 1972). Hydration can occur during deuteric alteration as the basalt cools, or during surficial weathering (e.g., Colman, 1982). Thus, lava flows that have a crystalline groundmass (i.e., holocrystalline) are more likely to yield meaningful K-Ar eruption ages than hyalocrystalline flows from the same volcano. Similar problems regarding element mobility under surficial conditions also apply to the U/Th isotopic system.

### 2.2 POTASSIUM/ARGON (<sup>40</sup>K/<sup>40</sup>Ar) METHOD

The K/Ar method is the most commonly used radiometric technique for dating Neogene and Quaternary volcanic rocks. The general principle is that <sup>40</sup>K, the radioactive isotope of potassium, decays with a half-life of  $1.4 \times 10^9$  years to the stable isotope <sup>40</sup>Ar (Dalrymple and Lanphere, 1969). The abundances of radiogenic <sup>40</sup>Ar (<sup>40</sup>Ar\*) and K are measured, and a date is calculated assuming that all the <sup>40</sup>Ar\* measured was produced through *in situ* decay of <sup>40</sup>K.

The K/Ar dating technique commonly is applied to samples that range in age from several billion years to less than a million years. K/Ar dates on mafic volcanic rocks older than several million years, and silicic volcanic rocks around one million years, are generally considered routine. Through a variety of analytical modifications (e.g., Cassagnol and Gillot, 1982), K/Ar dates as young as several tens of thousands of years, with equivalent uncertainties, can be produced. However, it is generally considered that ages of around 100 ka are the current lower limits to the K/Ar technique, if the laboratory is expressly calibrated to date young samples (Geyh and Schleicher, 1990).

Several details are important to understanding K/Ar systematics.  $^{40}\text{K}$ , which represents 0.01167 atomic percent of all potassium isotopes, follows a branched decay series with well-established decay constants (Steiger and Jäger, 1977). About 89 percent of  $^{40}\text{K}$  decay occurs as  $\beta^-$  decay to  $^{40}\text{Ca}$ , and has a half-life of  $1.40 \times 10^9$  years. The remainder of  $^{40}\text{K}$  decays to  $^{40}\text{Ar}$ , primarily through electron capture with a half-life of  $1.19 \times 10^9$  years. Both decay series must be considered when a K/Ar date is calculated. In addition to the general assumptions inherent in radiometric dating, the K/Ar method also has several specific requirements.

- $^{40}\text{Ar}$  is a naturally occurring stable isotope of Ar. For young volcanic rocks, a large percentage of the  $^{40}\text{Ar}$  in the sample will be from atmospheric contamination. The distinction between atmospheric and radiogenic  $^{40}\text{Ar}$  can be made by assuming the atomic ratio  $^{40}\text{Ar}/^{36}\text{Ar}=295.5$  for atmospheric  $^{40}\text{Ar}$  (Steiger and Jäger, 1977). The precision in measurement of this ratio is the most critical step in determining the date of a young volcanic rock.
- Ar is an inert noble gas and is not incorporated into mineral lattices at magmatic temperatures. At lower temperatures, however, Ar is trapped in the mineral lattice due to its relatively large (1.9 Å) atomic radius. The temperature at which Ar is retained is different for different minerals. Amphibole retains Ar between 700–500 °C, but feldspar retains Ar only at temperatures below about 230 °C (Geyh and Schleicher, 1990). Conversely, heating feldspar above 230 °C will result in Ar loss and anomalously young dates. Basaltic glass will allow Ar loss through diffusion under most conditions, and is thus unsuitable for K/Ar dating (e.g., Dalrymple and Lanphere, 1969).

### 2.2.1 Analytical Methods

The only required analyses for a K/Ar date are total K and  $^{40}\text{Ar}^*$  measurements. Analysis for K is usually through atomic absorption spectrophotometry, which has an accuracy of around 1 percent. Other methods used for K analysis include X-ray fluorescence, instrumental neutron activation analysis, isotope dilution analysis, wet-chemical (gravimetric) methods, and inductively coupled plasma spectrometry (Geyh and Schleicher, 1990). For the analysis of young volcanic rocks, the K content of the sample is a much smaller source of error than the measurement of  $^{40}\text{Ar}^*$ .

Isotope dilution is the technique used to measure  $^{40}\text{Ar}^*$ , and the procedure used by most labs follows Dalrymple and Lanphere (1969): The sample is weighed, heated to >1300 °C under high vacuum ( $<10^{-8}$  Torr), and the resulting gases are collected. Hydrogen and carbon monoxide are separated from the sample through oxidation over a hot copper oxide screen. Water and carbon dioxide are first precipitated in a cold trap, with the remainder being removed using a molecular sieve. Other reactive gases (e.g.,  $\text{O}_2$ ,  $\text{N}_2$ ) in the sample are adsorbed onto a titanium screen. An  $^{38}\text{Ar}$  spike

(i.e., tracer) with a purity of >99.9997 percent is added to the sample, and a mass spectrometer is used to measure  $^{40}\text{Ar}/^{38}\text{Ar}$  and  $^{38}\text{Ar}/^{36}\text{Ar}$ . The amount of  $^{38}\text{Ar}$  in the sample due to atmospheric contamination can be determined from the known ratio of  $^{38}\text{Ar}/^{36}\text{Ar}$  in the atmosphere, with the excess  $^{38}\text{Ar}$  from the spike. The fraction of atmospheric  $^{40}\text{Ar}$  can be calculated from the known ratio of 295.5 for  $^{40}\text{Ar}/^{36}\text{Ar}$  (Steiger and Jäger, 1977). After correcting for small amounts of  $^{36}\text{Ar}$  and  $^{40}\text{Ar}$  in the tracer and minor mass spectrometer fractionation effects, the exact amount of  $^{40}\text{Ar}^*$  in the sample can be calculated from the measured  $^{40}\text{Ar}/^{38}\text{Ar}$ . Using the constants of Steiger and Jäger (1977) the K/Ar date can then be calculated.

$$\text{date} = 1.804 \times 10^9 \ln \left( 9.540 \frac{^{40}\text{Ar}^*}{^{40}\text{K}} + 1 \right) \quad (2-1)$$

Cassagnol and Gillot (1982) proposed a modification of the conventional K/Ar technique in which the need for a  $^{38}\text{Ar}$  spike was eliminated. This technique requires a highly stable mass spectrometer in which gases other than Ar have been thoroughly removed. The mass spectrometer also is modified to increase the signal-to-noise ratio for  $^{36}\text{Ar}$  and  $^{38}\text{Ar}$  at low voltages. K/Ar dates in the 10–100-ka range produced with the Cassagnol technique are reported by Gillot and Cornette (1986) for highly potassic, silicic volcanic rocks in southern Italy. These dates appear to correlate well with known  $^{14}\text{C}$  and thermoluminescence dates (Gillot and Cornette, 1986).

### 2.2.2 Sources of Error

For conventional K/Ar analysis, the primary sources of uncertainty reported in a date are due to the difficulty in accurately distinguishing the radiogenic  $^{40}\text{Ar}$  component from atmospheric  $^{40}\text{Ar}$ . The amount of atmospheric  $^{40}\text{Ar}$  in young samples can be up to 98 percent of the total Ar measured. Although dates with <2-percent  $^{40}\text{Ar}^*$  may be at times accurate, they usually have large precision errors and are generally regarded as near the detection limits of the K/Ar technique (e.g., Dalrymple and Lanphere, 1969; Geyh and Schleicher, 1990). The other factor that limits precise determination of  $^{40}\text{Ar}^*$  is the difficulty in measuring the small amount of  $^{36}\text{Ar}$  in the sample. The low natural abundance of  $^{36}\text{Ar}$  (0.337 percent) and the large mass of  $^{38}\text{Ar}$  introduced in the spike result in an error of around 2 percent in measuring  $^{38}\text{Ar}/^{36}\text{Ar}$  (Dalrymple and Lanphere, 1969). Other analytical measurements can be combined with the uncertainty in determining  $^{40}\text{Ar}^*$  to derive the uncertainty typically reported for a K/Ar date (Dalrymple and Lanphere, 1969).

$$\sigma_{\text{date}} = \sqrt{(\sigma_K)^2 + (\sigma_x)^2 + \left(\sigma_{38}^{40}\right)^2 \left(\frac{1}{r}\right)^2 + \left(\sigma_{38}^{36}\right)^2 \left(\frac{1-r}{r}\right)^2} \quad (2-2)$$

where  $\sigma_K$  = uncertainty in K analysis  
 $\sigma_x$  = uncertainty in tracer calibration  
 $\sigma_{38}^{40}$  = uncertainty in the  $^{40}\text{Ar}/^{38}\text{Ar}$  ratio  
 $\sigma_{38}^{36}$  = uncertainty in the  $^{36}\text{Ar}/^{38}\text{Ar}$  ratio  
 $r$  = fraction of  $^{40}\text{Ar}$  that is radiogenic

Other sources of analytical error not included in Eq. (2-2) but generally assumed to be small, are uncertainties in sample weight (<0.01 percent), the fractionation factor of the mass spectrometer (<0.01 percent), and the decay constants used in the age equation (Steiger and Jäger, 1977).

Sample inhomogeneity also may be a large source of error in both the precision and accuracy of the K/Ar date. Analyses for K and Ar are made on different splits of the same sample, and errors associated with sample inhomogeneity can at times exceed analytical errors (Engles and Ingamells, 1970). Inhomogeneity in K-bearing phases can occur if different sample sizes are inadvertently used for these analyses. A common procedure to avoid sample inhomogeneity is to split the samples after they have been ground to a uniform size, commonly 0.5 mm (30 mesh) to 0.25 mm (60 mesh). Finer-grained samples typically are not used due to the difficulty in handling the sample under high vacuum.

The loss of Ar from the dated system must be considered when a K/Ar date is evaluated for accuracy. Once the sample has cooled to near-surface temperatures, Ar loss through diffusion is not a problem. At 20 °C, none of the materials routinely used in K/Ar dating will lose sufficient Ar to affect the resultant date (Dalrymple and Lanphere, 1969). However, heating plagioclase to about 200 °C can result in significant Ar loss and an erroneously young date for the sample (Dalrymple and Lanphere, 1969). In addition to heating, Ar loss commonly occurs during alteration of the rock. Small amounts of clay alteration along fractures or cleavage planes in plagioclase reflect generally unacceptable degrees of sample alteration. Volcanic glass also hydrates relatively easily under surficial conditions, which results in significant Ar loss (Kaneoka, 1972). Routine petrographic examination of the sample, which will quickly reveal significant degrees of alteration, is thus a mandatory step in determining the accuracy of the reported K/Ar date.

The problem of inherited  $^{40}\text{Ar}$  in the dated system is more difficult to evaluate than Ar loss. Magma is easily contaminated through the assimilation of the surrounding rock. If the assimilated rock is relatively old and contains significantly more  $^{40}\text{Ar}$  than the magma (i.e., more potassic), the magma will be anomalously enriched in  $^{40}\text{Ar}$  (McDougall and Harrison, 1988). The presence of excess  $^{40}\text{Ar}$  in the melt is not significant for minerals like plagioclase and amphibole, which have blocking temperatures well below the solidus of the melt. However, whole-rock samples that were cooled before the magma was completely degassed could retain some of the excess  $^{40}\text{Ar}$  and thus yield erroneously old K/Ar dates. The consistency of many K/Ar studies clearly indicates that most lavas are effectively degassed with respect to extraneous  $^{40}\text{Ar}$  (e.g., Dalrymple and Lanphere, 1969; McDougall and Harrison, 1988). However, petrographic evidence of disequilibrium crystallization, such as strongly resorbed or zoned plagioclase, should be viewed as evidence that wall-rock contamination and ensuing  $^{40}\text{Ar}$  enrichment might have occurred in the sample. A K/Ar date from such a sample will have a more questionable accuracy than dates from a sample that lacks disequilibrium effects.

From previous discussions on mineral blocking temperatures, it would appear intuitive that xenoliths and xenocrysts in a magma would be effectively degassed. However, the residence times for many xenoliths in magmas are too short to allow complete degassing through diffusion, even at temperatures well in excess of the blocking temperature of the xenocrysts (Dalrymple, 1964; Gillespie et al., 1982). Thus, the presence of xenoliths in a sample can significantly increase the apparent age of the dated rock. This apparent increase is of particular concern with whole-rock dates of young basaltic rocks, which will have relatively low amounts of K and  $^{40}\text{Ar}^*$ . The presence of only 1 volume percent of a 10-Ma basaltic xenolith in a 1-Ma basalt will result in a 10-percent error in the K/Ar age of the rock. If, however, the age of the basaltic xenolith is 100 Ma, then the 1-Ma basalt will have a date that is 100-percent in error of the true age of the rock (Dalrymple and Lanphere, 1969). Although relatively

large xenoliths can be easily removed from a crushed sample by hand, smaller fragments of the xenolith could easily escape detection during sample preparation. Samples should thus be selected in the field to avoid units with visible xenoliths. Although the absence of macroscopic xenoliths does not necessarily indicate the absence of microscopic xenoliths, such samples tend to lack xenoliths when examined under a petrographic microscope.

### 2.2.3 Material Dated

Most young igneous rocks can be dated by the K/Ar method. Both mineral separates and bulk-rock samples can be analyzed. For bulk-rock analysis, the most suitable samples are holocrystalline and as fine-grained and equigranular as possible (Engles and Ingamells, 1970). Strongly porphyritic samples increase the risk of inherited radiogenic Ar through xenocryst contamination, and large phenocrysts should be evaluated for equilibrium with the host-rock composition. Basaltic glass has poor Ar retentivity and is easily hydrated at surface conditions (Kaneoka, 1972), and is thus poorly suited for K/Ar dating. Mineral separates are preferred for analysis when the mineral contains more potassium than the bulk rock. Biotite, although uncommon in mafic volcanic rocks, contains about 7 to 9 weight percent  $K_2O$  and is thus one of the best minerals to date by the K/Ar method. Biotite usually yields accurate K/Ar dates even when slightly chloritized, because K and Ar are lost in the same proportions during weak chloritization (Geyh and Schleicher, 1990). Amphibole generally contains  $\leq 1$  weight percent  $K_2O$ , but has excellent Ar retention up to temperatures  $< 500$  °C (Dalrymple and Lanphere, 1969). Plagioclase also generally contains  $\leq 1$  weight percent  $K_2O$ , but is more common in occurrence than amphibole. However, Ar loss occurs in plagioclase at temperatures of around 200 °C, which may result in anomalously young dates for samples collected close to dikes. Sanidine contains about 14 weight percent  $K_2O$  and retains Ar like plagioclase, but is restricted to low-temperature rhyolitic rocks. Leucite contains high  $K_2O$  (16–18 weight percent) but only occurs in highly potassic, silica-undersaturated rocks. Other commonly occurring igneous minerals, such as pyroxene or olivine, are unsuitable for dating young volcanic rocks due to a low abundance of  $K_2O$  ( $< 0.1$  weight percent).

### 2.2.4 Application to the Yucca Mountain Region

#### 2.2.4.1 Quaternary Basaltic Volcanoes

K/Ar studies in the YMR have focused on Quaternary basaltic volcanoes. These dates are presented in Table 2-1, along with all published analytical information. None of the published K/Ar dates in the YMR present sufficient analytical information to independently calculate the date. In addition, analytical methods are rarely reported, there is no indication of petrographic examination of the dated samples, the samples have not been geochemically analyzed, and sample locations list only the name of the volcano. Independent determinations of precision and accuracy are thus extremely limited for these data.

Lathrop Wells (Figure 2-1) has long been recognized as the youngest volcanic center in the YMR based on a lack of cone degradation (Vaniman and Crowe, 1981). An evaluation (Connor and Hill, 1993) of existing data (Crowe et al; 1992b) suggests the best age estimate for Lathrop Wells is  $0.10 \pm 0.5$  Ma. Attempts at determining the age of Lathrop Wells through K/Ar dating have been unsuccessful (Vaniman and Crowe, 1981; Vaniman et al., 1982; Sinnock and Easterling, 1983). Analytical errors are generally large (Table 2-1), reflecting the difficulty in dating young (i.e.,  $< 1$  Ma) low-potassium basalt near the lower limits of the K/Ar technique. For dates with relatively low analytical

errors, the differences in the apparent ages of these samples often exceed several times the reported uncertainty, indicating that these dates do not accurately represent the age of Lathrop Wells. Splits from six Lathrop Wells samples were analyzed by three different laboratories in a study by Sinnock and Easterling (1983). These dates and associated errors are shown in Figure 2-2. They concluded that the amount of variation reported within each lab's sample set is considerably less than the age uncertainty represented by interlaboratory variations. Based on the amount of variation within the sample set, Sinnock and Easterling (1983) estimated the age of Lathrop Wells (sample site 1) at  $0.46 \pm 0.58$  Ma, which compares favorably with the average date of  $0.46 \pm 0.48$  Ma in Table 2-1 calculated from the reported analytical errors [Eqs. (1-1) and (1-2)].

Table 2-1. K/Ar dates for Quaternary volcanic rocks in the YMR. *Error* is the percentage error between Age and  $\pm 1\sigma$ . *Simple Avg* is the average and standard deviation of the reported ages. *Wgt Mean* is the weighted mean of the dates [Eq. (1-3)] *Average Date* reports propagated uncertainties [Eqs. (1-1 and 1-2)].

Volcano	Sample	Age (Ma)	$\pm 1\sigma$ (Ma)	$^{40}\text{Ar}^*$	% Error	Reference
Lathrop Wells 1	A	0.70	0.07	3.5	10	Sinnock & Easterling, 1983
Lathrop Wells 1	B	0.12	0.03	1.6	25	Sinnock & Easterling, 1983
Lathrop Wells 1	C	0.60	0.09	7.9	15	Sinnock & Easterling, 1983
Lathrop Wells 2	A	0.65	0.07	1.5	11	Sinnock & Easterling, 1983
Lathrop Wells 2	B	-0.01	0.29	0.1	-2900	Sinnock & Easterling, 1983
Lathrop Wells 2	C	0.61	0.16	4.0	26	Sinnock & Easterling, 1983
Lathrop Wells 3	A	0.77	0.08	2.8	10	Sinnock & Easterling, 1983
Lathrop Wells 3	B	-0.03	0.14	0.0	-467	Sinnock & Easterling, 1983
Lathrop Wells 3	C	0.66	0.10	6.5	15	Sinnock & Easterling, 1983
Lathrop Wells 4	A	0.59	0.06	1.6	10	Sinnock & Easterling, 1983
Lathrop Wells 4	B	0.08	0.03	1.1	38	Sinnock & Easterling, 1983
Lathrop Wells 4	C	0.56	0.09	7.3	16	Sinnock & Easterling, 1983
Lathrop Wells 5	A	1.10	0.30	2.4	27	Sinnock & Easterling, 1983
Lathrop Wells 5	B	0.13	0.18	0.4	144	Sinnock & Easterling, 1983
Lathrop Wells 5	C	0.59	0.21	3.4	36	Sinnock & Easterling, 1983
Lathrop Wells 6	A	0.58	0.08	2.3	14	Sinnock & Easterling, 1983
Lathrop Wells 6	B	0.18	0.09	0.9	51	Sinnock & Easterling, 1983
Lathrop Wells 6	C	0.39	0.07	6.6	18	Sinnock & Easterling, 1983
Simple Avg $0.46 \pm 0.30$		Wgt Mean $0.30 \pm 0.02$			Average Date $0.46 \pm 0.48$	
Lathrop Wells	TSV-1	0.29	0.20		69	Vaniman & Crowe, 1981

Volcano	Sample	Age (Ma)	$\pm 1\sigma$ (Ma)	$^{40}\text{Ar}^*$	% Error	Reference
Lathrop Wells		0.23	0.02		9	Vaniman et al., 1982
Lathrop Wells		0.30	0.10		33	Vaniman et al., 1982
Little Black Pk		0.29	0.11		38	Crowe et al., 1982
Little Black Pk		0.32	0.15		47	Crowe et al., 1982
Little Black Pk		0.24	0.22		92	Crowe et al., 1982
Little Black Pk		0.21	0.13		64	Crowe et al., 1982
Little Black Pk		0.22	0.10		45	Crowe & Perry, 1991
Simple Avg $0.26 \pm 0.04$		Wgt Mean $0.25 \pm 0.06$			Average Date $0.26 \pm 0.17$	
Hidden Cone		0.32	0.20		63	Crowe & Perry, 1991
Red Cone 7	A	1.70	0.20	5.9	12	Sinnock & Easterling, 1983
Red Cone 7	B	0.97	0.09	5.4	9	Sinnock & Easterling, 1983
Red Cone 7	C	1.46	0.11	12.4	8	Sinnock & Easterling, 1983
Red Cone 8	A	1.90	0.20	4.4	11	Sinnock & Easterling, 1983
Red Cone 8	B	0.95	0.11	3.6	12	Sinnock & Easterling, 1983
Red Cone 8	C	1.76	0.19	9.2	11	Sinnock & Easterling, 1983
Red Cone 9	A	1.50	0.20	2.0	13	Sinnock & Easterling, 1983
Red Cone 9	B	0.98	0.05	8.4	5	Sinnock & Easterling, 1983
Red Cone 9	C	1.40	0.13	12.4	9	Sinnock & Easterling, 1983
Red Cone 10	A	1.80	0.20	2.9	11	Sinnock & Easterling, 1983
Red Cone 10	B	1.66	1.52	1.5	92	Sinnock & Easterling, 1983
Red Cone 10	C	1.61	0.24	8.0	15	Sinnock & Easterling, 1983
Red Cone 11	A	0.99	0.15	4.2	15	Sinnock & Easterling, 1983
Red Cone 11	B	1.08	0.24	2.1	22	Sinnock & Easterling, 1983
Red Cone 11	C	1.64	0.35	4.0	21	Sinnock & Easterling, 1983
Red Cone 12	A	1.50	0.20	3.3	13	Sinnock & Easterling, 1983
Red Cone 12	B	1.11	0.13	3.8	12	Sinnock & Easterling, 1983
Red Cone 12	C	1.41	0.38	4.6	27	Sinnock & Easterling, 1983
Simple Avg $1.41 \pm 0.26$		Wgt Mean $1.17 \pm 0.03$			Average Date $1.41 \pm 0.60$	

Volcano	Sample	Age (Ma)	$\pm 1\sigma$ (Ma)	$^{40}\text{Ar}^*$	% Error	Reference
Red Cone	TSV-12 8	1.14	0.30		26	Vaniman & Crowe, 1981
Red Cone	W Rift	1.50	0.10		7	Vaniman et al., 1982
Red Cone Dike		0.98	0.10		10	Ho et al., 1991
Red Cone		1.01	0.06		6	Ho et al., 1991
Red Cone: Top		0.95	0.08		8	Ho et al., 1991
Northern Cone		1.14	0.30		26	Vaniman et al., 1982
Northern Cone	W Rift	1.07	0.04		4	Vaniman et al., 1982
Black Cone	TSV-2	1.09	0.30		28	Vaniman & Crowe, 1981
Black Cone	TSV-2A	1.07	0.40		37	Vaniman & Crowe, 1981
Little Cone SW	TSV-3	1.11	0.30		27	Vaniman & Crowe, 1981

The Sleeping Butte volcanoes (Figure 2-1) are somewhat more dissected and eroded than the Lathrop Wells cone and have long been regarded as late Quaternary vents (Crowe et al., 1983; Crowe and Perry, 1991). Five K/Ar dates have been determined for the Little Black Peak volcano (Table 2-1). Considering the associated analytical errors, these dates have an average of  $0.26 \pm 0.17$  Ma [Eqs. (1-1) and (1-2)]. The large analytical errors associated with these dates average 57-percent, and also reflect the difficulty in dating young low-potassium basalt near the lower limits of the K/Ar technique. Considering the large reported errors, an accurate age of Little Black Peak volcano is  $0.3 \pm 0.2$  Ma and  $0.3 \pm 0.2$  Ma for Hidden Cone. Both of these ages are indistinguishable from an age of either  $0.5 \pm 0.5$  Ma (Table 2-1) or  $0.10 \pm 0.05$  Ma for Lathrop Wells.

The other Quaternary volcanoes in the YMR consist of an arcuate alignment of five vents in Crater Flat (Figure 2-1). These volcanoes are more eroded than the Sleeping Butte or Lathrop Wells cones, but have long been recognized as Quaternary vents (Vaniman and Crowe, 1981). Samples from Red Cone were also included in the dating study of Sinnock and Easterling (1983), and these dates are reported in Table 2-1. As was observed for the Lathrop Wells dates, the amount of interlaboratory variation clearly exceeds the amount of intralaboratory variation (Figure 2-3). Dates that have low reported analytical errors range from  $0.98 \pm 0.05$  Ma to  $1.9 \pm 0.2$  Ma, which are distinct [Eq. (1-4)] at a 95-percent confidence level. Dating a roughly 1-Ma basalt is generally considered a routine procedure, which is reflected in the relatively low (< 10 percent) analytical errors (Table 2-1). However, the large variations in apparent age determined by the three labs clearly exceed the precision of the dates for Red Cone, which indicates the accuracy of these dates is questionable. A weighted mean age of  $1.17 \pm 0.03$  (Table 2-1) is clearly misleading and does not reflect the large range of precision and accuracy in these data. An average date [Eqs. (1-1) and (1-2)] of  $1.4 \pm 0.6$  Ma accurately represents the large amount of variation in these Red Cone dates. Other Crater Flat K/Ar dates (Table 2-1) are well represented by an age of  $1.2 \pm 0.4$  Ma.

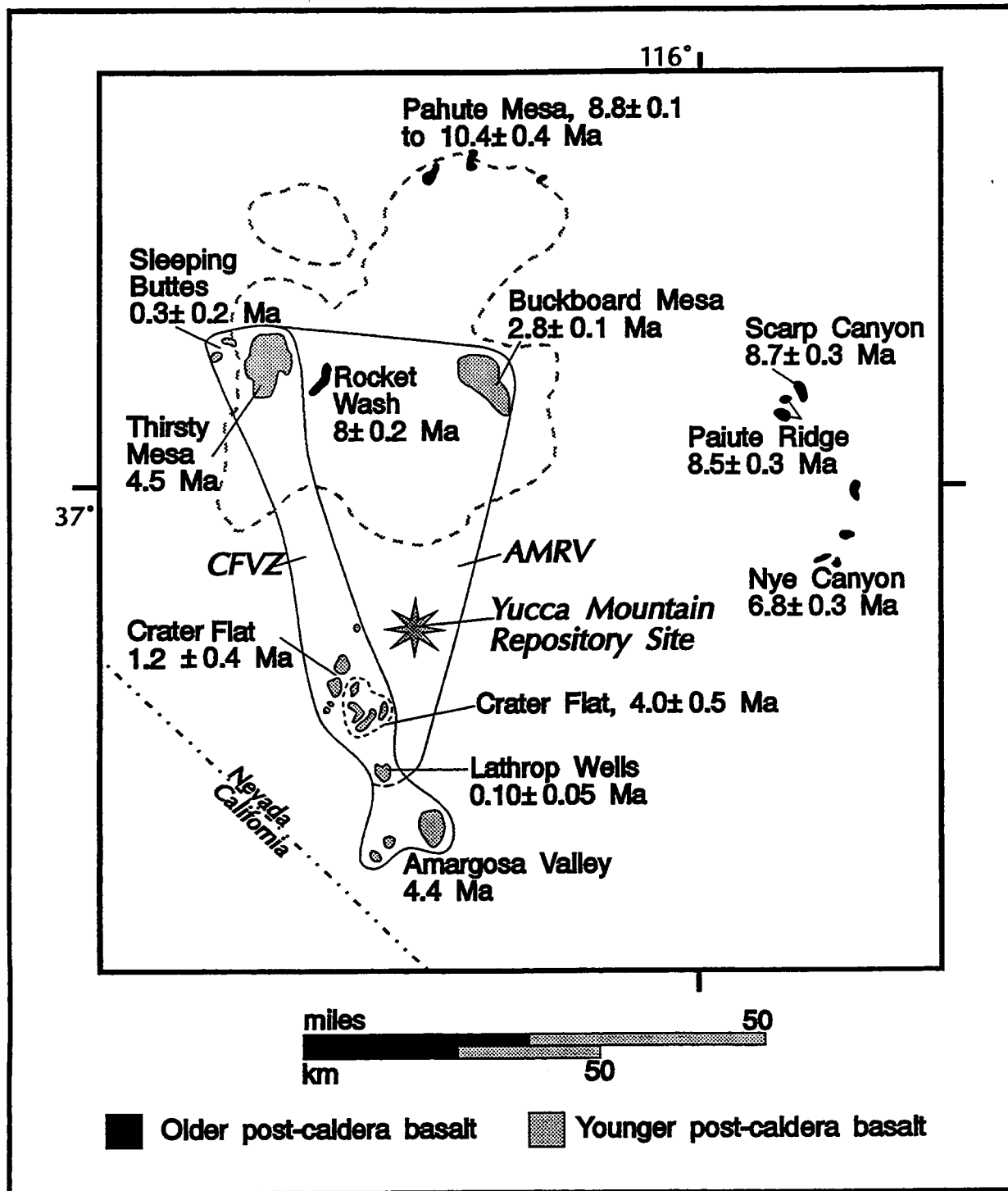


Figure 2-1. Locations and average ages of Neogene and Quaternary post-caldera basaltic volcanoes in the Yucca Mountain area, modified from Crowe (1990). Miocene calderas of the Timber Mountain complex are outlined by dashed lines. The area of most recent volcanism (AMRV) of Smith et al. (1990) and Crater Flat volcanic zone (CFVZ) of Crowe and Perry (1989) are outlined.

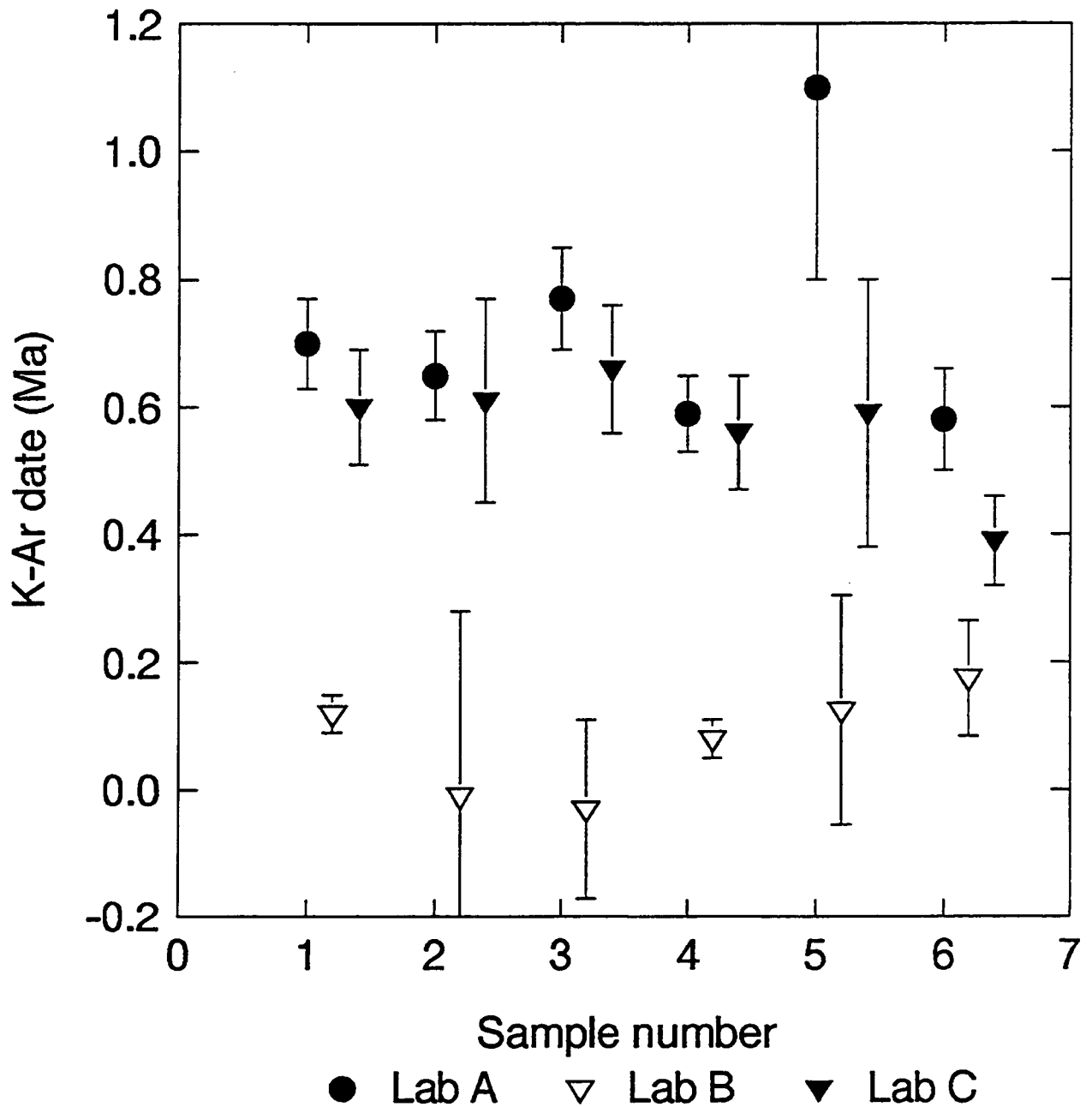


Figure 2-2. K-Ar dates for Lathrop Wells from Sinnock and Easterling (1983). Six sample splits from Lathrop Wells were sent to three geochronology laboratories for dating. Error bars represent 1σ analytical error. Note that intralaboratory and interlaboratory errors often exceed reported analytical error, strongly indicating that the accuracy of these dates is questionable. Using a variety of techniques, the best estimate for the age of Lathrop Wells is likely 0.10±0.05 Ma (Connor and Hill, 1993).

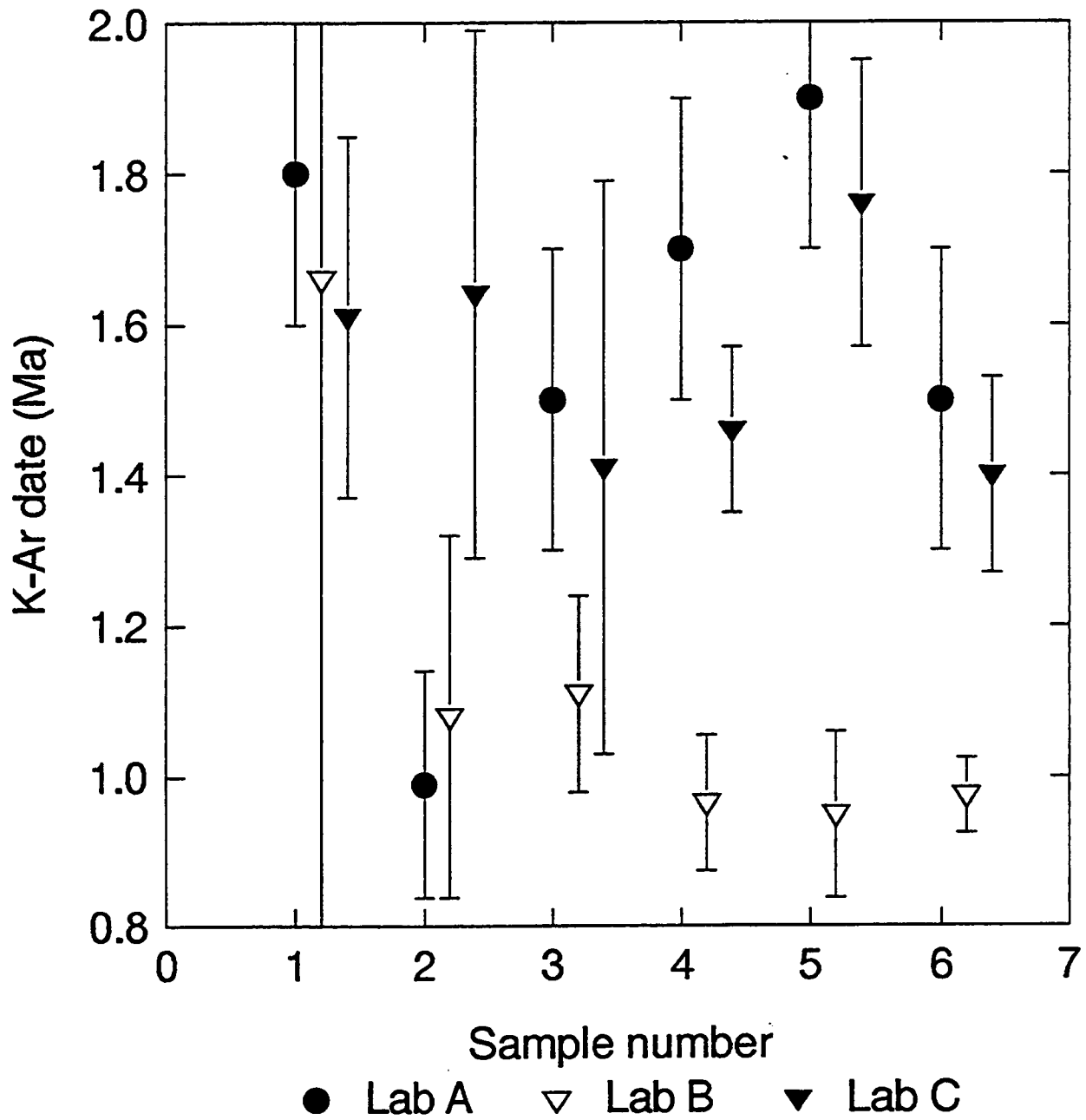


Figure 2-3. K-Ar dates for Red Cone from Sinnock and Easterling (1983). Six sample splits from Red Cone were sent to three geochronology laboratories for dating. Error bars represent 1σ analytical error. Note that intralaboratory and interlaboratory errors often exceed reported analytical error, strongly indicating that the accuracy of these dates is questionable. Using dates from several additional studies (Table 2-1), the best estimate for the age of Red Cone is likely  $1.2 \pm 0.4$  Ma.

### 2.2.4.2 Neogene Basaltic Volcanoes

Two dates are published for Buckboard Mesa (Figure 2-1), which average  $2.8 \pm 0.1$  Ma (Table 2-2). The Buckboard Mesa vent and associated lava flows are moderately dissected, and have a normal

**Table 2-2. K/Ar dates for Neogene basaltic rocks in the YMR. Error is the percentage error between Age and  $\pm 1\sigma$ . Simple Avg is the average and standard deviation of the reported ages. Wgt Mean is the weighted mean of the dates [Eq. (1-3)] Average Date reports propagated uncertainties [Eqs. (1-1 and 1-2)].**

Volcano	Sample	Age (Ma)	$\pm 1\sigma$ (Ma)	% <sup>40</sup> Ar*	%Error	Reference
Buckboard Mesa		2.82	0.04		1	Crowe et al., 1982
Buckboard Mesa		2.79	0.10		4	Crowe et al., 1982
SE Crater Flat 13	A	4.80	0.50	9.2	10	Sinnock & Easterling, 1983
SE Crater Flat 13	B	3.64	0.04	44.6	1	Sinnock & Easterling, 1983
SE Crater Flat 13	C	3.86	0.11	49.3	3	Sinnock & Easterling, 1983
SE Crater Flat 14	A	4.30	0.50	11.4	12	Sinnock & Easterling, 1983
SE Crater Flat 14	B	3.82	0.11	48.0	3	Sinnock & Easterling, 1983
SE Crater Flat 14	C	3.90	0.92	5.2	24	Sinnock & Easterling, 1983
SE Crater Flat 15	A	3.60	0.40	7.0	11	Sinnock & Easterling, 1983
SE Crater Flat 15	B	3.78	0.06	45.4	2	Sinnock & Easterling, 1983
SE Crater Flat 15	C	3.99	0.12	43.1	3	Sinnock & Easterling, 1983
SE Crater Flat 16	A	4.70	0.50	8.1	11	Sinnock & Easterling, 1983
SE Crater Flat 16	B	3.75	0.04	54.5	1	Sinnock & Easterling, 1983
SE Crater Flat 16	C	3.77	0.32	22.9	8	Sinnock & Easterling, 1983
SE Crater Flat 17	A	4.30	0.30	16.7	7	Sinnock & Easterling, 1983
SE Crater Flat 17	B	3.70	0.22	14.4	6	Sinnock & Easterling, 1983
SE Crater Flat 17	C	4.14	0.13	42.3	3	Sinnock & Easterling, 1983
SE Crater Flat 18	A	3.90	0.50	10.5	13	Sinnock & Easterling, 1983
SE Crater Flat 18	B	3.73	0.06	39.7	2	Sinnock & Easterling, 1983
SE Crater Flat 18	C	3.66	0.14	30.1	4	Sinnock & Easterling, 1983
Simple Ave $3.96 \pm 0.34$		Wgt Mean $3.75 \pm 0.02$			Average Date $3.96 \pm 0.65$	
SE Crater Flat 19	A	4.30	0.03	22.3	1	Sinnock & Easterling, 1983
SE Crater Flat 19	B	3.79	0.08	25.7	2	Sinnock & Easterling, 1983

Volcano	Sample	Age (Ma)	$\pm 1\sigma$ (Ma)	$\%^{40}\text{Ar}^*$	%Error	Reference
SE Crater Flat 19	C	3.99	0.10	66.5	3	Sinnock & Easterling, 1983
SE Crater Flat 20	A	4.20	0.30	24.5	7	Sinnock & Easterling, 1983
SE Crater Flat 20	B	3.80	0.05	47.7	1	Sinnock & Easterling, 1983
SE Crater Flat 20	C	3.99	0.12	43.6	3	Sinnock & Easterling, 1983
SE Crater Flat 21	A	4.20	0.30	33.4	7	Sinnock & Easterling, 1983
SE Crater Flat 21	B	3.56	0.04	58.5	1	Sinnock & Easterling, 1983
SE Crater Flat 21	C	4.14	0.11	67.2	3	Sinnock & Easterling, 1983
SE Crater Flat 22	A	4.20	0.03	24.5	1	Sinnock & Easterling, 1983
SE Crater Flat 22	B	3.64	0.10	31.7	3	Sinnock & Easterling, 1983
SE Crater Flat 22	C	4.02	0.12	47.1	3	Sinnock & Easterling, 1983
SE Crater Flat 23	A	4.30	0.30	18.2	7	Sinnock & Easterling, 1983
SE Crater Flat 23	B	3.68	0.06	35.6	2	Sinnock & Easterling, 1983
SE Crater Flat 23	C	3.76	0.11	52.1	3	Sinnock & Easterling, 1983
SE Crater Flat 24	A	4.10	0.40	24.4	10	Sinnock & Easterling, 1983
SE Crater Flat 24	B	3.71	0.05	39.9	1	Sinnock & Easterling, 1983
SE Crater Flat 24	C	4.10	0.15	34.5	4	Sinnock & Easterling, 1983
Simple Avg 3.97 $\pm$ 0.23		Wgt Mean 3.98 $\pm$ 0.02			Average Date 3.97 $\pm$ 0.39	
SE Crater Flat	72-24-8	3.84	0.20		5	Vaniman & Crowe, 1981
SE Crater Flat	79-26-1	3.64	0.10		3	Vaniman & Crowe, 1981
Pahute Mesa Ctrl		8.8	0.1		1	Crowe et al., 1983
Pahute Mesa W		10.4	0.4		4	Crowe et al., 1983
Pahute Mesa W		9.1	0.7		8	Crowe et al., 1983
Scarp Canyon		8.7	0.3		3	Crowe et al., 1983
Paiute Ridge		8.5	0.3		4	Crowe et al., 1983
Rocket Wash		8.0	0.2		3	Crowe et al., 1983
Nye Canyon		6.8	0.2		3	Crowe et al., 1983
Nye Canyon		7.2	0.2		3	Crowe et al., 1983
Nye Canyon		6.3	0.2		3	Crowe et al., 1983

paleomagnetic orientation consistent with an age of between 2.48 and 2.92 Ma (Lutton, 1969). Other Pliocene mafic volcanoes in the YMR (Figure 2-1) lack published dates by any technique, with the exception of flow and vent exposures in southeast Crater Flat.

Highly eroded vents and flows in southeast Crater Flat have been extensively dated by the K/Ar technique (Table 2-2). Two separate units were dated at three different labs by Sinnock and Easterling (1983). These analyses have low analytical errors typical of Pliocene basalt, although some problems in accuracy are apparent (Figure 2-4). The averages and standard deviations of the two sample sets ( $3.96 \pm 0.34$  and  $3.97 \pm 0.23$  Ma) closely reflect the average dates calculated [Eqs. (1-1 and 1-2)] with propagated analytical error ( $3.96 \pm 0.65$  and  $3.97 \pm 0.39$  Ma, respectively). The ages for these two units are thus indistinguishable and consistent with  $3.84 \pm 0.20$  and  $3.64 \pm 0.10$  dates of Vaniman and Crowe (1981). An age of  $4.0 \pm 0.5$  Ma [Eqs. (1-1 and 1-2)] gives equal weight to all reported dates and represents the best age estimate for the southeastern Crater Flat volcanoes.

Miocene basaltic volcanic centers that erupted after the formation of large silicic calderas (Crowe et al., 1983) have few published dates (Table 2-2). Analytical errors are generally low, and multiple dates for each distinct center are within reported error. Where stratigraphic relationships are present, these dates are consistent with relative position in the stratigraphic section (Crowe et al., 1983, 1986).

## 2.3 ARGON/ARGON ( $^{40}\text{Ar}/^{39}\text{Ar}$ ) METHOD

The  $^{40}\text{Ar}/^{39}\text{Ar}$  method is essentially a modification of the K/Ar dating technique. The primary difference is that the  $^{40}\text{Ar}/^{39}\text{Ar}$  method does not require measuring the K content of a sample aliquot, but instead directly measures  $^{39}\text{Ar}$  produced through neutron bombardment of  $^{39}\text{K}$ . The  $^{40}\text{Ar}/^{39}\text{Ar}$  method generally results in more precise dating of smaller samples than is possible with the K/Ar method, because isotopic ratios rather than elemental abundances are measured. However, analyses in the  $^{40}\text{Ar}/^{39}\text{Ar}$  method are considerably more complex than for the K/Ar method. In general, variable amounts of Ar are released from a sample that is heated in precise temperature increments. The isotopic composition of each increment is measured, and a date is calculated from the most stable increments, which are generally between 20 and 80 percent of total gas release.

The  $^{40}\text{Ar}/^{39}\text{Ar}$  technique is commonly applied to samples that range in age from several billion years to less than a million years. Dating fresh, 1-Ma volcanic rocks is generally considered routine for this technique, although lower age limits are strongly dependent on the laboratory technique used. Individual K-rich crystals also can be dated by the  $^{40}\text{Ar}/^{39}\text{Ar}$  method, and can yield high-precision dates of  $< 0.5$  Ma (e.g., Bogaard et al., 1987; Féraud et al., 1990).

Assumptions in the  $^{40}\text{Ar}/^{39}\text{Ar}$  method are identical to those used for the K/Ar method.  $^{40}\text{Ar}$  is produced by radioactive decay of  $^{40}\text{K}$  and retained in minerals at temperatures  $< 500\text{--}200$  °C. The mineral is assumed to remain closed to K and Ar, and thus, the amount of radiogenic  $^{40}\text{Ar}$  is proportional to the age and amount of  $^{40}\text{K}$  in the sample.

### 2.3.1 Analytical Methods

For general  $^{40}\text{Ar}/^{39}\text{Ar}$  analysis, samples are crushed to about 0.25 mm (60 mesh) and approximately 0.5 g are sealed in small quartz vials. The samples are irradiated with thermal neutrons

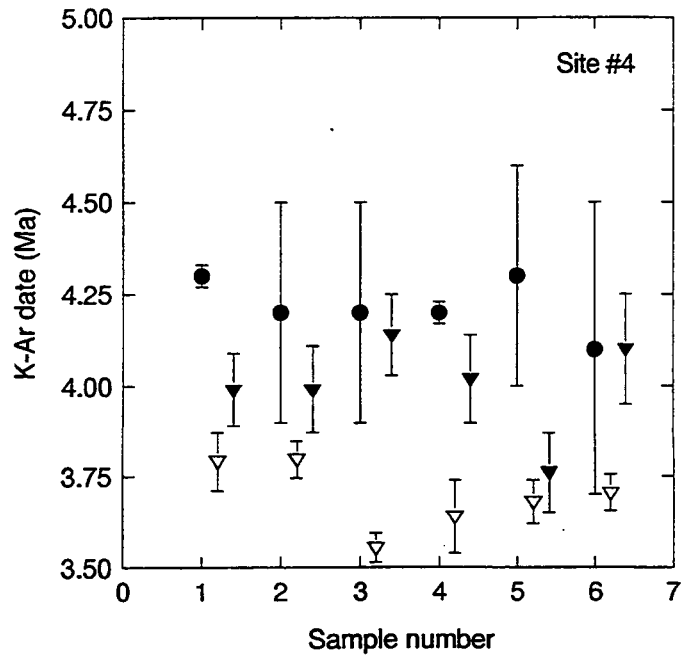
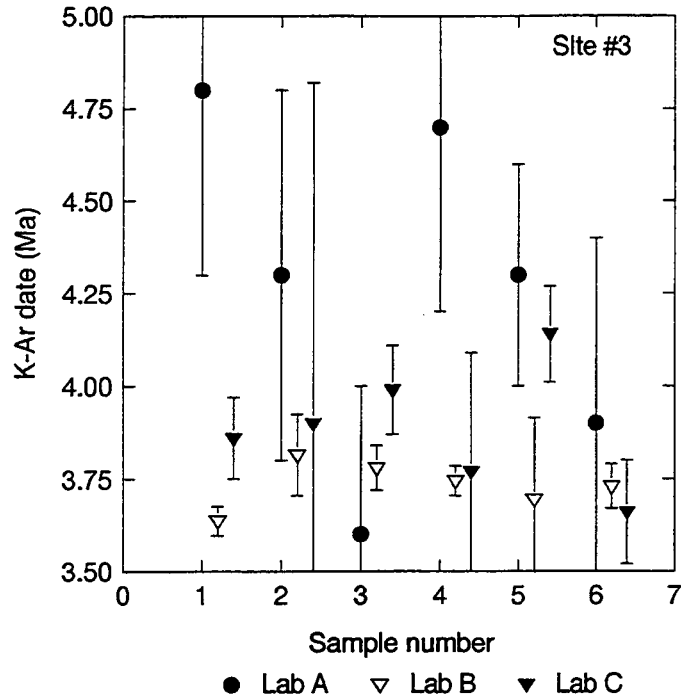


**Figure 2-4. K-Ar dates for two Neogene Crater Flat volcanoes from Sinnock and Easterling (1983). Six sample splits from sites 3 and 4 were sent to three geochronology laboratories for dating. Error bars represent  $1\sigma$  analytical error. Note that intralaboratory and interlaboratory errors often exceed reported analytical error, strongly indicating that the accuracy of these dates is questionable. Data from this and other studies indicate that the age of these volcanoes is probably  $4.0 \pm 0.5$  Ma.**

in a research reactor for several hours, and short-lived isotopes are allowed to decay for several weeks. The sample is incrementally heated under high vacuum, and Ar isotopic compositions are measured with a mass spectrometer. Single-mineral grains also can be fused using a laser microprobe attached to a mass spectrometer (e.g., Megrue, 1971). An older analytical technique that fused the total sample (e.g., Dalrymple and Lanphere, 1971) is rarely used, as it has roughly the same precision and accuracy as the conventional K/Ar technique (McDougall and Harrison, 1988).

The  $^{40}\text{Ar}/^{39}\text{Ar}$  method is based on the production of  $^{39}\text{Ar}_k$ , which has a half-life of 269 years, through neutron irradiation of  $^{39}\text{K}$ . The amount of  $^{39}\text{Ar}$  produced depends on the K content of the sample, duration of irradiation, neutron flux, and the neutron-capture cross section of  $^{39}\text{K}$  (McDougall and Harrison, 1988). In addition, sample irradiation in a nuclear reactor adds several complexities to the  $^{40}\text{Ar}/^{39}\text{Ar}$  method that must be corrected before an accurate date is produced.

- The primary source of  $^{39}\text{Ar}$  (i.e.,  $^{39}\text{Ar}_k$ ) produced through neutron bombardment is a  $^{39}\text{K}(n,p)$  reaction. However,  $^{39}\text{Ar}$  also can be produced by  $^{42}\text{Ca}(n,\alpha)$  reactions. Similarly,  $^{36}\text{Ar}$  is provided by the  $^{40}\text{Ca}(n,n,\alpha)$  reaction (Brereton, 1970). Fortunately,  $^{37}\text{Ar}$  is also produced from calcium reactions and can be used to calculate the amount of  $^{39}\text{Ar}$  and  $^{36}\text{Ar}$  produced by calcium reactions (e.g., Dalrymple et al., 1981).
- The production of  $^{39}\text{Ar}$  is extremely sensitive to the neutron flux gradients within the reactor. These inhomogeneities are minimized by irradiating the samples for several hours at the same height on a rotating sample rack. More detailed experiments utilize flux monitors such as nickel wire to account for variations in neutron fluence (Dalrymple et al., 1981).
- $^{39}\text{Ar}$  can be lost or redistributed during irradiation of the sample due to recoil effects associated with neutron bombardment (Turner and Cadogan, 1974; Harrison, 1983). Recoil redistribution of  $^{39}\text{Ar}$  occurs over distances of about  $0.1\ \mu\text{m}$  in silicate minerals, and thus can significantly affect the dates produced from very fine-grained ( $<4\ \mu\text{m}$ ) samples (Alexander et al., 1977; Foland et al., 1993). The loss of  $^{39}\text{Ar}$  through recoil effects will result in an anomalously old age for the sample (e.g., Villa et al., 1983).
- It is possible that differential neutron absorption could occur within a dense sample due to shielding of the sample interior by the outer parts of the sample. Although Dalrymple et al. (1981) were able to detect self-shielding in a solid core of diabase, they concluded that self-shielding effects were negligible for granular samples (i.e., about  $0.25\ \text{mm}$ ).

In order to compensate for uncertainties in irradiation parameters, a mineral standard of known age is irradiated with the samples. Isotopic analysis of the standard yields

$$J = \frac{e^{\lambda t} - 1}{^{40}\text{Ar}^*/^{39}\text{Ar}_k} \quad (2-3)$$

The total decay constant for  $^{40}\text{K}$  ( $\lambda$ ) and the age of the standard ( $t$ ) are known, and the value for  $J$  is used to derive the age of the sample.

$$t = \frac{1}{\lambda} \ln \left( 1 + J \frac{{}^{40}\text{Ar}^*}{{}^{39}\text{Ar}_K} \right) \quad (2-4)$$

One of the main advantages of the  ${}^{40}\text{Ar}/{}^{39}\text{Ar}$  method is that the sample can be incrementally heated at temperatures well below fusion (400–1100 °C). Although the temperature may be well above the blocking temperature of the abundant minerals in the sample, only partial Ar degassing occurs due to the relatively low diffusivity of Ar (McDougall and Harrison, 1988). If the sample is thought to have a uniform distribution of  ${}^{40}\text{Ar}^*$  and  ${}^{39}\text{Ar}$ , then a date can be calculated for each heating increment. A sample that has remained completely closed with respect to K and Ar should have the same calculated date for each heating increment (Merrihue and Turner, 1966). However, most basaltic rocks generally show some apparent Ar loss from low-temperature sites, which results in anomalously young dates for the initial release fraction (e.g., Fleck et al., 1977). Conversely, samples that have lost K due to low-temperature alteration will show anomalously old dates for the first increments of heating (Harrison, 1983). In addition, the presence of excess  ${}^{40}\text{Ar}^*$  will often result in an anomalously old date for the lowest and highest release fractions (e.g., Lanphere and Dalrymple, 1976). Thus, to calculate the date of the sample, the increments that have anomalous dates are discarded and only the increments that show relatively similar dates are used to calculate the *plateau date*. An example of an incremental heating  ${}^{40}\text{Ar}/{}^{39}\text{Ar}$  date for a weakly altered tholeiite is given in Figure 2-5A.

The incremental heating technique also can be used to calculate an  ${}^{40}\text{Ar}/{}^{39}\text{Ar}$  date that requires no assumptions about the initial  ${}^{40}\text{Ar}/{}^{36}\text{Ar}$ . By measuring the total  ${}^{40}\text{Ar}/{}^{36}\text{Ar}$  and  ${}^{39}\text{Ar}/{}^{36}\text{Ar}$  in each increment and plotting these ratios on an isochron diagram (Figure 2-5B), the slope of the resulting line is the date of the sample and the ordinate intercept is the  ${}^{40}\text{Ar}/{}^{36}\text{Ar}$  for nonradiogenic Ar (Dalrymple and Lanphere, 1974). One potential limitation to the isochron technique is that  ${}^{36}\text{Ar}$  is the least abundant Ar isotope in the sample. Errors associated with  ${}^{36}\text{Ar}$  are thus associated with both axes on the isochron plot and could lead to apparent linear correlations (McDougall and Harrison, 1988). To avoid this problem, inverse isochron plots (Turner, 1971) are used, in which  ${}^{39}\text{Ar}_K/{}^{40}\text{Ar}^*$  is the abscissa,  ${}^{36}\text{Ar}/{}^{40}\text{Ar}$  is the ordinate, and the abscissa intercept represents the  ${}^{40}\text{Ar}^*/{}^{39}\text{Ar}_K$  used in Eq. (2-4) to calculate the age of the sample (Figure 2-5C). A common practice is to calculate the plateau date and the isochron dates for each sample. These dates all should be within analytical error if the date is to represent the age of the sample.

### 2.3.2 Sources of Error

The  ${}^{40}\text{Ar}/{}^{39}\text{Ar}$  dating method has sources of error that are very similar to the K/Ar technique. With young mafic rocks, uncertainties in determining low amounts of  ${}^{40}\text{Ar}^*$  will produce the largest errors in the reported date. For example, if the amount of  ${}^{40}\text{Ar}^*$  is <5 percent, small errors in the calibration of the mass spectrometer can lead to large errors in the measured  ${}^{40}\text{Ar}^*$  and thus large uncertainties in the date (McDougall and Harrison, 1988). In addition, determining the small amounts of  ${}^{36}\text{Ar}$  in the sample also is a significant source of error in young basalt dates. With these limitations,  ${}^{40}\text{Ar}/{}^{39}\text{Ar}$  dates for young basaltic rocks generally have errors of around 10 percent, although smaller uncertainties are possible by utilizing very clean Ar extraction lines or an extremely stable mass spectrometer (e.g., Gillot and Cornette, 1986). The uncertainty associated with a date is generally calculated from Dalrymple and Lanphere (1971).

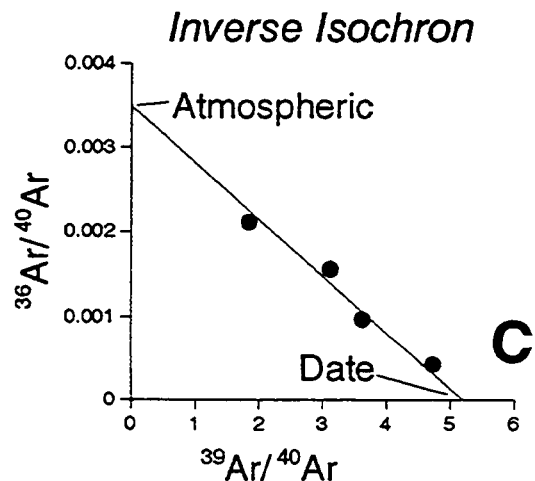
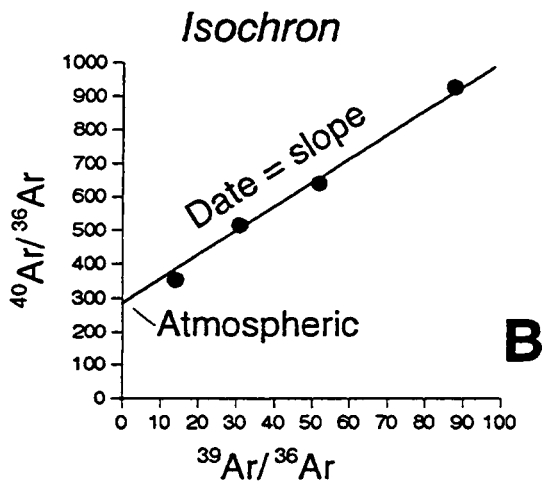
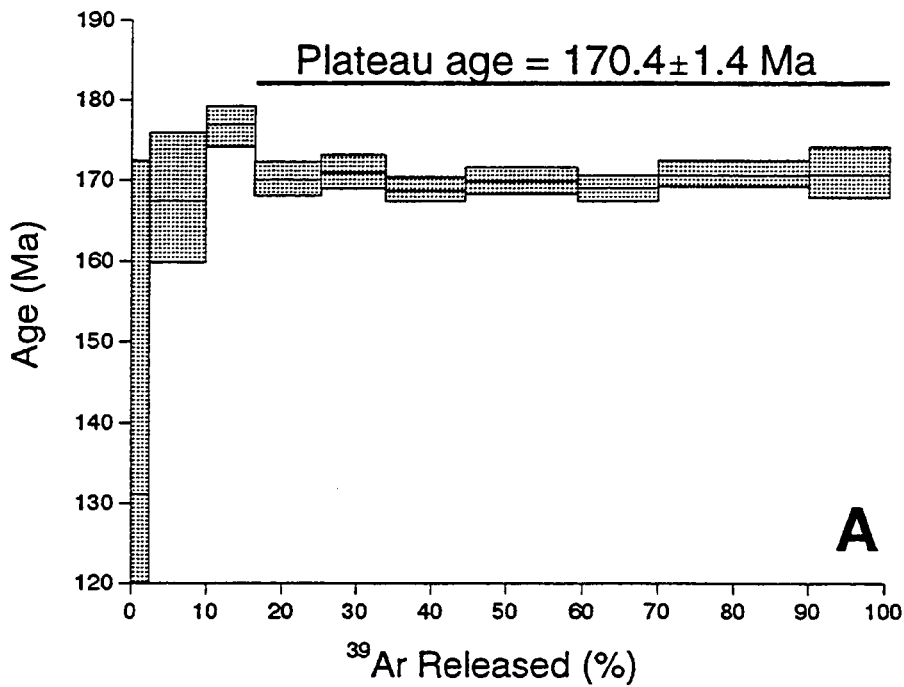


Figure 2-5. (A) Example of a  $^{40}\text{Ar}/^{39}\text{Ar}$  incremental heating date, modified from Fleck et al. (1977). Size of shaded boxes represent  $1\sigma$  errors for each incremental date. Note that the approximately 3-percent release date is younger and has significantly larger errors than the plateau dates. Plateau position is determined empirically (e.g., Harrison, 1983). (B) Example of an isochron plot, modified from McDougall and Harrison (1988). Ar isotopic ratios are measured for each increment of heating and plotted. The slope of the line represents the date of the sample. (C) Example of an inverse isochron plot, modified from McDougall and Harrison (1988). Ar isotopic ratios are measured for each increment of heating and plotted. The intercept of the line on the abscissa is used to calculate the date of the sample.

$$\sigma_t^2 = \frac{J^2 \sigma_F^2 + F^2 \sigma_J^2}{\lambda^2 (1 + FJ)^2} \quad (2-5)$$

where  $F = {}^{40}\text{Ar}^*/{}^{39}\text{Ar}_K$   
 $J =$  irradiation parameter (Eq. 2-3)  
 $\sigma_x =$  uncertainty in parameter  $x$

Several additional sources of error that are present in the K/Ar technique do not occur in the  ${}^{40}\text{Ar}/{}^{39}\text{Ar}$  method. Uncertainties in the sample weight are not important for the  ${}^{40}\text{Ar}/{}^{39}\text{Ar}$  method, because only isotopic ratios are measured. Sample heterogeneity is rarely a concern, because all the analyses are conducted on the same small sample aliquot. Although the  ${}^{40}\text{Ar}/{}^{39}\text{Ar}$  technique is more analytically complex than the K/Ar technique, the sources of error are smaller and more easy to quantify for  ${}^{40}\text{Ar}/{}^{39}\text{Ar}$  dates.

The incremental heating technique is extremely useful in determining if the sample was open with respect to K or Ar. Dates can be calculated using only the data from increments that show no significant Ar or K mobility. Although the determination of which increments constitute the plateau age is largely subjective (Albarède, 1978; Harrison, 1983), most  ${}^{40}\text{Ar}/{}^{39}\text{Ar}$  age spectra have relatively clear plateaus and anomalous age ranges (e.g., Dalrymple and Lanphere, 1974). The incremental dates are thus more accurate than conventional K/Ar dates for complex geologic systems, because the analyzed isotopes are not totally released at one fixed temperature.

### 2.3.3 Material Dated

The same materials used for K/Ar dates are used in the  ${}^{40}\text{Ar}/{}^{39}\text{Ar}$  technique. An additional consideration is that fine-grained (i.e., <0.01–0.03 mm) samples will yield anomalously young dates due to recoil effects during irradiation. Fine silts and clays are thus inappropriate samples to date by the  ${}^{40}\text{Ar}/{}^{39}\text{Ar}$  technique.

The ability to analyze extremely small samples through laser-fusion is of particular interest in Quaternary studies. For example, apparently accurate dates have been produced for single sanidine crystals in the Massif Central, France (Lo Bello et al., 1987; Féraud et al., 1990) and the East Eifel Volcanic Field, Germany (Bogaard et al., 1987).

Granitic xenoliths in Quaternary basaltic lavas can at times yield extremely precise eruption ages through incremental  ${}^{40}\text{Ar}/{}^{39}\text{Ar}$  analysis (Gillespie et al., 1982). These xenoliths are only partially degassed upon entrainment and eruption. The lower temperature release fractions should thus represent the time since degassing occurred (i.e., eruption), but the higher temperature fractions reflect the initial age of the xenolith. For a Cretaceous granitic xenolith, an accurate eruption age can usually be determined for the 25–50-percent  ${}^{39}\text{Ar}$ -release intervals (Gillespie et al., 1982). Using this technique, Gillespie et al. (1983) were able to derive a  $1.18 \pm 0.05$  Ma ( $2\sigma$ ) age for a basaltic lava from the Big Pine Field, California. Another Big Pine basalt in Sawmill Canyon was dated by Gillespie et al. (1984) at  $119 \pm 7$  ka ( $2\sigma$ ), further demonstrating the utility of this technique.

### 2.3.4 Application to the Yucca Mountain Region

For post-caldera basalts in the YMR, the  $^{40}\text{Ar}/^{39}\text{Ar}$  method has been used only to determine dates for the Lathrop Wells eruptive center (Figure 2-1). These dates were published in Turrin and Champion (1991) and Turrin et al. (1991), and are presented in Table 2-3. Considerable controversy surrounds these data (Wells et al., 1992; Turrin et al., 1992; Crowe et al., 1992b), primarily on the methods used to calculate average ages and the significance of reported analytical errors.

Although the  $^{40}\text{Ar}/^{39}\text{Ar}$  technique is at times capable of producing high-precision dates for relatively young basaltic rocks, the dates for Lathrop Wells reflect the difficulties inherent in the analysis of low-potassium  $\approx 100$ -ka basalt (Turrin and Champion, 1991; Turrin et al., 1991). These basalts generally contain  $< 2$ -percent  $^{40}\text{Ar}^*$  and consequently have large analytical errors (Figure 2-6). The errors do not appear normally distributed about a mean age (Figures 2-6 and 2-7), although the uncertainties in the reported dates are very large. As discussed previously, the application of a weighted mean to a data set is only appropriate when data errors are normally distributed about the mean (e.g., Taylor, 1990). Although a probability plot of the dates may show a roughly normal distribution (Figure 2-7), the large errors associated with these data prevent any rigorous statistical determination of the true shape of this distribution. Thus, a weighted mean may not accurately reflect the large analytical uncertainties reported for these dates (Wells et al., 1992) and will be inherently biased towards older dates (Turrin and Champion, 1991; Turrin et al., 1991). Propagation of reported analytical errors through average and standard deviation calculations using Eqs. (1-1) and (1-2) results in average dates with large uncertainties, which reflect the poor precision of these data (Table 2-3). Using these  $^{40}\text{Ar}/^{39}\text{Ar}$  dates, the most accurate age of the Lathrop Wells eruptive center is  $0.15 \pm 0.30$  Ma.

Several other objections to the Turrin and Champion (1991) dates focus on the possibility of inherited  $^{40}\text{Ar}^*$  (Poths and Crowe, 1992) and recoil effects (Wells et al., 1992). Poths and Crowe (1992) detected  $^{40}\text{Ar}/^{36}\text{Ar}$  ratios of  $371 \pm 8$  and  $328 \pm 7$  in crushed olivine separates from Lathrop Wells, which are well above the standard atmospheric ratio of 295 (Steiger and Jäger, 1977). Although some of the excess  $^{40}\text{Ar}$  may be due to trapped melt inclusions or adhering basalt matrix, it is possible that excess  $^{40}\text{Ar}$  is present in some Lathrop Wells units (Poths and Crowe, 1992). Isochron and reverse isochron plots for some Lathrop Wells dates (Turrin et al., 1991) show significant scatter and are at times controlled by outlying points (Wells et al., 1992), but do not support the conclusion of Poths and Crowe (1992) that  $^{40}\text{Ar}/^{36}\text{Ar}$  was greater than 300. Recoil effects (Wells et al., 1992) were shown by Turrin et al. (1992) to be insignificant for the sizes of the potassium sites ( $> 10$ - $20 \mu\text{m}$ ) in these samples.

## 2.4 URANIUM-SERIES METHODS

The uranium-series methods rely on radioactive disequilibrium between a parent and daughter isotope in the  $^{238}\text{U}$ ,  $^{232}\text{Th}$ , and  $^{235}\text{U}$  natural decay chains [Eq. (2-6)] to be established by a chemical or physical process. The half-lives of the isotopes in the partial decay chains are listed below the isotope.

Table 2-3.  $^{40}\text{Ar}/^{39}\text{Ar}$  dates for Lathrop Wells, Nevada, from Turrin and Champion (1991). *Unit* is the unit designation reported by Turrin and Champion, *Crowe* refers to the unit names of Crowe et al., 1992b, for Lathrop Wells. *Error* is the percentage error between *Age* and  $\pm 1\sigma$ . *Simple Avg.* is the average and standard deviation of the reported ages. *Wgt Mean* is the weighted mean of the dates [Eq. (1-3)] *Average date* reports propagated uncertainties [Eqs. (1-1 and 1-2)].

Unit	Sample	Crowe	Age (Ma)	$\pm 1\sigma$ (Ma)	$^{40}\text{Ar}^*$ (%)	Error (%)
LW Qs5	1569-2	Qs2b	0.007	0.374	0.0	5343
LW Qs5	1569-2	Qs2b	0.170	0.180	0.9	106
LW Qs5	1569-3	Qs2b	0.151	0.197	1.0	130
LW Qs5	1569-4	Qs2b	0.228	0.165	1.2	72
Simple Avg: $0.14 \pm 0.08$		Wgt Mean: $0.18 \pm 0.10$		Average date: $0.14 \pm 0.34$		
LW Q13	1561-1	Q13	0.392	0.215	1.6	55
LW Q13	1561-2	Q13	0.194	0.186	0.8	96
LW Q13	1561-4	Q13	0.261	0.232	1.1	89
LW Q13	1553-1	Q13	0.187	0.243	0.6	130
LW Q13	1553-2	Q13	0.110	0.327	0.2	297
LW Q13	1553-3	Q13	0.042	0.185	0.2	440
LW Q13	1553-4	Q13	0.145	0.088	1.3	61
LW Q13	1553-11	Q13	0.144	0.084	1.8	58
LW Q13	1553-13	Q13	0.126	0.082	1.1	65
LW Q13	1552-1	Q13	0.172	0.039	5.9	23
LW Q13	1552-2	Q13	0.099	0.196	1.2	198
LW Q13	1552-4	Q13	0.211	0.041	7.0	19
LW Q13	1557-1	Q13	0.177	0.212	2.7	120
LW Q13	1557-2	Q13	0.147	0.134	2.7	91
LW Q13	1557-3	Q13	0.294	0.379	1.9	129
LW Q13	1557-4	Q13	0.112	0.282	1.2	252
Simple Avg: $0.18 \pm 0.08$		Wgt Mean: $0.18 \pm 0.02$		Average date: $0.18 \pm 0.22$		

Table 2-3. Continued. *Contam* refers to samples recognized as contaminated by Turrin and Champion (1991).

Unit	Sample	Crowe	Age (Ma)	$\pm 1\sigma$ (Ma)	$^{40}\text{Ar}^*$ (%)	Error (%)
LW Q13	1554-1	Q14a	0.143	0.088	1.5	62
LW Q13	1554-2	Q14a	0.311	0.078	4.2	25
LW Q13	1554-3	Q14a	0.066	0.216	0.3	LW Q13 327
LW Q13	1554-4	Q14a	0.093	0.212	0.5	228
Simple Avg: $0.15 \pm 0.10$		Wgt Mean: $0.22 \pm 0.06$		Average date: $0.15 \pm 0.28$		
LW Q15	1555-10	Q15	0.112	0.090	0.6	80
LW Q15	1555-11	Q15	0.107	0.155	0.4	145
LW Q15	1555-12	Q15	0.235	0.521	0.4	222
LW Q15	1555-13	Q15	0.228	0.200	1.2	88
LW Q15	1555-1	Q15	0.168	0.318	0.6	189
LW Q15	1555-2	Q15	-0.020	0.263	-0.1	1315
LW Q15	1555-3	Q15	0.368	0.644	0.7	175
LW Q15	1555-4	Q15	0.164	0.089	0.9	54
LW Qs5	1557-10	Qs5	0.139	0.081	2.2	58
LW Qs5	1557-11	Qs5	0.182	0.125	1.4	69
LW Qs5	1557-12	Qs5	0.020	0.285	0.1	1425
LW Qs5	1557-13	Qs5	0.138	0.080	1.3	58
Simple Avg: $0.15 \pm 0.10$		Wgt Mean: $0.14 \pm 0.04$		Average date: $0.15 \pm 0.32$		
Contam Q13	1561-3	Q13	0.776	0.162	2.9	21
Contam Q13	1553-12	Q13	0.947	0.024	62.3	3
Contam Q13	1553-10	Q13	0.452	0.086	4.3	19
Contam Q13	1552-3	Q13	0.450	0.073	7.0	16

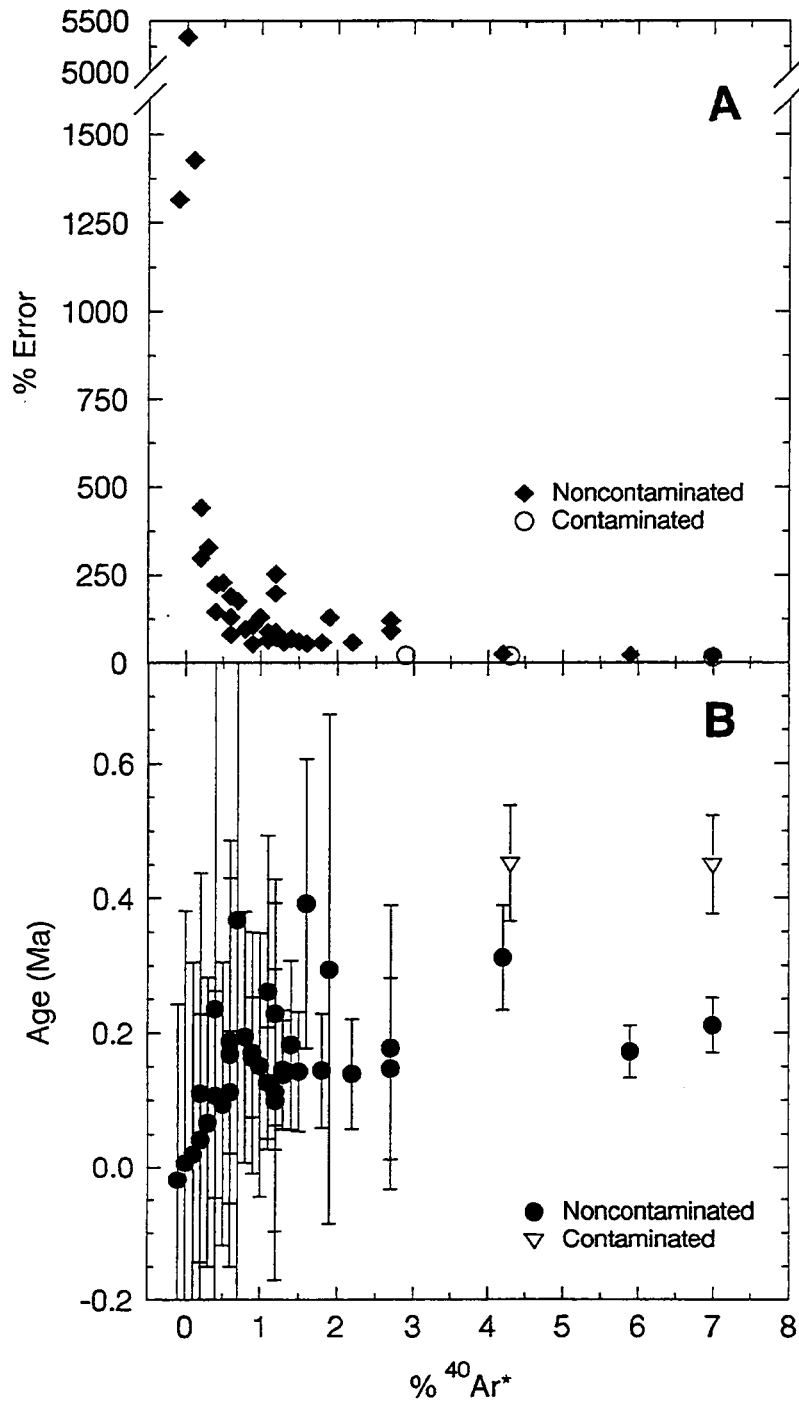


Figure 2-6.  $^{40}\text{Ar}/^{39}\text{Ar}$  data for Lathrop Wells from Turrin and Champion (1991). Contaminated samples contain xenoliths of Miocene ignimbrite (Turrin and Champion, 1991). (A) The amount of analytical error correlates with the amount of  $^{40}\text{Ar}^*$ ; note that samples with <2-percent  $^{40}\text{Ar}^*$  have large analytical errors. (B) The dates for these samples have large errors in both precision and accuracy, which reflects the difficulty in determining the age of relatively young basalt.

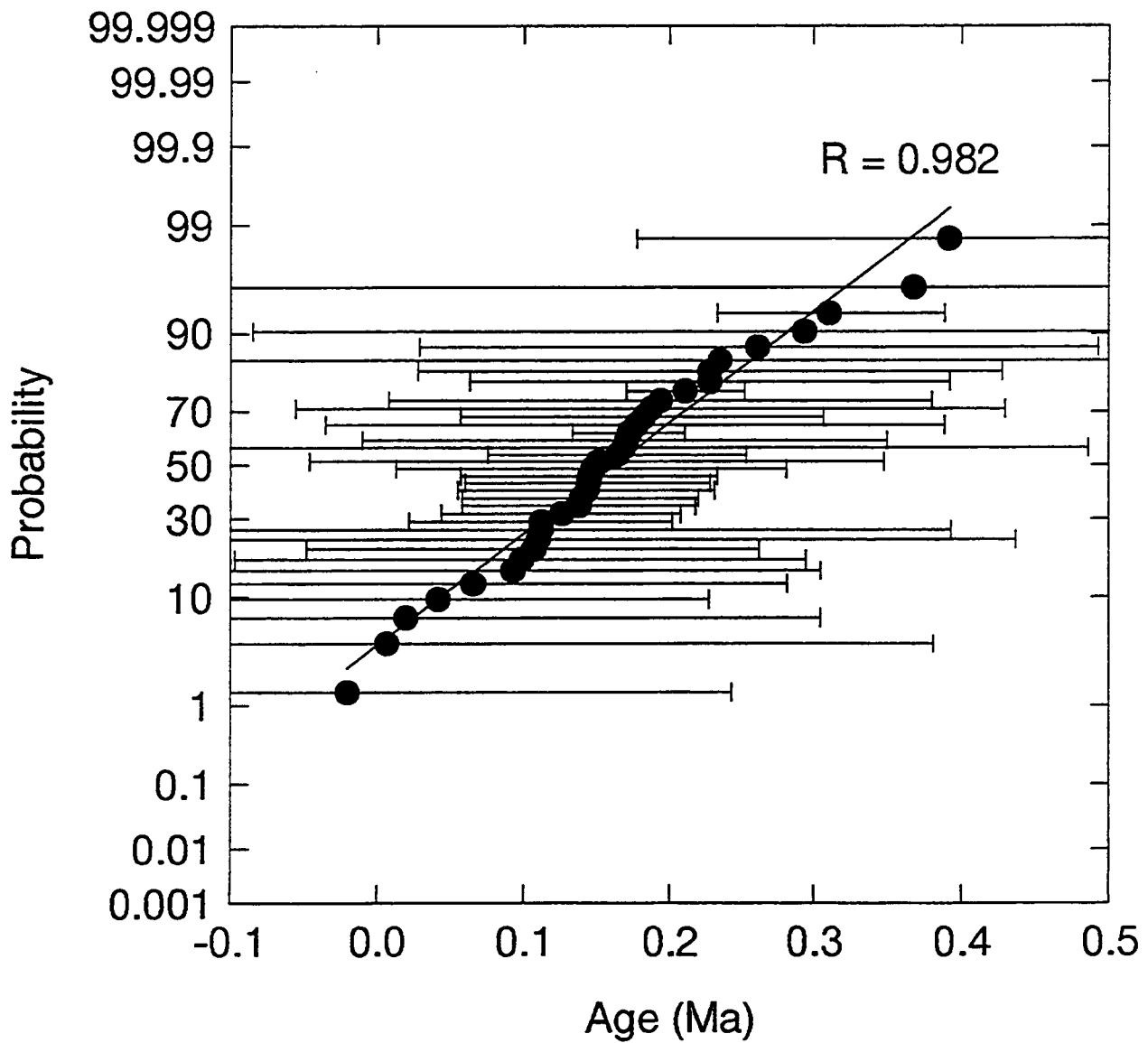
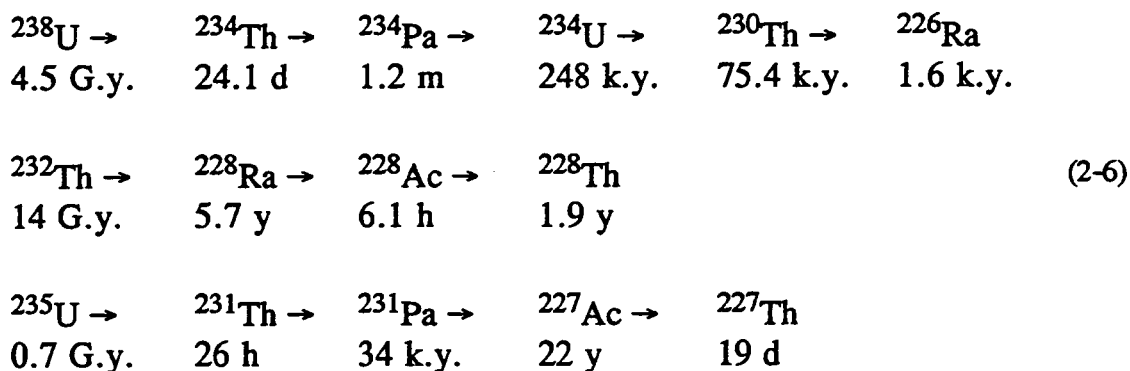


Figure 2-7. The large errors associated with  $^{40}\text{Ar}/^{39}\text{Ar}$  dates for Lathrop Wells by Turrin and Champion (1991) obscure the population distribution of the data; both log-normal and normal distributions can be fit to these data. Application of a weighted mean to this sample set is inappropriate and results in mean errors that are an order of magnitude smaller than reported analytical errors.



The fractionation between these isotopes during chemical or physical processes usually is caused by chemical differences between the elements. For instance, the large difference in solubility between U and Th in natural waters causes authigenic minerals such as carbonate to record the isotopic disequilibrium of the water. This difference in solubility forms the basis for U-series dating of Quaternary carbonate deposits. Similarly, magmatic processes such as melting or crystallization can produce radioactive disequilibrium between members of the uranium decay series. Once disequilibrium is established in a closed phase, then with time, the disequilibrium will decrease at a rate that is dependent upon the half-lives of both the parent and daughter isotopes (Geyh and Schleicher, 1990). To derive a date from the measured disequilibrium in a phase, it is necessary to know or derive the initial disequilibrium. From measured disequilibrium in several mineral phases from a volcanic rock, the initial isotopic disequilibrium can be determined, thus the time since eruption for a volcanic rock can be determined (Gill et al., 1992).

Depending on the parent-daughter isotopic pair measured, the time span that can be dated ranges from 0–30 years for the  $^{228}\text{Ra}/^{232}\text{Th}$  isotopic pair to 0–350 k.y. for the  $^{230}\text{Th}/^{238}\text{U}$  isotopic pair (Gill et al., 1992). The half-life of  $^{230}\text{Th}$  is 75.4 k.y., and thus, the practical limit for measuring disequilibrium between  $^{230}\text{Th}$  and  $^{238}\text{U}$  is about 350 k.y. Several assumptions are required to utilize  $^{230}\text{Th}/^{238}\text{U}$  disequilibrium for dating young volcanic rocks and  $^{230}\text{Th}/^{234}\text{U}$  disequilibrium for dating carbonate deposits. First, the U and Th isotopic systems should be closed to exchange; this includes exchange during residence within the magma chamber, during eruption, and after eruption (i.e., weathering of both carbonates and rock). Second, the residence time of minerals in the magma chamber after crystallization or in ascent to the surface must be short, relative to the radioactive half-lives of interest. For dating carbonates, this assumption translates into the requirement that precipitation of carbonate is fast relative to the half-lives of the isotopes used to date the deposit. To be able to generate a  $^{230}\text{Th}/^{238}\text{U}$  date for a young volcanic rock requires that measurable parent-daughter fractionation has occurred in the parent magma, as reflected by the mineral isotopic contents, and that pure mineral separates be obtained. The purity and characterization of mineral separates is essential to differentiate between minerals that may have different sources or ages.

The most common isotopic pair used to date young volcanic rocks is the  $^{230}\text{Th}/^{238}\text{U}$  pair (Gill et al., 1992). Equations similar to those below [Eq (2-7) and (2-8)] can be derived for other isotopic pairs (Gill et al., 1992); however, those equations will not be discussed here. Decay of the long-lived radionuclide  $^{238}\text{U}$  to the shorter-lived  $^{230}\text{Th}$  may be used to date uranium-thorium fractionation events in crystallizing magma chambers. In igneous systems the intermediate nuclides are either sufficiently short-lived to be neglected, or else are not fractionated from their parent (e.g.,  $^{234}\text{U}$  from  $^{238}\text{U}$ ). The magnitude of the original U-Th disequilibrium may be assessed by reference to the very long-lived pair  $^{238}\text{U}$  and  $^{232}\text{Th}$ . In the case of this pair, the activities of these radionuclides will not change appreciably

by decay in 350 k.y. and activity measurements may be normalized to  $^{232}\text{Th}$ . If activity ratios of different mineral phases are measured, an internal isochron for the system can be written

$$\left(\frac{^{230}\text{Th}}{^{232}\text{Th}}\right)_t = \left(\frac{^{230}\text{Th}}{^{232}\text{Th}}\right)_i e^{-t\lambda_{230}} + \left(\frac{^{238}\text{U}}{^{232}\text{Th}}\right)_i [1 - e^{-t\lambda_{230}}] \quad (2-7)$$

where  $\lambda_{230}$  is the decay constant of  $^{230}\text{Th}$ . The slope,  $m$ , on any isochron will yield the sample date from the relationship

$$m = 1 - e^{-t\lambda_{230}} \quad (2-8)$$

On the  $^{230}\text{Th}/^{232}\text{Th}$  against  $^{238}\text{U}/^{232}\text{Th}$  isochron diagram (Figure 2-8), a chemically homogeneous melt containing crystals ( $a, b, c$ ) with different uranium and thorium contents but identical  $^{230}\text{Th}/^{232}\text{Th}$  activity ratios will define a horizontal isochron at zero age (0 k.y.). At the time when the minerals and melt become separate systems, so that chemical diffusion no longer maintains isotopic homogeneity between them, the isochron will rotate with time about the point  $(^{230}\text{Th}/^{232}\text{Th})_i$  on the equiline. This point is the initial  $^{230}\text{Th}/^{232}\text{Th}$  activity ratio when the system closed (used in Eq 2-7). This time may or may not coincide with the eruption age. For example, it will pre-date the eruption time if the minerals were isolated at the outer margins of the magma reservoir, or if the minerals were compositionally zoned (Gill et al., 1992). When secular equilibrium is reached and  $^{230}\text{Th} = ^{238}\text{U}$ , then the isochron has a slope of 45 degrees. This line is commonly called the equiline. The  $^{230}\text{Th}$ - $^{238}\text{U}$  system can be used to date crystallization, irrespective of whether or not the melt itself was out of radioactive equilibrium at the time crystallization began, as long as crystallization was rapid (i.e., less than 1 k.y.) and the system remained closed to postcrystallization migration of radionuclides.

For dating carbonate deposits, the disequilibrium between  $^{230}\text{Th}$  and  $^{234}\text{U}$  is most commonly used. In most cases, due to their differing solubilities in water, most authigenic phases precipitating out of natural solutions have very low  $^{232}\text{Th}/^{238}\text{U}$  and  $^{230}\text{Th}/^{238}\text{U}$  ratios. The  $^{230}\text{Th}$  ingrowth method of dating [Eq. (2-9)], these mineral phases may be employed with confidence by assuming  $^{230}\text{Th}/^{234}\text{U} = 0$  at their time of formation ( $t=0$ ). This dating method is feasible, however, only for cases in which U-containing authigenic phases essentially free of  $^{232}\text{Th}$  are available for dating. If a sample contains no  $^{230}\text{Th}$  at the time of formation, then at any later time the  $^{230}\text{Th}/^{234}\text{U}$  ratio is given by the relationship:

$$\frac{^{230}\text{Th}}{^{234}\text{U}} = \left( \frac{1 - e^{-t\lambda_{230}}}{^{234}\text{U} / ^{238}\text{U}} \right) + \left( 1 - \left[ \frac{1}{^{234}\text{U} / ^{238}\text{U}} \right] \right) \frac{\lambda_{230}}{\lambda_{230} - \lambda_{234}} (1 - e^{-(\lambda_{230} - \lambda_{234})t}) \quad (2-9)$$

where  $\lambda_{234}$  is the decay constant of  $^{234}\text{U}$  and  $\lambda_{230}$  is the decay constant for  $^{230}\text{Th}$ . Figure 2-9 is an isochron plot showing a graphical solution of this equation. It illustrates the relationship between  $^{230}\text{Th}/^{234}\text{U}$  and  $^{234}\text{U}/^{238}\text{U}$  activity ratios for closed systems of varying initial  $^{234}\text{U}/^{238}\text{U}$  ratio. Given the corrected  $^{230}\text{Th}/^{234}\text{U}$  and  $^{234}\text{U}/^{238}\text{U}$  activity ratios for a sample (see description of correction procedures used for impure carbonates below), an age can be calculated by iteratively solving Eq. (2-9) or by plotting the results graphically on Figure 2-9. Isochrons are the near vertical lines, whose slopes decrease with increasing age (Figure 2-9). Thus for ages less than 50 k.y., the values of the  $^{234}\text{U}/^{238}\text{U}$  activity ratio have little influence on the age. Ages are determined graphically by interpolating between isochrons. The age error limits are determined by drawing an ellipse whose major and minor axes correspond to the  $\pm 1\sigma$  error bars for the two activity ratios. The upper and lower age limits are then given by the

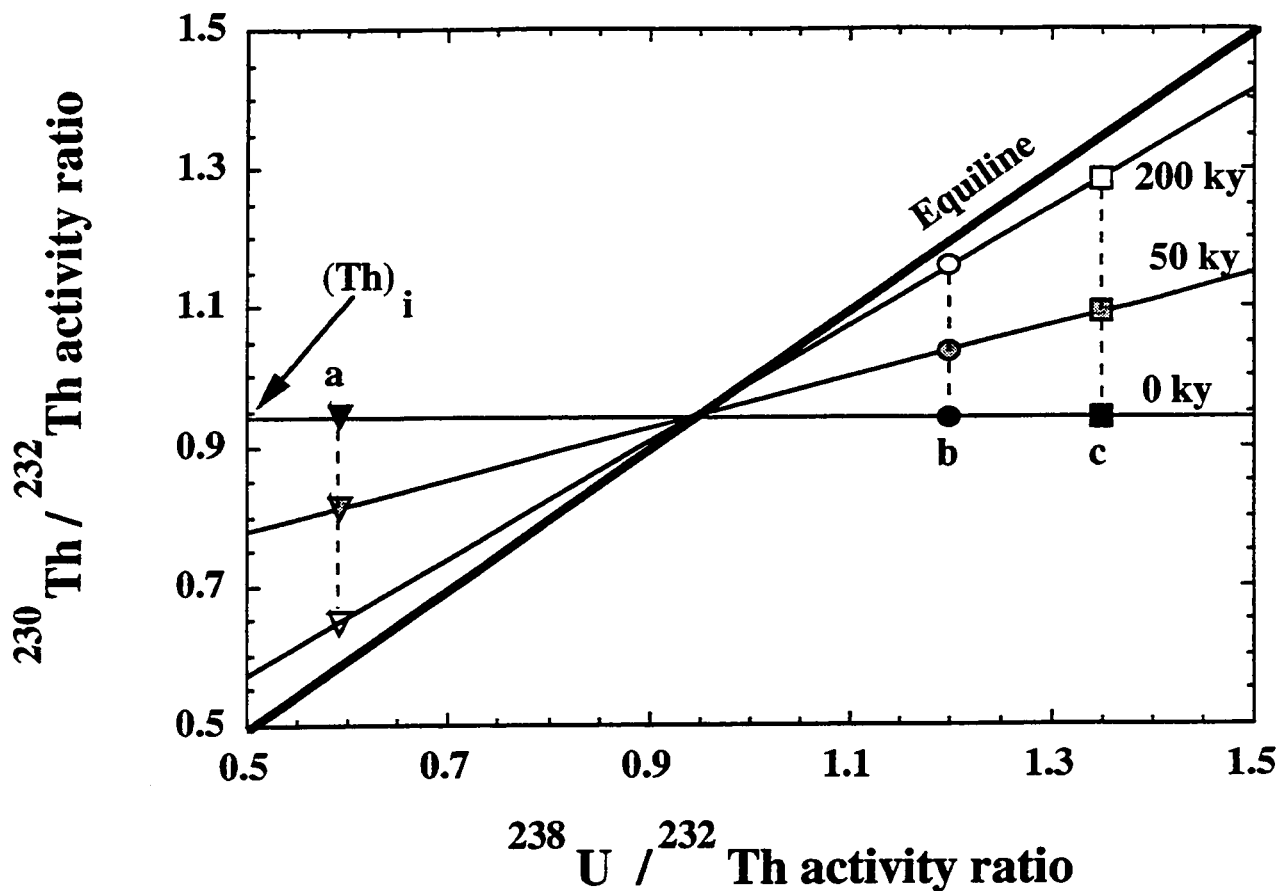


Figure 2-8.  $^{230}\text{Th}/^{232}\text{Th}$ - $^{238}\text{U}/^{232}\text{Th}$  isochron diagram showing the schematic evolution of an initially isotopically homogenous crystallizing magma. At 0 yr, the system crystallized three phases, *a*, *b*, and *c*, then erupted and became isotopically closed. All the crystals had the same initial  $^{230}\text{Th}/^{232}\text{Th}$  activity ratios  $(\text{Th})_i$ . With time,  $^{230}\text{Th}$  grows in or decays towards radioactive equilibrium with  $^{238}\text{U}$ , and the isochron will rotate about the point  $(\text{Th})_i$  on the equiline, which is a line of slope 45 degrees. Isochrons are shown for 50 and 200 k.y. At any time after 350 k.y.,  $^{230}\text{Th} = ^{238}\text{U}$  and points *a*, *b*, and *c* will lie along the equiline.

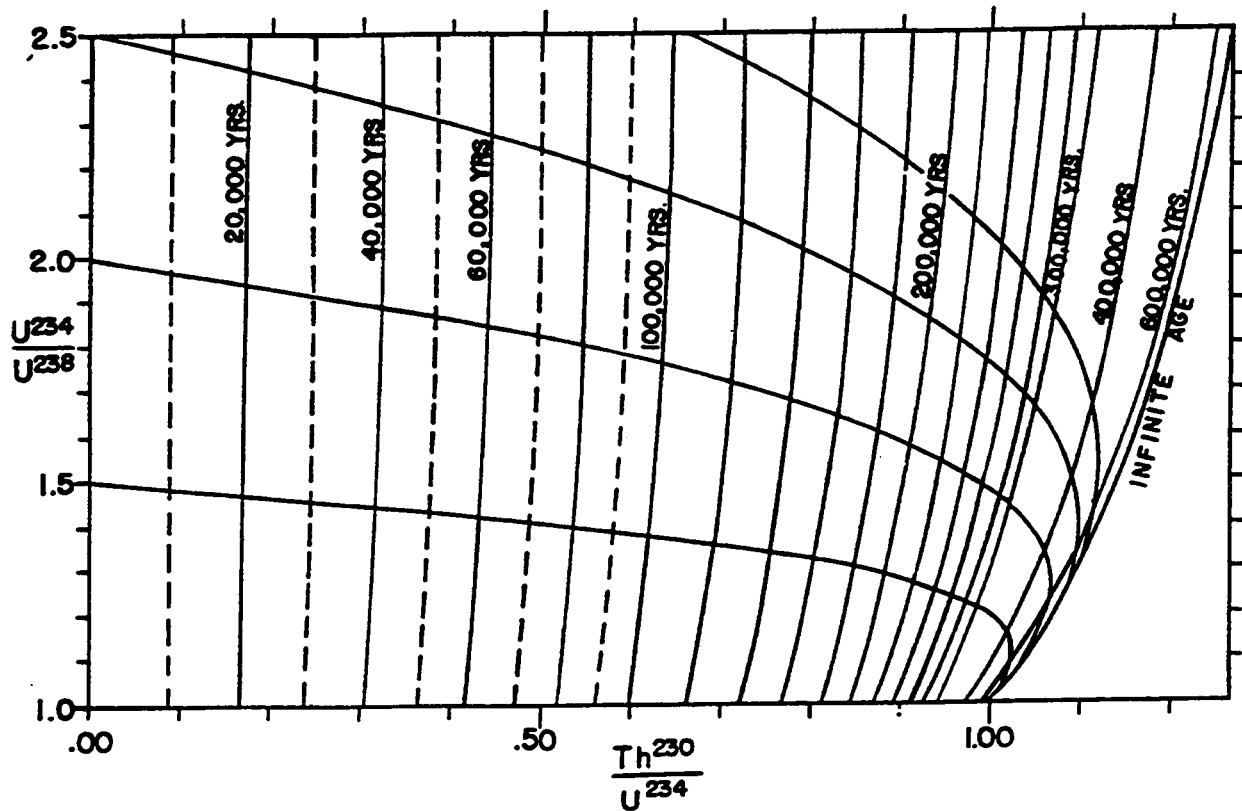


Figure 2-9. Variation of  $^{234}\text{U}/^{238}\text{U}$  and  $^{230}\text{Th}/^{234}\text{U}$  ratios with time in a closed system free of initial  $^{230}\text{Th}$ . The near-vertical lines are isochrons (i.e, loci of points for samples of the same age but different initial  $^{234}\text{U}/^{238}\text{U}$  ratios). The horizontal curves denote age paths of samples with initial  $^{230}\text{U}/^{238}\text{U}$  ratios of 1.5, 2.0, and 2.5.

isochrons touching the ellipse spaced furthest apart. The graphical technique leads to unsymmetrical errors in the age estimation, since isochrons are more closely spaced at higher  $^{230}\text{Th}/^{234}\text{U}$  ratios (Figure 2-9).

If the carbonate or authigenic deposit being dated is impure (i.e., contains detrital particles), then the isotopic measurements must be corrected for the  $^{230}\text{Th}$  that accompanies the  $^{232}\text{Th}$  in the detrital fraction (Luo and Ku, 1991; Kaufman, 1993). The correction schemes either involve acid leaching of the authigenic-allochthonous mixture (Kaufman, 1993) or total dissolution of several aliquots of the sample with differing proportions of detrital contamination (Bischoff and Fitzpatrick, 1991; Luo and Ku, 1991). For the leaching techniques, the U and Th isotopic signals of the leachate are combined with those of either the residue (the L/R method; Szabo et al., 1981) or the leachates from coeval samples (the L/L method; Kaufman, 1993) to derive the authigenic  $^{234}\text{U}/^{238}\text{U}$  and  $^{230}\text{Th}/^{234}\text{U}$  activity ratios. The total dissolution correction scheme requires that isochron plots of  $^{230}\text{Th}/^{232}\text{Th}$  versus  $^{234}\text{U}/^{232}\text{Th}$  and  $^{234}\text{U}/^{232}\text{Th}$  versus  $^{238}\text{U}/^{232}\text{Th}$  be used to derive the authigenic  $^{234}\text{U}/^{238}\text{U}$  and  $^{230}\text{Th}/^{234}\text{U}$  activity ratios (Luo and Ku, 1991). Once the corrected authigenic  $^{234}\text{U}/^{238}\text{U}$  and  $^{230}\text{Th}/^{234}\text{U}$  ratios have been determined, the ratios can be used to determine the date of the deposit by the procedures outlined above [Figure (2-9) or Eq. (2-9)].

### 2.4.1 Analytical Methods

Analytical methods are similar for dating both young volcanic rocks and carbonate deposits. In essence, the material to be dated must be dissolved, U and Th separated from each other and other cations, and solid sources from these pure U and pure Th solutions must be prepared. The number of published analytical schemes to get to the final solid source exceeds 50 (Lally, 1992). In general, solids are totally dissolved using mineral acids, U and Th are scavenged on some carrier phase, and sources of purified U and Th solutions obtained either by selective precipitation, or more commonly, by ion exchange chromatography methods. Once the purified solutions of U and Th are obtained, then solid sources are prepared either for mass spectrometry (Chen et al., 1992) or alpha spectrometry (Luo and Ku, 1991). Again the exact technique used to prepare the solid sources is highly dependent upon the investigator involved (Chen et al., 1992; Goldstein et al., 1989; McDermott et al., 1993; Lally, 1992). For both mass spectrometry and alpha spectrometry techniques, calibrated and isotopically pure spike solutions of U ( $^{232}\text{U}/^{228}\text{Th}$  or  $^{236}\text{U}$  for alpha spectrometry and a  $^{233}\text{U}$ - $^{236}\text{U}$  double spike for mass spectrometry) and Th isotopes ( $^{232}\text{U}/^{228}\text{Th}$  or  $^{229}\text{Th}$  for alpha spectrometry and  $^{229}\text{Th}$  for mass spectrometry) are used to correct for incomplete recovery during chemical procedures and variable counting geometries and efficiencies. The mass spectrometry technique is much more sensitive than the alpha spectrometry technique, however, the number of mass spectrometers available for these measurements is limited and most results for carbonate deposits are derived from alpha spectrometry.

### 2.4.2 Sources of Error

Analytical uncertainty, derived due to aliquot spiking after dissolution, for U and Th concentration measurement is small using mass spectrometric techniques (<2 percent) and slightly larger for alpha spectrometry techniques (3-5 percent). The mass spectrometric technique is much more precise in the determination of isotope ratios with common  $2\sigma$  uncertainties of 5‰ for  $^{230}\text{Th}/^{238}\text{U}$  and  $^{234}\text{U}/^{238}\text{U}$ ;  $2\sigma$  errors for alpha spectrometry measurements on a similar sample would be larger by a factor of 20 and 5, respectively, for the two isotopic ratios (Chen et al., 1992; Goldstein et al., 1989). Normally counting errors reported for alpha spectrometry results reflect a  $1\sigma$  error, but it is common practice to report  $2\sigma$  errors for mass spectrometric results (Chen et al., 1992). The resultant uncertainty

in the calculated date is a factor of 10 higher for alpha spectrometry compared to mass spectrometry results (Chen et al., 1992). The overall uncertainty in a calculated date is influenced by the concentration of U and Th in the phases being dated. More precise measurements are possible for carbonates compared to silicates due to the stronger fractionation of Th from U in the carbonate. Precision of the  $^{230}\text{Th}/^{238}\text{U}$  isochron technique is limited by the small degree of Th/U fractionation for the separated phases (e.g., Crowe et al., 1992b; Anthony, 1993).

The accuracy of the U-series disequilibrium dates is dependent on the assumptions used in the particular dating scheme. For instance, dating both volcanic rocks and carbonates by U/Th disequilibria requires that the system remains closed with respect to isotopic exchange after the process that fractionates U and Th occurs (i.e., crystallization for a magma and precipitation for a carbonate). The accuracy of the  $^{230}\text{Th}/^{238}\text{U}$  isochron technique is dependent upon, and necessarily presumes, thorium and uranium isotopic homogeneity in the melt that formed the unit dated (Gill et al., 1992), and that the  $^{234}\text{U}/^{238}\text{U}$  activity ratio is equal to one. The assumption of uranium isotopic homogeneity and isotopic equilibrium between  $^{234}\text{U}$  and  $^{238}\text{U}$  is rarely checked (Gill et al., 1992). However, when checked, the activity ratio for  $^{234}\text{U}/^{238}\text{U}$  is equal to one within the experimental uncertainty (Goldstein et al., 1989), which for mass spectrometry is better than 5‰ at  $2\sigma$ . The assumption of initial thorium isotopic homogeneity often is not true (Gill et al., 1992) and may be addressed by careful petrographic study.

The accuracy of  $^{230}\text{Th}/^{234}\text{U}$  dates of carbonate deposits also is dependent upon other assumptions that vary depending on the method of analysis. For instance, the total dissolution method (Luo and Ku, 1991; Bischoff and Fitzpatrick, 1991) requires that the detrital fraction of the impure carbonate deposit has uniform U and Th isotopic compositions. Partial dissolution techniques (Kaufman, 1993) requires that the leaching treatment of the samples does not preferentially solubilize one isotope relative to the other, or if it does, the degree of fractionation remains constant for a given suite of coeval samples (Luo and Ku, 1991). The total sample dissolution technique provides adequate information to address the assumption of isotopic homogeneity of the detrital phase. However, the assumption of no fractionation during leaching is often violated (Bischoff and Fitzpatrick, 1991). In addition, the discussion of Kaufman (1993) clearly demonstrates that ages derived by L/R methods may be invalid theoretically, but often give dates that are similar to the more theoretically robust L/L method. The accuracy of  $^{230}\text{Th}/^{234}\text{U}$  dates of pure carbonates can also be addressed by looking at the  $^{231}\text{Pa}/^{235}\text{U}$  disequilibrium in the same sample. The dates generated by both methods should be concordant.

### 2.4.3 Material Dated

Young igneous rocks can be dated by U-series disequilibrium methods. Both whole-rock samples and mineral separates can be analyzed for U- and Th-series isotopes. Pure mineral separates and phases containing U and Th are required. The whole rock and mineral separates also should be characterized using petrographic techniques in order to differentiate between a true isochron and the case of isotopic mixing, which could result from a mixture of minerals from different sources or of different ages. The amount of material needed for isotopic analysis depends on the method of analysis; alpha spectrometry requires large samples (1–5 g, or enough to yield 1  $\mu\text{g}$  of  $^{238}\text{U}$  and 1  $\mu\text{g}$  of  $^{232}\text{Th}$ ), but mass spectrometric analysis of U and Th isotopes only requires much smaller masses for Th (50 to 400 ng, Goldstein et al., 1989; McDermott et al., 1993) and U (10 to 100 ng, Goldstein et al., 1989; Chen et al., 1992). For  $^{226}\text{Ra}$ - $^{230}\text{Th}$  disequilibrium measurements, which would be applicable for volcanic rocks less than about 8 ka (half-life of  $^{226}\text{Ra}$  is 1600 yr), require less than 20 mg of rock for mass spectrometric

analysis of  $^{226}\text{Ra}$  (Cohen and O'Nions, 1991). This quantity is about 100 times smaller than that required for  $^{226}\text{Ra}$  analysis by radioactive counting methods.

Uranium-series methods also can be applied to deposits of impure carbonate such as soil caliche and carbonate coatings on lavas and surge deposits. Poorly cemented samples of soil caliche are crushed and cleaned by sieving and removal of visible rock fragments (Szabo et al., 1981). For purer and more densely cemented samples, crushing and grinding to a fine powder are required. For the total sample dissolution method, it is necessary to obtain subsamples with varied mineral compositions, and hence, varied U/Th ratios (Bischoff and Fitzpatrick, 1991; Luo and Ku, 1991). For both partial dissolution (leachate/residue) or total sample dissolution analytical schemes, different size fractions of the impure carbonate are obtained by gentle grinding and sieving (Luo and Ku, 1991; Paces et al., 1993). Carbonate tends to be fractionated into the smaller size ranges, thus sieving would fulfill the requirement of the total dissolution method to obtain subsamples of varying U/Th ratios. Isotopic analysis for U and Th isotopes can be accomplished using either alpha spectrometry or mass spectrometry. Sample mass requirements are similar to those required for analysis of young volcanic rocks and are smaller for mass spectrometric analyses (Chen et al., 1992). The  $^{230}\text{Th}/^{234}\text{U}$  dates of carbonate deposits can be used to bound cosmogenic and other radiogenic dating techniques. In addition, this method could be used to verify the accuracy of thermoluminescence dates.

#### 2.4.4 Application to the Yucca Mountain Region

Uranium-series methods have been applied to the young volcanic rocks at Lathrop Wells and to carbonate deposits at this site and throughout the YMR. Samples from three flow units at Lathrop Wells have been analyzed for  $^{230}\text{Th}/^{238}\text{U}$  disequilibrium using solid-source mass spectrometry (Crowe et al., 1992b). None of the  $^{230}\text{Th}/^{238}\text{U}$  disequilibrium dates for the volcanic units at Lathrop Wells present sufficient analytical information to independently calculate the date. In addition, insufficient analytical data were presented to independently evaluate analytical precision and accuracy. For example, the atom ratio or activity ratio and associated analytical uncertainties for the  $^{230}\text{Th}/^{232}\text{Th}$  and  $^{234}\text{U}/^{238}\text{U}$  isotopic pairs should be reported in order to distinguish between the precision of the measurement and the uncertainty in the reported date.

An internal mineral isochron date for the  $\text{Ql}_4$  lava of Lathrop Wells (subunit  $\text{Ql}_{4a}$ ) of  $150 \pm 40$  ka was graphically presented in Crowe et al. (1992b). Although it was stated that the error in the date for  $\text{Ql}_4$  was a  $2\sigma$  error, it was not clear if the error reflects only the mass spectrometric measurement or if it is a  $2\sigma$  error associated with the fit of the isochron. An additional U-Th isochron date was reported for subunit  $\text{Ql}_6$  by Crowe et al. (1993); however, no isotopic data were reported, and the method to generate an error estimate of the date was not given. The reported U-Th isochron date for subunit  $\text{Ql}_6$  was  $135 \pm 35$  ka, -25 ka.

Although it was stated by Crowe et al. (1993) that different disequilibrium was observed for plagioclase and olivine of different sizes in the  $\text{Ql}_6$  sample, without any other analytical data it is difficult to determine the significance of this observation. If the different disequilibrium for the different mineral sizes reflects initial  $^{230}\text{Th}/^{232}\text{Th}$  heterogeneity, which would be determined by the intersection of the isochron for each size fraction and the equiline, then this differing initial  $^{230}\text{Th}/^{232}\text{Th}$  could provide petrologic constraints on the evolutionary history of the Lathrop Wells complex. For example, one possible explanation is that the differing disequilibrium for different mineral sizes indicates magma mixing (Gill et al., 1992). The magmas would necessarily be derived from melts of similar major element

composition, which crystallized under similar conditions and had variable amounts of otherwise similar minerals. If the melts were of different isotopic compositions, then the resulting mineral isotopic signatures could differ from either of the two melt compositions (Gill et al., 1992). An alternative explanation is that the coarser-grained olivine and plagioclase were altered by an uranium-rich fluid (Crowe et al., 1993).

Previous  $^{230}\text{Th}/^{234}\text{U}$  dates at Lathrop Wells by Szabo et al. (1981) indicated that a minimum age of the lava flows was  $25 \pm 10$  ka. One dated sample (Sample No. 59) consisted of caliche from the base of loess overlying a rubbly lava flow near Highway 95. The technique used to analyze the impure carbonate was to dissolve the ashed impure carbonate in dilute acid and analyze both the soluble and insoluble residues for isotopic content. Additionally, a stalactitic laminated calcrete in cavities between boulders immediately beneath the basalt flow were analyzed for  $^{230}\text{Th}/^{234}\text{U}$  disequilibrium (Szabo et al., 1981). This stalactitic material (Sample No. 60) contained well-developed laminae, so that the sample was split into an inner and outer portion. Analysis of Sample No. 60 gave dates of  $345 + 180$  ka,  $-71$  ka, and  $345$  ka  $+ 180$  to  $70$ -ka for the two portions. These dates for the carbonate underlying the basalt provide a maximum bounding age for the Lathrop Wells center of  $525$  ka. Other workers are using U-series methods to date carbonates in the YMR (Luo and Ku, 1991; Paces et al., 1993); however, no other attempts to reproduce or further constrain the limiting dates for Lathrop Wells complex (Szabo et al., 1981) have been completed.

The overall utility of U-series disequilibrium methods to constrain the eruption history of the Lathrop Wells center will be limited. Insufficient fractionation of U and Th to precisely determine  $^{230}\text{Th}/^{238}\text{U}$  isochron ages appears to prevail in the young volcanic rocks, thus limiting the resolution of the technique to young volcanic rocks that differ in age by  $50$ – $75$  ka. Although better precision for  $^{230}\text{Th}/^{234}\text{U}$  disequilibrium dates is possible for total sample dissolution of soil carbonates and caliches (i.e., 10-percent precision), their formation is not likely to exactly reflect the eruptive history of the deposit. The dates generated will reflect minimum ages for the volcanic rock if the carbonate deposit overlies the volcanic feature, and maximum ages for carbonate deposits that underlie the volcanic unit being constrained. If sufficient carbonate was found to accumulate between different stratigraphic flow units, then it might be possible to date these accumulations and further constrain the eruptive history of the Lathrop Wells complex.

## 2.5 CARBON-14 ( $^{14}\text{C}$ ) METHOD

The  $^{14}\text{C}$  method is the technique most often used to date organic material associated with geologic events younger than about  $40$  ka. The general principle is that  $^{14}\text{C}$  is produced by cosmic-ray bombardment of  $^{14}\text{N}$  in the upper atmosphere (Libby, 1946). The rate of  $^{14}\text{C}$  production is assumed to be in equilibrium with the rate of  $^{14}\text{C}$  decay through  $\beta^-$  emission, which has a half-life of  $5,730 \pm 40$  yr. This half-life results in an equilibrium concentration of about  $1.2 \times 10^{-12}$  atoms of  $^{14}\text{C}$  for every  $^{12}\text{C}$  atom in living organic matter. When an organism dies,  $^{14}\text{C}$  is no longer replenished and begins to decay. A date is produced by analyzing the amount of  $^{14}\text{C}$  in the organic material relative to a standard of known age.

The  $^{14}\text{C}$  method is routinely used to date organic material up to about  $40$  ka. The theoretical upper limit to the technique is about  $57$  ka, by which time 99.9 percent of the available  $^{14}\text{C}$  will have decayed. Application of the technique is limited to geologic events that trap and kill living organic

material, typically through burning or rapid burial. Such material commonly occurs beneath lava flows or in pyroclastic fall deposits, and within rapidly deposited sediments.

### 2.5.1 Analytical Methods

Analysis for a  $^{14}\text{C}$  date is relatively simple. Cleaned organic samples that contain gram quantities of C are burned, and the ensuing  $\text{CO}_2$  is collected and purified. The activity of  $^{14}\text{C}$  in gas can then be measured directly with a heavily shielded gas-filled proportional counter (e.g., Ralph, 1971). Samples can also be converted to benzene through dissolution in acetylene, then counted in liquid-scintillation detectors (Geyh and Schleicher, 1990). Count rates are generally low ( $\approx 14$  decays per minute per gram C), requiring count times between 2 to 7 days for most samples.

A date is calculated by assuming that the initial  $^{14}\text{C}$  activity in the sample is the same as in atmospheric  $\text{CO}_2$  (Anderson et al., 1947; Stuiver and Polach, 1977). The measured  $^{14}\text{C}$  activity in the sample must then be corrected for small isotopic fractionation effects that occur as a result of  $\text{CO}_2$  assimilation by plants, due to significant differences in size, mass, and reaction rate between  $^{14}\text{C}$  and  $^{12}\text{C}$ . This correction is made by using a mass spectrometer to measure the  $^{13}\text{C}/^{12}\text{C}$  of the sample and a carbonate standard, which gives

$$\delta^{13}\text{C} = \frac{\left(\frac{^{13}\text{C}}{^{12}\text{C}}\right)_{\text{samp}} - \left(\frac{^{13}\text{C}}{^{12}\text{C}}\right)_{\text{std}}}{\left(\frac{^{13}\text{C}}{^{12}\text{C}}\right)_{\text{std}}} * 1000\text{‰} \quad (2-10)$$

The isotopic fractionation between  $^{14}\text{C}$  and  $^{12}\text{C}$  is 2.3 times greater than between  $^{13}\text{C}$  and  $^{12}\text{C}$ . By convention, this fractionation factor is rounded to 2 and the activity of  $^{14}\text{C}$  is corrected to reflect a  $\delta^{13}\text{C}$  of  $-25\text{‰}$  (e.g., Stuiver and Polach, 1977)

$$A_{\text{cor}} = A_{\text{meas}} \left[ 1 - \frac{2(\delta^{13}\text{C} + 25)}{1000} \right] \quad (2-11)$$

where  $A_{\text{cor}}$  = corrected  $^{14}\text{C}$  activity  
 $A_{\text{meas}}$  = measured  $^{14}\text{C}$  activity

The corrected  $^{14}\text{C}$  activity is then used to calculate the date

$$t = \left( \frac{5568}{\ln 2} \right) \ln \frac{A_o}{A_{\text{cor}}} \quad (2-12)$$

By convention, the 5,568-yr  $^{14}\text{C}$  half-life of Libby (1946) is used in all dates, and the initial activity of  $^{14}\text{C}$  ( $A_o$ ) is determined from an international standard (Stuiver and Polach, 1977). In addition, 1950 A.D. is considered the reference year for dates that report years before present (B.P.); a  $^{14}\text{C}$  date of 5000 B.P. thus refers to the year 3050 B.C.

One of the inherent assumptions in the  $^{14}\text{C}$  method is that the production of  $^{14}\text{C}$  in the ancient atmosphere occurred at the same rate as the present. However, cosmic-ray production rates of  $^{14}\text{C}$  are known to have changed over the last 10,000 yr due to variations in the earth's magnetic field, changes in solar-wind magnetic properties, and sun-spot cyclicity (e.g., Geyh and Schleicher, 1990).  $^{14}\text{C}$  dates are thus corrected using calibration tables or curves, which account for these variations (Stuiver and Kra, 1986). Dates older than about 10,000 yr generally are not corrected, although  $^{14}\text{C}$  production-rate errors may result in several thousands of years difference between the date and the actual age of the sample (e.g., Stuiver, 1978).

A  $^{14}\text{C}$  date can also be produced for very small samples (< 1 mg) using high-energy particle accelerators (Bennett et al., 1977). This technique has the ability to determine  $^{14}\text{C}$  dates for samples as old as 70 ka, and avoids many of the contamination problems inherent in bulk carbon samples (e.g., Bennett, 1979). Particle accelerators are the only instruments capable of the high sensitivities needed to resolve mass differences between  $^{14}\text{C}$  and  $^{14}\text{N}$ . These mass differences cannot be resolved using conventional mass spectrometers (Bennett, 1979). This technique is thus limited to high-energy physics laboratories.

### 2.5.2 Sources of Error

The largest source of error in  $^{14}\text{C}$  dates originates in contamination of the sample with younger carbon (Geyh and Schleicher, 1990). Contamination can easily occur through root growth into the sample area, bioturbation, bacterial action, or seepage of carbonate into the sample horizon. Sample preparation usually involves removing visible contamination and chemical treatment to remove surficial organic material. Other significant sources of error generally originate in the difficulties of counting low-radioactivity samples, which have less than the 14 decays per minute per gram carbon of modern atmospheric  $\text{CO}_2$ . A total of at least 10,000 decays must be counted before  $\leq 1$  percent error in the  $^{14}\text{C}$  activity is achieved (e.g., Wang et al., 1975). Assuming no contamination, conventional  $^{14}\text{C}$  dates generally have analytical precision of around  $\pm 50$ –100 yr for Holocene dates, with greater than about 100 yr uncertainty for pre-Holocene dates (e.g., Geyh and Schleicher, 1990).

The accuracy of some  $^{14}\text{C}$  dates is questionable due to significant, but not easily quantified, variations in ancient  $^{14}\text{C}$  production rates. Although relative  $^{14}\text{C}$  dates are generally accurate, comparison of older  $^{14}\text{C}$  dates with dates produced through U-Th,  $^3\text{He}$ , or other geochronologic analyses can show up to 5,000-yr differences between these techniques and the  $^{14}\text{C}$  dates (e.g., Vogel, 1983; Bard et al.,

1990). Bard and coworkers (1990) recently have developed a 30,000-yr  $^{14}\text{C}$  timescale calibrated with U/Th dates of coral, in an attempt to minimize the inaccuracies of pre-Holocene  $^{14}\text{C}$  dates.

### **2.5.3 Material Dated**

Most organic material can be dated by the  $^{14}\text{C}$  method, including humus, rock varnish, bones, and mollusk shells (Geyh and Schleicher, 1990; Dorn et al; 1989). Volcanic events are usually dated through the analysis of intraformational charcoal. Although a sample size of about 5 g is preferred, clean samples of less than about 1 g can be dated through conventional methods (Simonsen, 1983). Samples of peat or humus generally require at least 10 g for dating, and several kilograms of soil must generally be processed in order to recover enough organic material for a reliable date (Geyh and Schleicher, 1990). Samples analyzed by accelerator mass spectrometry require about 1 mg of carbon, although smaller amounts are datable using detailed preparation techniques (Bennett, 1979).

### **2.5.4 Application to the Yucca Mountain Region**

There have been no dates for Quaternary basaltic volcanoes in the YMR produced through the  $^{14}\text{C}$  method, although several late Quaternary to Holocene ages have been proposed for the Lathrop Wells volcanic center (Crowe et al., 1992b; Wells et al., 1992, 1990). If Lathrop Wells is significantly older than about 40 ka, organic material buried by lava flows or scoria falls could provide a useful confirmation of the minimum age of the deposit through  $^{14}\text{C}$  analysis. Holocene ages proposed for Lathrop Wells could be easily verified through conventional  $^{14}\text{C}$  dating.

## 3 RADIATION INTERACTION METHODS

### 3.1 GENERAL PRINCIPLES

Ionizing alpha, beta, gamma, and cosmic radiation can interact with dielectric solids and change their physical and chemical properties. These changes can produce defects in a mineral's crystal lattice, create new elements through spallation or n-capture reactions, and excite electrons to unstable energy states. Some of these changes are stable over geological periods of time, and can be used as geochronometers. For example, the spontaneous fission of  $^{238}\text{U}$  creates defects in a crystal lattice, which is the principle used for fission-track dating. Additionally, cosmogenic isotopes can form through spallation reactions between cosmic-ray neutrons and the major elements of a rock. These isotopes are produced at a relatively constant rate and their accumulation is the basis for the cosmogenic isotope dating technique. Finally, the interaction of ionizing radiation with a crystalline lattice can excite electrons to metastable energy states, which accumulate with time and form the basis of thermoluminescence dating. These techniques are sometimes viewed as experimental and do not always provide dates with the same precision and accuracy as some radiogenic isotope techniques. They can, however, provide dates for Quaternary deposits that cannot be analyzed by conventional radiogenic methods.

The use of radiation interaction methods in geochronology is based on two primary assumptions.

- The radiation effects acquired by the sample during exposure are stable for the length of time under consideration, and the magnitude of the effect is proportional to the age of the sample.
- The irradiation rate for the sample has remained constant through time. This assumption generally considers that the system has remained closed with respect to naturally occurring radioisotopes and that variations in cosmic-ray flux for the sample can be determined.

Radiation interaction methods differ from radiogenic isotope methods in several important ways. The ability of a mineral to accommodate isotopic decay products is essentially infinite; there are many more available lattice sites than there are atoms to fill them. For radiation interaction methods, mineral lattices have a finite number of stable sites that can store time-dependent phenomena. After these sites are used, continued exposure to radiation interaction will not result in detectable effects. Radioactive decay also occurs at a constant rate. However, the effects of cosmogenic radiation are not always produced at a constant rate. Variations in cosmic-ray production have occurred through time (e.g., Kurz, 1986a), although these variations may be relatively minor over geologic periods of time. In addition, the effects of cosmogenic radiation will vary with altitude, latitude, irradiation geometry, and thickness of the sample (e.g., Lal, 1991). These effects must be quantified before any cosmogenic method can be used effectively in geochronology.

After these basic assumptions are constrained, a date can be produced by measuring the amount of radiation the sample has been exposed to and determining the radiation dose rate needed to produce the measured radiation effects. The date is then calculated by simply dividing the radiation dose (signal) by the dose rate. Although this procedure appears simple, determining the radiation dose and dose rate for young basaltic samples is usually difficult and involves significant uncertainties.

## 3.2 THERMOLUMINESCENCE METHOD

The thermoluminescence (TL) method is based on the interaction of ionizing radiation with electrons in a crystal lattice (Daniels et al., 1953; Aitken, 1967). Defects within the crystal lattice result in "traps", which can accommodate electrons that have been excited to higher energy states through interaction with ionizing radiation. Although only some of these traps are stable, the number of occupied traps increases linearly with age if the radiation dose rate remains constant (Aitken, 1967). The stability of a trap increases with its excitation energy. Upon heating, energy is imparted to the metastable electrons in these traps. Electrons are released from the traps, and excess energy is emitted as light when the electron moves to a ground state (Aitken, 1967; 1978). The intensity of the emitted light is measured as a function of temperature to produce the TL signal used for dating.

A trapped electron has a finite lifetime at an excited energy state. In general, electron traps that emit light upon heating at low temperatures have relatively short lifetimes, whereas high-temperature (i.e., 300 °C) traps have lifetimes in excess of about 10,000 yr (Figure 3-1; Aitken, 1967). In order to produce a TL date that represents the age of the sample, electron traps with lifetimes equal to or greater than the sample's age must be empty when the sample forms. For minerals in lavas or tephra, temperatures above 400 °C are sufficient to empty all electron traps (May, 1979). Exposure to sunlight for about a day also empties much of a sample's electron traps (Wintle, 1982; Forman, 1989), which permits the dating of eolian deposits.

### 3.2.1 Analytical Methods

The TL signal is sensitive to self-shielding effects; smaller samples show a larger TL signal than larger size fractions of the same sample (Sabels, 1963; May, 1979). For this reason, samples are usually sieved prior to analysis and only a narrow range of grain size is used (Geyh and Schleicher, 1990). The sample aliquot is mounted on a stainless steel disk and placed in a heating chamber filled with an inert gas such as nitrogen or argon. The sample is heated at a constant rate of 10–20 °C/sec, to a maximum temperature of 450–500 °C (May, 1979). Emitted light is measured with a photomultiplier and plotted versus temperature to produce a glow curve. Most geologic samples have a maximum TL signal between 300–400 °C, which represents emissions by relatively stable electron traps (Aitken, 1967).

After cooling, several aliquots of the sample are exposed to successively larger doses of  $\beta$  radiation from an isotopic source such as  $^{90}\text{Sr}$ , which refills the electron traps that stored the original TL signal (e.g., Geyh and Schleicher, 1990). The samples generally are held at an elevated temperature of about 50 °C following irradiation to permit spontaneous decay of the least stable sites (May, 1979). The samples are then reheated in the same manner as that used to measure the natural TL signal. The ratio between consecutive areas of the natural TL and artificial TL curves should reach a constant value near 300 °C, which indicates that a stable natural TL signal was acquired (Aitken, 1978). Areas under specific temperature intervals of the glow curves are measured and plotted versus the radiation dose (Figure 3-2). The abscissa intercept of a straight line through these data represents the apparent radiation dose to the sample. However, the relationship between TL signal and total radiation dose is not linear for low doses, because additional electron traps probably are being created in the early stages of irradiation (Aitken, 1978). This effect is referred to as supralinearity (Aitken, 1978), and is compensated for by measuring

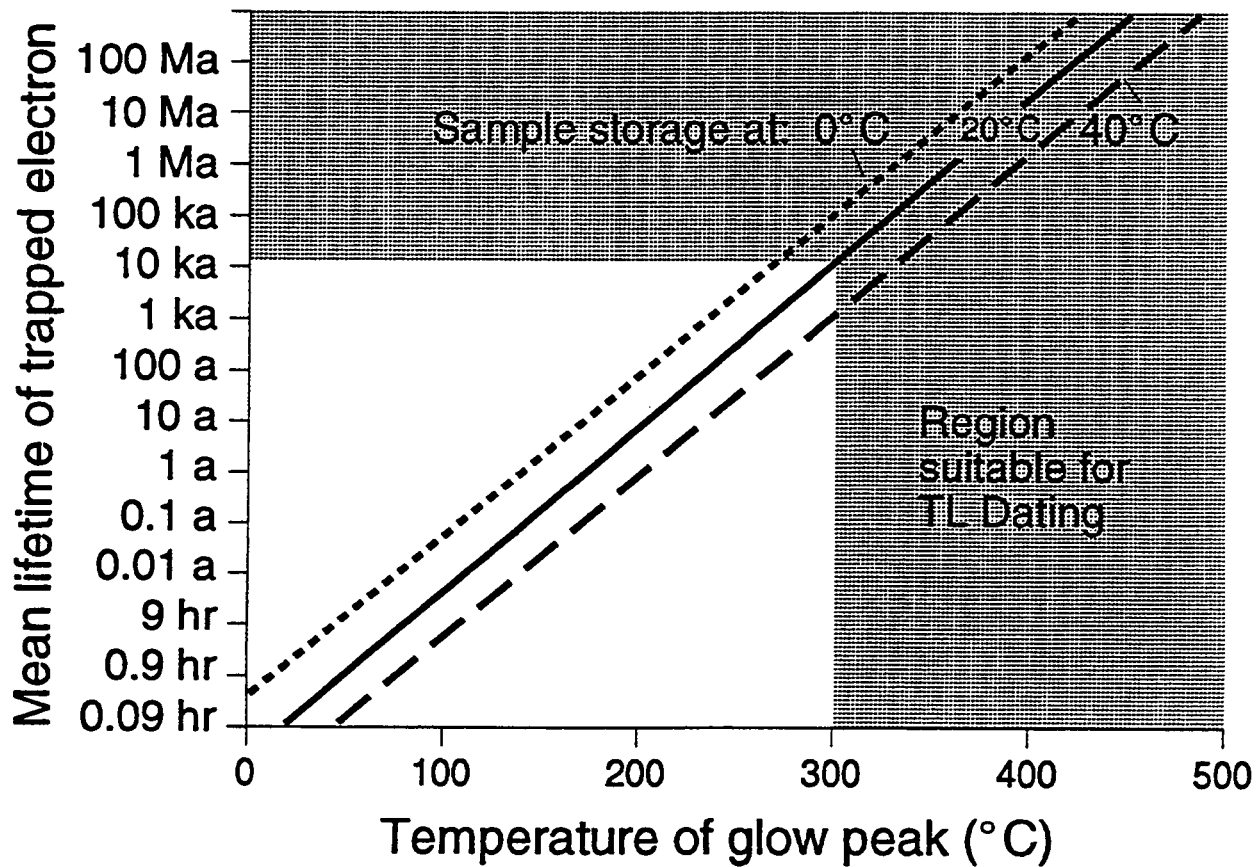


Figure 3-1. Mean lifetime of electron traps as a function of glow-peak and sample storage temperatures, modified from Aitken (1967). Sample with presumed ages in excess of 10 ka can only be dated accurately if the TL signal originates from electron traps with stabilities above 300 °C. Lower temperature traps have mean lifetimes that are significantly less than the age of the sample and will yield erroneously young dates.

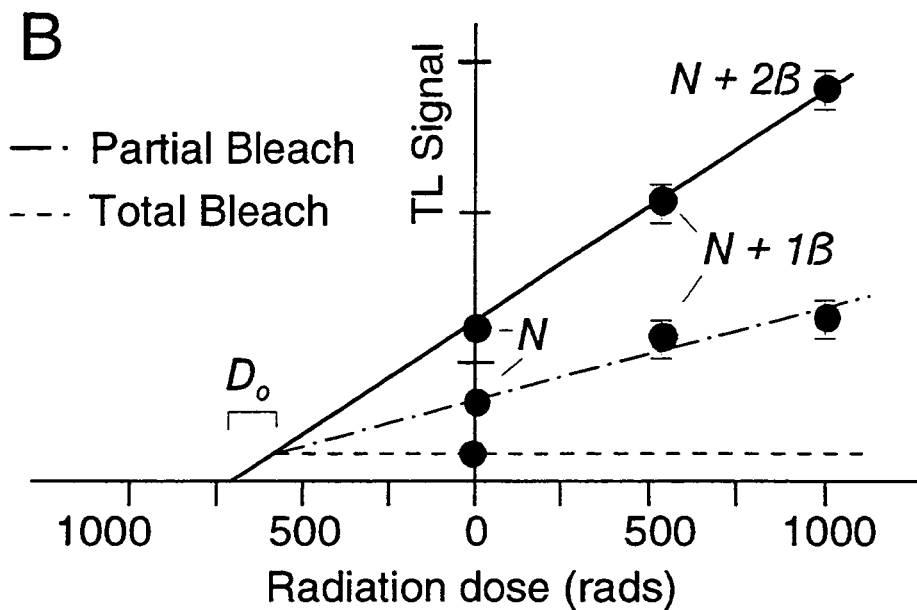
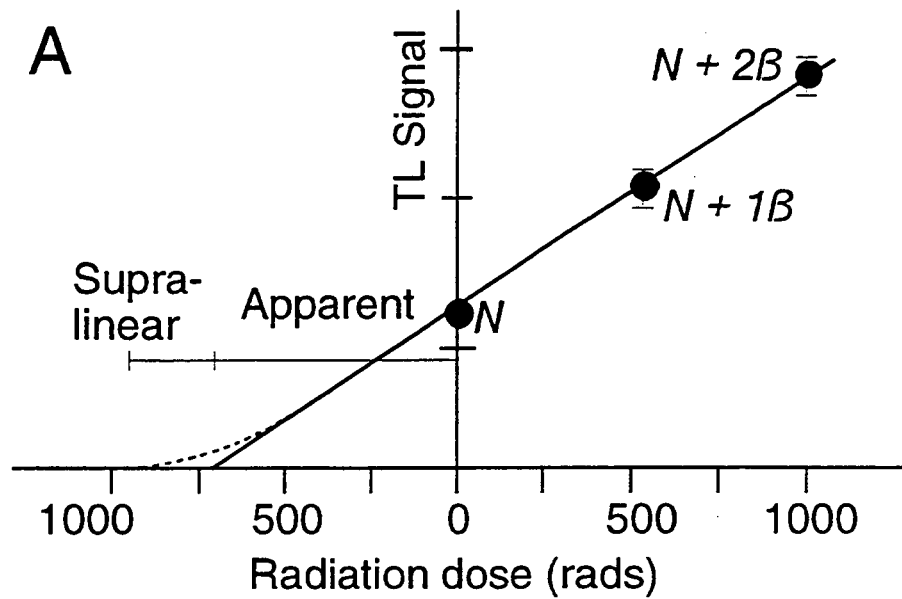


Figure 3-2. (A) Additive dose method for determining the accumulated radiation dose of a sample, modified from Aitken (1978). The natural TL signal,  $N$ , is measured during heating to about 400 °C. Sample aliquots are then exposed to  $1\beta$  and  $2\beta$  doses of artificial radiation and heated to measure the natural plus artificial TL signal. The accumulated dose consists of the apparent dose of the sample plus an additional component related to supra-linearity effects. (B) Partial and Total Bleach methods of TL dating, modified from Geyh and Schleicher (1990). Samples are exposed to small (Partial) and large (Total) amounts of UV light and analyzed by the additive dose method. Differences between the nonbleached and bleached trends represent  $D_0$ , the original TL signal of the sample, which is subtracted from the accumulated dose of the sample.

the TL response for samples from which the natural TL signal has been removed and adding the appropriate amount to the measured dose of the sample (Figure 3-2A). The corrected value represents the total dose of radiation received by the natural sample and is commonly referred to as the *accumulated dose*.

In order to calculate a date from the accumulated dose of the sample, the annual dose rate must be determined. The dose rate is the sum of alpha, beta, gamma, and cosmic-ray activity both within and proximal to the sample. Ideally, the external dose rate is measured directly by emplacing a dosimeter at the sample site for several months to a year (Geyh and Schleicher, 1990). Internal dose rates are calculated by determining the abundances of naturally occurring radioisotopes in the sample. The same procedure can be used to estimate the external dose rate, assuming the material around the sample is reasonably homogeneous. Alpha particles only have a range of about 20  $\mu\text{m}$  and are thus limited to U and Th decay within minerals. With an attenuation factor of about 15 percent, equilibrium alpha dose rates are around 50 mrad per year for a sample containing 1 ppm Th and 1 ppm U (Bell, 1979). Beta radiation has a range of about 2 mm, and a sample containing 1 ppm each of Th and U, and 1 weight percent  $\text{K}_2\text{O}$ , will have an annual beta dose rate of about 86 mrad (Bell, 1979). Gamma radiation has an annual dose rate of about 37 mrad for samples containing 1 ppm Th, U, and 1 weight percent  $\text{K}_2\text{O}$  (Bell, 1979). After the annual dose rate to the sample has been determined, the TL date is calculated by simply dividing the dose rate into the accumulated dose measured for the sample (Aitken, 1967).

The dating of eolian sediments requires additional analysis in order to resolve the low TL signal present in these deposits and account for electron traps that were not completely emptied upon deposition (Berger, 1986; Geyh and Schleicher, 1990). The *partial bleach method* (Singhvi and Mejdahl, 1985; Forman, 1989) is similar to the additive dose method described above, except that the original and irradiated samples are exposed to sunlight or UV light for a short interval of time and then reanalyzed. The intersection of the original and secondary trends yields the amount of the initial TL signal, which is subtracted from the accumulated dose of the sample (Figure 3-2B). The *total bleach method* (Singhvi and Mejdahl, 1985; Forman 1989) exposes a single sample to UV light until the TL signal is no longer lowered. The residual TL signal represents the initial TL signal of the sample and is subtracted from the accumulated dose (Figure 3-2B).

### 3.2.2 Sources of Error

The primary sources of error in the TL dating method are uncertainties in the external and internal radiation dose rates (e.g., Geyh and Schleicher, 1990). External dose rates are usually calculated based on an estimated composition of the material surrounding the sample, because *in situ* measurements are very time consuming. In addition to uncertainties in radioisotope abundances and cosmic-ray irradiation rates, the moisture of the material surrounding the sample will strongly affect the alpha dose-rate to the sample. For 5-MeV alpha particles, which are produced by the U and Th decay series and have a range of about 3.5 cm in air, a layer of water about 40  $\mu\text{m}$  thick will completely shield the sample from irradiation (Wang et al., 1975). Compaction of the sample will retard the flow of soil-gas radon, which also will affect the external dose rate to the sample (e.g., Berger, 1985). Thus, TL dates cannot be evaluated unless the methods used to determine external and internal dose rates are explicitly described. Assuming minimal errors in the estimate of these rates, TL dates of geologic materials commonly have uncertainties of around 25 percent, although more precise dates are possible if external dose rates are measured at the sample site (Geyh and Schleicher, 1990).

The TL signal is very sensitive to the grain size of the sample. In general, smaller sample sizes show a larger TL signal than larger size fractions of the same sample (Sabels, 1963; May, 1979). This effect may be due to both self-shielding and the larger activation area per unit volume of smaller grain sizes (e.g., Geyh and Schleicher, 1990). For these reasons, it is important to know what size fraction of a sample was used to produce a TL date. In addition, the TL growth curve may be nonlinear for samples older than about 50 ka (Forman, 1989). Failure to account for nonlinearity will underestimate the accumulated dose, and underestimate the age of the sample.

The total bleach method commonly produces TL dates that are significantly older than the age of the sample (Berger, 1986). Prolonged exposure of the sample to a UV light source will excessively bleach the sample, resulting in an anomalously small estimate of the initial TL signal and erroneously old dates. To avoid excess bleaching effects, samples are usually exposed to the UV light source for no more than 24 h (Geyh and Schleicher, 1990). For all TL samples, exposure to UV light sources during sample collection and preparation will produce anomalous fading of the TL signal and erroneously young dates for the sample. This effect is particularly important when unconsolidated sediments are dated, and extreme care during sample collection is required to avoid exposure to sunlight (Geyh and Schleicher, 1990).

### **3.2.3 Material Dated**

The most suitable materials for dating by the TL method are mineral separates that have electron traps emptied through heating above 400 °C or prolonged exposure to sunlight. All minerals have a limited number of stable electron traps that will become filled after a specific interval of time. The electron traps in quartz become completely filled after about 100 ka (Geyh and Schleicher, 1990). Plagioclase traps become saturated by several 100 ka (e.g., May, 1979). Silicic ash up to about 200 ka also can be dated by the TL method (Berger, 1985, 1991).

### **3.2.4 Application to the Yucca Mountain Region**

The TL dating method has had limited application to the Quaternary volcanic rocks of the YMR. Data presented to date fail to report most of the details necessary to independently evaluate the precision and accuracy of the data, and many of the assumptions necessary in TL dating are not addressed. A TL date of  $24.5 \pm 2.5$  ka is reported in Crowe et al. (1992b) for baked soil several decimeters under lava Q1<sub>3</sub> at the Lathrop Wells volcanic center. However, <sup>3</sup>He exposure dates for this and other temporally equivalent units are generally twice as old as this date. Crowe et al. (1992b) state that this date is preliminary and that additional work on baked soils in the Snake River Plains of Idaho will be used to confirm the procedure used for this date.

Multiple analyses of three nonbaked soil samples from Lathrop Wells were presented in Crowe et al. (1992b). These soils are interbedded with primary fall deposits associated with the latest stage of activity at Lathrop Wells, which is called chronostratigraphic unit 1 by Crowe et al. (1992b). Chronostratigraphic unit 1 has <sup>3</sup>He exposure dates up to  $44 \pm 5$  ka (Crowe et al., 1992b). Soil 1, the oldest soil in the dated sequence, has TL dates of  $8.9 \pm 0.7$ ,  $9.9 \pm 0.7$ , and  $8.7 \pm 1.0$  ka. Soil 2 has a date of  $3.7 \pm 0.4$  ka, and Soil 3, the youngest soil in the sequence, has dates of  $3.7 \pm 0.4$  and  $4.5 \pm 0.4$  ka. The reproducibility of the dates demonstrates the precision of the technique used to obtain these values. However, there is no way to evaluate the accuracy of these dates, nor is it at all clear how the measured TL signal was acquired by the sample. Apparently these samples were heated to only 100 °C to remove

the least stable time signal. Crowe et al. (1992b) do not state what temperatures were used to measure the TL signal, nor are glow curves or plateaus presented. Although Crowe et al. (1992b) state that the TL technique applied to these soils is preliminary, the large disparity between the  $^3\text{He}$  exposure dates and the TL dates is difficult to reconcile.

### 3.3 COSMOGENIC NUCLIDES METHODS

Cosmogenic nuclides including  $^3\text{He}$ ,  $^{10}\text{Be}$ ,  $^{14}\text{C}$ ,  $^{21}\text{Ne}$ ,  $^{26}\text{Al}$ , and  $^{36}\text{Cl}$  are produced by direct cosmic-ray irradiation of rocks at the surface of the earth (Lal, 1987, 1988). The production of these nuclides occurs via high-energy spallation reactions, neutron-capture reactions, and muon-induced nuclear disintegrations (Table 3-1). Cosmogenic nuclide methods are based upon the *in situ* accumulation of the cosmogenic nuclides in rocks exposed at the earth's surface (Dorn and Phillips, 1991). The rate of accumulation of the cosmogenic nuclides is dependent on altitude, geomagnetic latitude, rock chemistry, geometry of exposure to cosmic rays, and on the cosmic-ray flux. These factors can be measured to varying degrees of success (Zreda et al., 1991; Cerling, 1990; Kurz et al., 1990). The measurements of the cosmogenic nuclides in the exposed rocks allows the generation of an exposure age of the rock at the earth's surface. To assume that an exposure age of a rock is equivalent to the true age (eruption age) of the rock, the surface dated by cosmogenic nuclide techniques must have been continuously exposed. Any erosion, cover, or disturbance of the surface will yield a minimum age for the surface and will not reflect the true age of the rock.

The production rate of these nuclides is small, and measurement of the radioactive cosmogenic nuclides ( $^{10}\text{Be}$ ,  $^{14}\text{C}$ ,  $^{26}\text{Al}$ , and  $^{36}\text{Cl}$ ) requires an accelerator mass spectrometer, usually a tandem-accelerator. The stable cosmogenic nuclides  $^3\text{He}$  and  $^{21}\text{Ne}$  require measurement with a rare-gas mass spectrometer. Although all these nuclides have been used in exposure age dating, only  $^3\text{He}$ ,  $^{21}\text{Ne}$ , and  $^{36}\text{Cl}$  methods will be discussed here. Other methods ( $^{10}\text{Be}$  and  $^{26}\text{Al}$ ) either require minerals (i.e., quartz; Nishiizumi et al., 1991) that are not readily available in the basaltic volcanic rocks in the YMR, or the method is not yet fully developed ( $^{14}\text{C}$ ; Bierman and Gillespie, 1991a). Both  $^3\text{He}$  and  $^{21}\text{Ne}$  are stable isotopes; however,  $^{36}\text{Cl}$  is radiogenic with a half life of  $3.08 \times 10^5$  yr.

Unlike the radiometric methods, cosmogenic surface exposure dating assumes negligible initial concentration of the cosmogenic isotope. The system also is open with respect to accumulation of cosmic-ray induced isotope but closed chemically and isotopically with respect to other noncosmogenic sources of the isotope. For stable nuclides such as  $^3\text{He}$ , exposure time to cosmic rays is assessed assuming a linear accumulation with time. For cosmogenic radionuclides, it is necessary to include the effects of both buildup and radioactive decay to determine the exposure age. It is important to note that these techniques have only been in use for the past 10 yr, and many of the assumptions used in the techniques (e.g., constant production rates) have not been fully tested. However, where well-constrained and carefully selected samples have been subjected to cosmogenic surface exposure dating, age agreement with other independent dating techniques has been good (Phillips et al., 1991; Anthony and Poths, 1992; Anthony, 1993).

The cosmogenic  $^{36}\text{Cl}$  method is based on the fundamental difference between high surface (cosmogenic) and low subsurface (radiogenic or background) production rates of  $^{36}\text{Cl}$ . In the subsurface,  $^{36}\text{Cl}$  forms almost exclusively by thermal-neutron activation of  $^{35}\text{Cl}$  by slow neutrons associated with radioactive decay of U and Th. In rocks exposed at the surface,  $^{36}\text{Cl}$  is produced primarily by spallation reactions on  $^{39}\text{K}$  and  $^{40}\text{Ca}$  due to fast secondary neutrons and by thermal-neutron activation of  $^{35}\text{Cl}$ . The subsurface  $^{36}\text{Cl}$  concentration is in secular equilibrium between radiogenic production and decay. The

**Table 3-1. Selected cosmogenic isotopes production reactions in terrestrial rocks.**

Isotope	Thermal Neutron	Negative mu-meson Principal target	Spallation
$^3\text{He}$	$^6\text{Li}(n, \alpha)^3\text{H}$	—	$^{14}\text{N}(n, ^3\text{He})^{12}\text{B}$ $^{19}\text{F}(n, ^3\text{He})^{17}\text{N}$ $^{40}\text{Ca}(n, ^3\text{He})^{38}\text{Ar}$
$^{21}\text{Ne}$		Na, Mg, Al, Si	
$^{36}\text{Cl}$	$^{35}\text{Cl}(n, \gamma)^{36}\text{Cl}$	$^{40}\text{Ca}(\mu^-, \alpha)^{36}\text{Cl}$	$^{39}\text{K}(n, 2n2p)^{36}\text{Cl}$ $^{40}\text{Ca}(n, 2n3p)^{36}\text{Cl}$

radiogenic  $^{36}\text{Cl}$  can thus be subtracted from the measured  $^{36}\text{Cl}$  to yield the cosmogenic component (Zreda et al., 1992).

The cosmogenic  $^3\text{He}$  method is based on the production of  $^3\text{He}$  primarily through cosmogenic spallation reactions (Kurz, 1986b; Lal, 1987). The total  $^3\text{He}$  in a sample reflects both magmatic and cosmogenic sources (Kurz, 1986a,b). In order to use  $^3\text{He}$  derived only from cosmic-ray interaction, it is necessary to subtract the magmatic component. The basic procedure to differentiate between the two components requires that the gas released during both crushing and during melting is analyzed for rare gas isotopes (Kurz, 1986b; Anthony and Poths, 1992). Unlike the  $^{36}\text{Cl}$  and methods based on the K/Ar system, measurements of  $^3\text{He}$  must be completed on mineral separates, because diffusional loss of helium isotopes can occur in groundmass material. The production rate of cosmogenic  $^3\text{He}$  is poorly known, and the effects of elevation, latitude, and depth of sample must be determined. Uncertainty in these parameters results in an overall accuracy of only 30 percent for  $^3\text{He}$  surface age dates (Anthony and Poths, 1992).

### 3.3.1 Analytical Methods

Several analyses, including major elements, B, REE (particularly Gd), total Cl, and mass spectrometric analysis of  $^{36}\text{Cl}$ , are needed for a  $^{36}\text{Cl}$  exposure date of a whole rock sample. The rock samples are cleaned of any organic material present at the surfaces, ground, and leached in 5-percent nitric acid to remove any secondary carbonates in the vesicles and micropores within the rock matrix. Chlorine for  $^{36}\text{Cl}$  analysis is obtained by dissolution of powdered rocks in a hot mixture of concentrated nitric and hydrofluoric acids with subsequent precipitation of Cl as AgCl (Zreda et al., 1992). The preparation and purification of the AgCl to remove isobaric isotopes require several wet chemistry steps prior to drying (Zreda et al., 1992). The dried, purified AgCl is mixed with a low-sulfur AgBr binder (not to exceed 3:1 AgBr:AgCl), loaded into custom-made, low-sulfur tantalum holders, and submitted for  $^{36}\text{Cl}$  analysis by tandem-accelerator mass spectrometry (Zreda et al., 1992; Elmore and Phillips, 1987). Major element composition is determined by x-ray fluorescence on fused disks, B and Gd by ICP-AE and prompt gamma emission spectrometry, and total Cl by combination ion-selective electrode (Zreda et al., 1992).

The calculation of an exposure date for the  $^{36}\text{Cl}$  method is equally complicated as the analysis [Eq. (3-1)]. The rates of  $^{36}\text{Cl}$  production due to spallation reactions are calculated from the measured Ca and K concentrations (Zreda et al., 1991), rates of  $^{36}\text{Cl}$  production due to thermal neutron activation of  $^{35}\text{Cl}$  are calculated from the whole rock chemical measurements, particularly influenced by B and Gd measurements (Zreda et al., 1991). Each of these rates must then be corrected for the effects of elevation, latitude, and depth below the surface (Zreda et al., 1991). Additionally, the production rate of  $^{36}\text{Cl}$  from negative muon capture is calculated from the Ca measurements and must be corrected for the effects of elevation and latitude (Zreda et al., 1991). The amount of cosmogenic  $^{36}\text{Cl}$  accumulated in a given sample after  $t$  yr of exposure to cosmic rays and with negligible erosion can be expressed as

$$R - R_0 = \left( \frac{E_n L_n D_n [\Psi_K C_K + \Psi_{Ca} C_{Ca} + \Psi_n] + E_\mu L_\mu \Psi_\mu}{\lambda N} \right) \times (1 - e^{-\lambda t}) \quad (3-1)$$

where

$R$	= atomic ratio of $^{36}\text{Cl}$ to stable Cl
$R_0$	= background $^{36}\text{Cl}/\text{Cl}$ supported by U- and Th-derived neutrons
$\Psi_K, \Psi_{Ca}$	= production rates due to spallation of $^{39}\text{K}$ and $^{40}\text{Ca}$ , in atoms $(\text{kg rock})^{-1} \text{yr}^{-1}$ per unit concentration of K or Ca, at sea level and latitudes $\geq 60^\circ$
$C_K, C_{Ca}$	= concentrations of K or Ca
$\Psi_n$	= production rate due to thermal neutron activation of $^{35}\text{Cl}$ , in atoms $(\text{kg rock})^{-1} \text{yr}^{-1}$ , at sea level and latitudes $\geq 60^\circ$
$\Psi_\mu$	= production rate due to slow negative muon capture by $^{40}\text{Ca}$ , in atoms $(\text{kg rock})^{-1} \text{yr}^{-1}$ , at sea level and latitudes $\geq 60^\circ$
$E, L, D$	= scaling factors for dependence of cosmic-ray neutron ( $n$ ) and muon ( $\mu$ ) fluxes based on elevation above sea level ( $E$ ), geomagnetic latitude ( $L$ ), and depth below surface ( $D$ )
$t$	= time of exposure, in years
$N$	= stable Cl concentration, in atoms $(\text{kg rock})^{-1}$
$\lambda$	= decay constant for $^{36}\text{Cl}$ , $2.30 \times 10^{-6} \text{yr}^{-1}$

Analysis for  $^3\text{He}$  and  $^{21}\text{Ne}$  requires preparation of 250- to 420- $\mu\text{m}$  olivine or clinopyroxene separates. Samples are analyzed on a static mass spectrometer equipped with ion-counting detectors (Anthony and Poths, 1992). The mineral separate is first crushed in vacuum, and the inherited (i.e., magmatic) component released is analyzed for the amount and isotopic composition of helium and neon. The same sample is then melted in a double-walled, all-metal vacuum furnace. The helium and neon released in this step is a combination of cosmogenic and residual magmatic components (Kurz, 1986a, b). Both the crushing and melting take place on-line to the mass spectrometer. For both steps, the heavy noble gases are removed by sorption on charcoal at liquid nitrogen temperatures, and the remaining gas is admitted to the mass spectrometer (Anthony and Poths, 1992). Blanks for  $^3\text{He}$ ,  $^4\text{He}$ , and neon isotopes are measured for both the crushing and melting steps for each sample (Anthony and Poths, 1992). Blanks for neon have atmospheric compositions. Cosmogenic  $^{21}\text{Ne}$  concentrations are calculated by assuming all  $^{20}\text{Ne}$  in the melt fraction is due to a component with atmospheric isotopic

composition and subtracting the corresponding amount of  $^{21}\text{Ne}$ . Atmospheric compositions of noble gases serve as standards. The helium analyses must be corrected for blank and mass fractionation (Anthony and Poths, 1992). Cosmogenic  $^3\text{He}$  is calculated by subtracting from the total  $^3\text{He}$  a magmatic component equal to the total  $^4\text{He}$  released in the melting step multiplied by the  $^3\text{He}/^4\text{He}$  ratio released in the crushing step. This method assumes that all the  $^4\text{He}$  released by heating is due to a magmatic component that has a helium isotopic composition identical to that released in the crushing step. This assumption is reasonable for low-uranium phases such as olivine (Anthony and Poths, 1992).

Neon isotopic concentrations can be used to monitor the assumption that all the  $^4\text{He}$  in the melt step belongs to the magmatic component (Anthony and Poths, 1992). Neon has three isotopes -  $^{20}\text{Ne}$ ,  $^{21}\text{Ne}$ , and  $^{22}\text{Ne}$ . Only the low-abundance  $^{21}\text{Ne}$  has a significant cosmogenic component. In the absence of radiogenic  $^4\text{He}$ ,  $^4\text{He}/^{20}\text{Ne}$  should be similar in both the crush and melt steps. Thus, the measured  $^4\text{He}/^{20}\text{Ne}$  is used to partition  $^4\text{He}$  in the melt step between magmatic and radiogenic components. In addition, neon data can be used to check for diffusive loss of  $^3\text{He}$  from the olivine. Because the diffusivity of He isotopes is much greater than the diffusivity of neon isotopes, the measured cosmogenic  $^3\text{He}/^{21}\text{Ne}$  for a sample that has not lost He via diffusion should be approximately 2.1 (Marti and Craig, 1987).

The calculation of  $^3\text{He}$  surface exposure dates is based upon a measured production rate at a given latitude and elevation, which is then corrected for the sample elevation, latitude, and sample thickness (Anthony and Poths, 1992; Lal, 1991). The surface exposure age is then given by

$$N = P_o t \quad (3-2)$$

where  $N$  is the measured cosmogenic  $^3\text{He}$ ,  $P_o$  is the corrected production rate, and  $t$  is time in years.

### 3.3.2 Sources of Error

Accuracy for  $^{36}\text{Cl}$  dates is primarily dependent on uncertainty in the production rates, which have been estimated to be less than 10 percent (Zreda et al., 1991) for the Great Basin area. Potential problems with temporal variations in cosmogenic nuclide production rates that affect young samples (< 10 ka) probably are negligible for older samples, because these variations are averaged over time (Zreda et al. 1991). Analytical errors associated with the determination of major and trace elements, and stable Cl, are on the order of a few percent. Analytical errors for  $^{36}\text{Cl}$  range from 5–10 percent and lead to similar uncertainties in  $^{36}\text{Cl}$  ages. Another possible source of error is from geometrical corrections, which can reduce the thermal-neutron absorption rate by 30 percent (Zreda et al., 1993). An overall conservative estimate of accuracy for this dating method is about 20 percent, given the uncertainties in the production rates and the calibration of these production rates to the uncorrected  $^{14}\text{C}$  timescale (Zreda et al., 1991). Precision of  $^{36}\text{Cl}$  dates depends mainly on rates of postdepositional processes occurring on sampled surfaces. Erosional removal of < 80 cm of soil since surface formation results in a small overestimation of the age, whereas removal of thicker material will have an opposite effect (Zreda et al., 1991, 1993). Multiple analyses from the same surface by Zreda et al. (1993) indicate a precision of 10 percent or better for surface exposure dating of young volcanic rocks. Thus, the precision of this technique is much better than those methods based on the K/Ar and U/Th system for very young volcanic rocks.

A reasonable uncertainty for  $^3\text{He}$  is about 30 percent. This uncertainty can be attributed primarily to assumptions about the constancy and accuracy of the  $^3\text{He}$  production rate (Cerling, 1990; Kurz et al., 1990). The production rate has been precisely calibrated at only around 15 ka and may vary by 10 to 20 percent due to changes in the intensity of cosmic-ray flux with time. Also, the production rate is tied to the  $^{14}\text{C}$  timescale, and all ages, to date, would increase by approximately 17 percent if adjusted to the proposed revisions in that timescale (Bard et al., 1990; Anthony 1993). A 30-percent uncertainty for this technique should be used when comparing the results to other dating techniques (Anthony and Poths, 1992). Analytical uncertainties, which represent full error propagation in the experiments, are usually smaller than 30 percent (Table 3-2; Poths and Crowe, 1992; Anthony and Poths, 1992). Comparison of dates derived from different samples of the same surface indicates the best estimate for precision of  $^3\text{He}$  surface exposure ages is 14 percent (Anthony and Poths, 1992).

### 3.3.3 Material Dated

For  $^{36}\text{Cl}$  surface exposure dating, the whole rock is analyzed with whole-rock chemical analysis, selective extraction of Cl via acid extraction, and Cl measurements on completely dissolved rock. Multiple samples for  $^{36}\text{Cl}$  analysis are collected from the top 5 cm, with hammer and chisel, of carefully selected rocks (Zreda et al., 1991). Surfaces should be chosen that minimize the chances that the material to be dated has been modified by erosional processes. Suitable rocks should exhibit primary flow feature, such as spatter, flow lineation, and cooling rinds (Anthony and Poths, 1992); sites also should be checked to ascertain whether the sample surface had been previously covered by eolian deposits or altered by weathering (Zreda et al., 1993). Samples containing noticeable quantities of secondary minerals should be avoided. However, a correction method, which introduces further uncertainty in the calculated exposure age, can be applied to those samples containing secondary minerals (Zreda et al., 1993).

For  $^3\text{He}$  surface exposure dating, olivine and pyroxene are both satisfactory. However, plagioclase, volcanic glass, and quartz are unsuitable because they do not quantitatively retain helium isotopes in the crystal lattice (Kurz et al., 1990; Cerling, 1990). A similar sample surface evaluation procedure to that used in the  $^{36}\text{Cl}$  method also should be used for  $^3\text{He}$  exposure dating (Anthony and Poths, 1992).

### 3.3.4 Application to the Yucca Mountain Region

Use of cosmogenic nuclide methods to determine the exposure ages of surfaces has been limited to  $^3\text{He}$  and  $^{36}\text{Cl}$  measurements of samples from the Lathrop Wells volcanic center (Poths and Crowe, 1992; Crowe et al., 1993; Zreda et al., 1993). The  $^3\text{He}$  dates are presented in Table 3-2, along with all the available analytical data. As has been observed for most geochronological data in the YMR, details of the analytical methods used and the sample locations were not provided for the  $^3\text{He}$  dates (Poths and Crowe, 1992; Crowe et al., 1993). As pointed out by Anthony and Poths (1992), the absolute accuracy for  $^3\text{He}$  dates is probably only 30 percent. However, because the precision of the measurements is much less than 30 percent, this technique is applicable for relative dating of surfaces at a particular site. Within the resolution of this technique, the three lava units dated by Poths and Crowe (1992) apparently are the same age. Only minimum ages are generated using the  $^3\text{He}$  technique on samples that might have been wholly or partially covered by eolian or alluvial deposits during residence at the earth's surface. Using the 30-percent accuracy figure of Anthony and Poths (1992), and the oldest age generated (44 ka) for the Lathrop Wells scoria cone, a minimum exposure age of Lathrop Wells is thus  $44 \pm 13$  ka.

Table 3-2.  $^3\text{He}$  dates for units from the Lathrop Wells complex, from Poths and Crowe (1992), and Crowe et al. (1993) unit designations from Crowe et al. (1993). *Error* is the percentage error between *Age* and  $\pm 1\sigma$ . *Simple Avg* is the average and standard deviation of the reported ages. *Wgt Mean* is the weighted mean of the dates [Eq. (1-3)] *Average Date* reports propagated uncertainties [Eqs. (1-1 and 1-2)].

Unit	Rock	Age (ka)	$\pm 1 \sigma$ (ka)	%Error	Reference
Qs <sub>2a</sub>	Scoria	22	4	18	Poths and Crowe, 1992
Qs <sub>2a</sub>	Scoria	28	4	14	Poths and Crowe, 1992
Qs <sub>2a</sub>	Scoria	44	6	14	Poths and Crowe, 1992
Qs <sub>2a</sub>	Scoria	36	4	11	Crowe et al., 1993
Ql <sub>3</sub>	Lava	65	7	11	Poths and Crowe, 1992
Ql <sub>3</sub>	Lava	73	9	12	Poths and Crowe, 1992
Ql <sub>4</sub>	Lava	48	5	10	Poths and Crowe, 1992
Ql <sub>4</sub>	Lava	> 49			Poths and Crowe, 1992
Ql <sub>5</sub>	Lava	64	6	9	Poths and Crowe, 1992
Ql <sub>5</sub>	Lava	59	6	10	Poths and Crowe, 1992
Simple Avg $48.8 \pm 17.8$		Wgt Mean $33.6 \pm 2.1$		Average Date $48.8 \pm 25.2$	

Only the  $^{36}\text{Cl}$  study by Zreda et al. (1993) provided sufficient analytical information to independently calculate the reported dates. The sample ages and accompanying data for the  $^{36}\text{Cl}$  analyses are presented in Table 3-3. Sufficient information also was presented in this study to determine that erosional modification and secondary mineralization had not occurred for each sample and to make the necessary correction for thermal-neutron leakage associated with the irregular geometry of pressure-ridge samples. Note that the units used for Table 3-3 reflect those of Turrin et al. (1991). As concluded by Zreda et al. (1993), the average ages for the main scoria cone and stratigraphically older Q1<sub>5</sub> lava flow (Crowe et al., 1988) are statistically indistinguishable. However, the  $1\sigma$  statistics of the combined data still provide a 16-k.y. interval within which the center could have erupted more than once.

### 3.4 FISSION-TRACK DATING

Although the fission-track dating method has several potential applications to dating late Neogene and Quaternary volcanic rocks in the YMR, it has not been so applied. The fission-track dating method basically involves counting the number of tracks left in a mineral or glass by the spontaneous fission of  $^{238}\text{U}$ , which has a half-life for spontaneous fission of about  $8.6 \times 10^{15}$  years (Geyh and Schleicher, 1990). Assuming that the fission tracks do not fade or anneal with time, the date of the sample is proportional to the density of tracks. Lower age limits for fission-track dating of uranium-rich minerals such as zircon is  $10^3$  years, and for apatite it is about  $10^4$  years. The minerals become saturated with fission-tracks after about  $10^8$  years (Geyh and Schleicher, 1990).

Fission tracks are annealed in sphene, epidote, and allanite at temperatures around 300 °C, about 200 °C for zircon, and 150 °C for apatite (Fleischer et al., 1965; Green et al., 1986). The exact temperatures and duration of heating necessary for annealing depend on the number of tracks initially in the mineral, mineral composition, and crystal size (Fleischer et al., 1965). The low temperature of annealing may permit the dating of suitable minerals in small silicic xenoliths commonly found in young basaltic volcanoes.

#### 3.4.1 Analytical Methods

The primary analysis for fission-track dating is the precise determination of the uranium concentration in the sample. The uranium concentration is usually determined by irradiating the sample to produce neutron-induced fission of  $^{238}\text{U}$ . By counting the density of spontaneous ( $\rho_{sf}$ ) and artificially induced ( $\rho_i$ ) fission tracks, a date can be calculated (Price and Walker, 1963)

$$\text{Date} = \frac{1}{\lambda_{238\text{tot}}} \ln \left[ 1 + \frac{\rho_{sf}}{\rho_i} \frac{\lambda_{238\text{tot}} \Phi \sigma_{235}}{\lambda_{238\text{sf}}} \left( \frac{^{235}\text{U}}{^{238}\text{U}} \right) \right] \quad (3-3)$$

where	$\lambda_{238\text{tot}}$	= total decay constant for $^{238}\text{U}$
	$\lambda_{238\text{sf}}$	= decay constant for the spontaneous fission of $^{238}\text{U}$
	$\Phi$	= thermal neutron fluence during irradiation
	$\sigma_{235}$	= neutron capture cross-section for $^{235}\text{U}$ fission
	$^{235}\text{U}/^{238}\text{U}$	= 1/137.88

Table 3-3.  $^{36}\text{Cl}$  exposure age dates for units of the Lathrop Wells center (Zreda et al., 1993). Unit designations from Turrin et al. (1991) and Crowe et al. (1993) in braces. Samples LWC88 3-6 are loose volcanic bombs from the main scoria cone resting on alluvium or pyroclastic surge deposits west of the main Lathrop Wells cone. Samples LWC89-S and -W are from the summit of the Lathrop Wells Cone. *Error* is the percentage error between *Age* and  $\pm 1\sigma$ . *Simple Avg* is the average and standard deviation of the reported ages. *Wgt Mean* is the weighted mean of the dates [Eq. (1-3)] *Average Date* reports propagated uncertainties [Eqs. (1-1 and 1-2)].

Unit	Sample	Age (ka)	$\pm 1 \sigma$ (ka)	% Error
Qs <sub>5</sub> (Qps <sub>1</sub> )	LWC88-3	79	3.4	4
Qs <sub>5</sub> (Qps <sub>1</sub> )	LWC88-4	96	4.5	5
Qs <sub>5</sub> (Qps <sub>1</sub> )	LWC88-5	85	4.6	5
Qs <sub>5</sub> (Qps <sub>1</sub> )	LWC88-6	78	4.6	6
Ql <sub>5</sub>	LWC88-1	93	7.2	8
Ql <sub>5</sub>	YM88-5	73	6.8	9
Ql <sub>5</sub>	YM88-6L	81	5.4	7
Ql <sub>5</sub>	YM88-6M	77	6.0	8
Ql <sub>5</sub>	YM88-8	79	6.1	8
Qs <sub>5</sub>	LWC89-S	83	9.2	11
Qs <sub>5</sub>	LWC89-W	68	5.7	8
Simple Avg 81. $\pm$ 5.8		Wgt Mean 84 $\pm$ 2		Average Date 81 $\pm$ 16

Many of the uncertainties in these values can be eliminated if a standard with known age is irradiated with the sample (Geyh and Schleicher, 1990). The date of the sample is calculated by counting the natural ( $\rho_{msf}$ ) and induced ( $\rho_{mi}$ ) fission tracks in the standard, and a date calculated by.

$$\text{date} = \frac{\text{std age} \left( \frac{\rho_{sf}}{\rho_i} \right) \rho_{mi}}{\rho_{msf}} \quad (3-4)$$

After irradiation, the mineral grains are mounted in epoxy and polished to remove the upper 25  $\mu\text{m}$ . The minerals are etched with either strong acids or bases to enhance identification of fission tracks and counted under a microscope. Track densities between  $10/\text{cm}^2$  and  $2 \times 10^7/\text{cm}^2$  are required for accurate dates (Geyh and Schleicher, 1990).

### 3.4.2 Sources of Error

The largest source of error in fission-track dates is the uncertainty associated with the choice of a decay constant for natural  $^{238}\text{U}$  fission, which ranges from  $6.85 \times 10^{-17} \text{yr}^{-1}$  to  $8.57 \times 10^{-17} \text{yr}^{-1}$  and imparts an error of about 10 percent to the sample date (Geyh and Schleicher, 1990). Dates determined using a calibrated standard method may have uncertainties of about 5 percent, depending on the age of the standard and material being dated (Geyh and Schleicher, 1990). Errors in track density can be minimized by counting  $10^4$  tracks, which reduces this uncertainty to 1 percent (Wang et al., 1975). Counting  $10^3$  tracks will increase this uncertainty to 3 percent, with 10-percent uncertainty resulting from counting only 100 tracks.

Another potentially significant source of error for fission-track dating is the assumption that uranium is homogeneously distributed throughout the sample. Uranium is often zoned in zircons that have a complex geologic history (e.g., Watson and Harrison, 1984), which may lead to erroneous fission-track dates.

### 3.4.3 Material Dated

Minerals that contain relatively high abundances of uranium commonly are dated through the fission-track method. For Quaternary dates, zircon or silicic glass generally contain uranium abundances sufficient for fission-track dating (e.g., Westgate, 1989). Apatite, sphene, and allanite also can be used for late Quaternary to Neogene dates.

### 3.4.4 Application to the Yucca Mountain Region

The fission-track dating method has not been applied to post-10-Ma volcanic rocks in the YMR. Basaltic rocks are undersaturated with  $\text{P}_2\text{O}_5$  at water contents  $< 5$  weight percent (Green and Watson, 1982) and thus commonly lack phenocrysts of apatite. However, local saturation of  $\text{P}_2\text{O}_5$  can occur at phenocryst-melt interfaces and result in the crystallization of microphenocrysts of apatite in basalt (Green and Watson, 1982; Bacon 1989). Apatite is reported as a groundmass mineral in some YMR basalt (e.g., Vaniman et al., 1982), although these microlites are probably too small to yield meaningful fission-track dates. Basaltic magmas are too undersaturated with zirconium to crystallize zircon under reasonable conditions (Watson and Harrison, 1983).

A potential application of the fission-track dating technique to young basaltic rocks was demonstrated by Calk and Naeser (1973), who obtained fission-track dates from granitic xenoliths in shallow basaltic intrusions. The heat from the basalt was sufficient to completely anneal pre-existing fission tracks in the trace minerals upon incorporation of the xenolith. Subsequent fission tracks formed after the xenolith cooled below about 300 °C and represent the age of the host basalt. Shallow crustal xenoliths in basaltic volcanoes of the YMR primarily consist of Tertiary rhyolitic ignimbrite, which commonly contains trace amounts of sphene and zircon (e.g., Byers et al., 1976). Centimeter-sized xenoliths are likely to have reached temperatures in excess of 300 °C if they were erupted in lava flows, and may have attained this temperature if erupted with basaltic scoria. Pre-existing fission tracks may have been annealed upon eruption of the xenolith. Existing fission tracks would have formed subsequent to eruption and thus reflect the age of the host basalt.

## 4 INDIRECT DATING METHODS

### 4.1 GENERAL PRINCIPLES

A number of widely applied geochronology techniques utilize basic geological information to derive relative, and at times absolute, ages of volcanic units. These methods are based on correlating specific features of a sample, such as the orientation of remnant magnetization, with the same features on a unit of known age. Application of these methods requires that the ages of reference units are well-constrained through direct dating, and that specific geological features can be uniquely identified in the studied samples. Although these methods are generally incapable of producing absolute ages, they often provide useful age constraints and can be used to test the precision and accuracy of radiometric and radiation-interaction dates.

Many of the indirect dating methods are based on stratigraphic relationships, which can be poorly developed in young volcanic terranes. Most flows and pyroclastic units have restricted occurrences due to pre-existing topography or prevailing winds. Determining these stratigraphic relationships usually requires detailed studies, including geochemical analyses, age determinations, and subsurface information. Regionally extensive marker beds generally occur in large depositional basins and are only rarely preserved in basaltic volcanic fields (e.g., Sarna-Wojcicki et al., 1985). The tephra from basaltic volcanoes is not regionally extensive and generally lacks the compositional distinctions necessary for robust stratigraphic correlations. Most volcanic eruptions are spatially and temporally isolated and, thus, do not have useful stratigraphic relationships. Fossiliferous sediments occur in relatively low-energy pluvial systems that receive large inputs of silicic ash, and are thus rare in young basaltic volcanic terranes.

### 4.2 PALEOMAGNETIC DATING

The orientation of a lava's magnetic field reflects the orientation of the earth's magnetic field at the time the lava cooled. Because the orientation of the earth's magnetic field has changed markedly through time, remnant magnetization can be used to date or correlate basaltic rocks (e.g., Tarling, 1983).

About 80 percent of the earth's geomagnetic field can be modeled as a simple dipolar magnet, which presently has a north pole inclined about 12 degrees from the earth's axis of rotation. Changes in the dipole field consist of episodes of polarity reversal, which have durations of  $10^4$  to  $10^6$  years (e.g., Cox, 1969; Mankinen and Dalrymple, 1979). The ages and durations of these reversals are relatively well-constrained for rocks younger than about 5 Ma (Figure 4-1). Magnetic polarity timescales with less precision and accuracy also have been developed for rocks as old as 100 Ma (Harland et al., 1982).

The remaining nondipolar component to the magnetic field consists of about 12 large regions on the earth's surface (Tarling, 1983). Changes in the intensity and directions of the nondipolar field occur over periods of  $10^0$  to  $10^3$  years, and are referred to as *secular variations* (e.g., Creer, 1981). For the western United States, the present drift of the nondipolar (i.e., secular) field is about 0.25 degree westward per year (Tarling, 1983). Secular variations of about 4.5 degrees per century also were determined by Holcomb et al. (1986) for the last 200 years of volcanic activity on Hawaii. For sites at middle latitudes, secular variation over time can result in declination changes of about 20 degrees and inclination changes of about 25 degrees, relative to the average magnetic field direction (e.g., Champion, 1991).

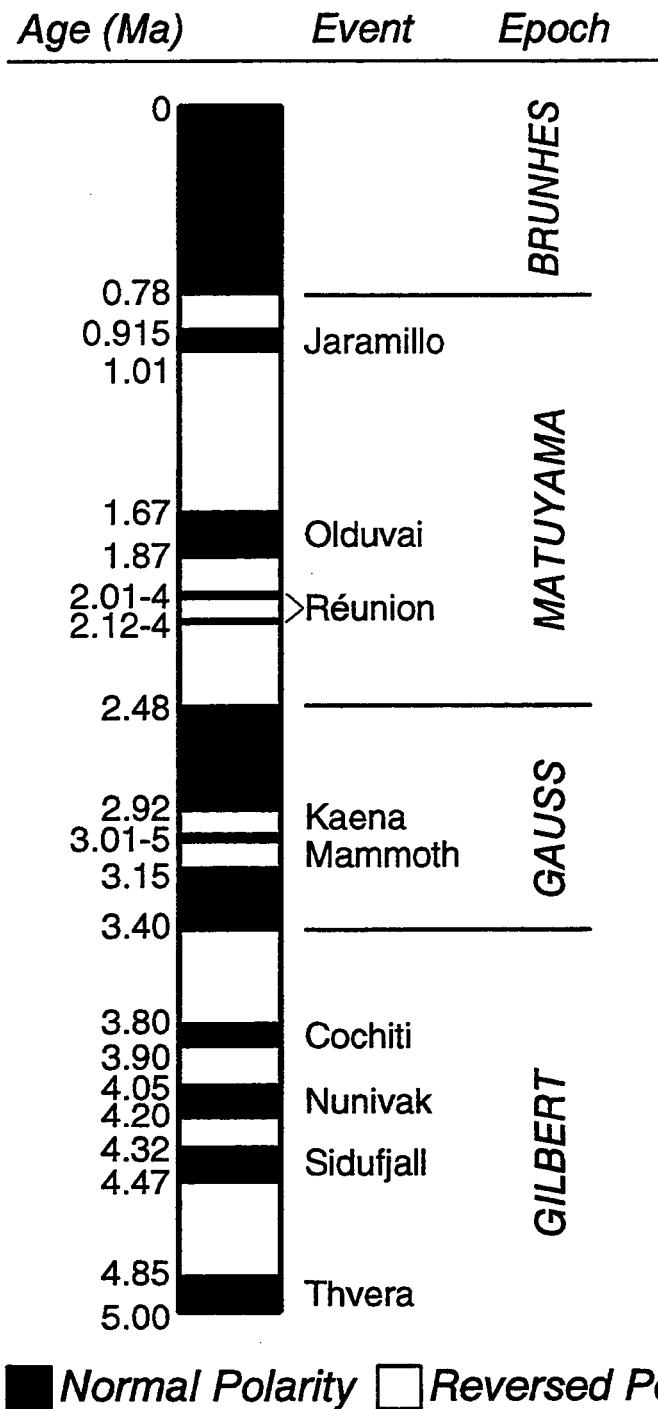


Figure 4-1. Late Cenozoic paleomagnetic polarity timescale from Mankinen and Dalrymple (1979), modified to include new age determinations by Spell and McDougall (1992). Age ranges of short events are for last significant figure, that is, 2.01-4 represent 2.01 to 2.04 Ma.

When a lava cools below about 580 °C, magnetic minerals such as the iron-oxides begin to acquire a remnant magnetization that is oriented in the same direction as the geomagnetic field. The temperature at which a mineral acquires this magnetization is commonly referred to as the *Curie temperature* or *blocking temperature*. The stability of the thermoremanent magnetization depends on the size, composition, and postcooling alteration of the magnetic minerals (e.g., Geyh and Schleicher, 1990). Fine-grained sediments also can acquire a remnant magnetization through the alignment of detrital magnetic grains with the geomagnetic field present during deposition (e.g., Negrini et al., 1988).

Paleomagnetic orientations obtained from lavas can be compared to assess the likelihood that the lavas erupted at the same time. Assuming that the units have not been rotated since cooling, differences in paleomagnetic orientation clearly indicate that the lavas formed at different times. In addition, lavas with similar paleomagnetic orientations may be of similar age. However, the directions of the secular field have not been unique through time and lavas with very similar paleomagnetic orientations may have significantly different ages (e.g., Champion, 1980). It is important to remember that resolvable differences in the nondipolar component of earth's magnetic field can develop in under 100 years (e.g., Mankinen et al., 1986), which may not represent a significant interval of time in some geologic studies.

#### 4.2.1 Analytical Methods

Samples are collected in the field by using a portable drill to cut centimeter-size oriented cores from intact outcrops. A general practice is to collect about ten cores from each sample site and to have several sample sites within each unit (e.g., Holcomb et al., 1986). Paleomagnetic orientation measurements are generally made with a spinner magnetometer, which rotates the sample in the center of a large flux-gate coil. A potential proportional to the magnetic field of the sample is produced in these coils (e.g., Sharma, 1986). This potential is recorded at specific positions during each rotation and calculated into a magnetic field vector, which has the following components.

- Declination ( $D$ ), which is the difference in azimuth between the geographic and magnetic poles measured in degrees clockwise from north
- Inclination ( $I$ ), which is the dip angle of the magnetic pole measured in degrees from horizontal
- Field intensity ( $J$ ), which is the intensity of the magnetic field present when the rock cooled below the curie temperature measured relative to the present-day geomagnetic field intensity

Following the measurement of the natural remnant magnetization (NRM), several additional steps can be performed to evaluate the quality of the paleomagnetic signal. Samples can be exposed to progressive alternating-field demagnetization, which incrementally reduces the paleomagnetic signal of the sample. Above a demagnetization field of around 20 milliteslas (mT), the paleomagnetic field vectors should form a straight line when direction is plotted on orthogonal projection plot. This higher coercivity component represents the paleomagnetic field preserved by the sample during formation. The lower coercivity component (<20 mT) generally represents a secondary viscous remnant magnetization (VRM), which is produced by long-term exposure of the sample to the earth's magnetic field (Sharma, 1986). If the lower coercivity component plots along the same trend as the higher coercivity component, both components are generally reported as the NRM. If, as is often the case, the VRM is a different direction

than the higher coercivity component, the lower coercivity component is removed from the sample and the magnetization field at which it was removed is reported (e.g., Mankinen et al., 1986). VRM also can be removed by incrementally heating the sample up to about 150 °C and cooling it in a magnetic field-free environment (Sharma, 1986).

The paleomagnetic orientation for each sample is then averaged to produce the paleomagnetic orientation for the unit (Sharma, 1986). The declination ( $D_s$ ) and inclination ( $I_s$ ) for each sample first is used to calculate directional cosines ( $l, m, n$ )

$$l = \cos D_s \cos I_s \quad m = \sin D_s \cos I_s \quad n = \sin I_s \quad (4-1)$$

The mean of these vectors is then calculated to determine the unit's declination ( $D_U$ ) and inclination ( $I_U$ ) vector, which has a length of  $R$

$$R = [(\sum l)^2 + (\sum m)^2 + (\sum n)^2]^{1/2} \quad (4-2)$$

$$D_U = \cot [(\sum m)/(\sum l)]; \quad I_U = \csc [(\sum n)/R] \quad (4-3)$$

In addition, two additional parameters are usually calculated to provide a measure of the precision of the mean paleomagnetic orientation (Fisher, 1953). The parameter  $K$  provides a measure of the scatter in the population containing  $N$  samples

$$K = (N-1)/(N-R) \quad (4-4)$$

A  $K$  value of about 1 indicates a random distribution of paleomagnetic orientations, and will equal infinity for identical direction.  $K$  values are commonly around 10 for units that show large amounts of scatter in sampled paleomagnetic orientation, and range between about 100 to 1000 for tightly clustered data. The parameter  $\alpha_{95}$  (Fisher, 1953) is used to show that at a 95-percent probability level, the given mean orientation lies within a circular cone with a semivertical angle given by

$$\alpha_{95} = \sec \left\{ 1 - \frac{N-R}{R} \left[ \left( \frac{1}{0.05} \right)^{1/(N-1)} - 1 \right] \right\} \quad (4-5)$$

In general,  $\alpha_{95}$  values tend to be less than about 5 degrees for tightly clustered data and greater than about 10 degrees for dispersed data.

The unit's paleomagnetic orientation can then be compared with other units in the area or to secular variation curves for the region under investigation. If two units have the same paleomagnetic orientation within analytical error, there is a likelihood that the units are contemporaneous. However, additional stratigraphic or volcanologic data are needed to robustly demonstrate that the paleomagnetically similar units are truly contemporaneous, or merely formed during different periods of similar geomagnetic orientation (e.g., Bogue and Coe, 1981). In contrast, a lack of paleomagnetic correlation shows that the units are not temporally equivalent. The length of time necessary to produce the directional

differences is poorly constrained for most rocks, because large changes in paleomagnetic orientation can develop over geologically unresolvable periods of time (e.g., Champion, 1980).

#### 4.2.2 Sources of Error

The most significant sources of error in paleomagnetic dating occur during sample selection and preparation. In young volcanic terranes, it is often difficult to determine if the outcrop has remained in place since cooling below a Curie temperature of about 580 °C (Tarling, 1983). Lava flow interiors commonly yield more consistent paleomagnetic orientations than flow exteriors, due to the mobility of large blocks along flow boundaries. Small degrees of tilting also may be difficult to detect in localized Quaternary deposits, which could affect correlations with secular variation curves. Weathering and alteration will commonly produce a large viscous remnant magnetization that may cause large systematic errors if uncorrected (e.g., Bogue and Coe, 1981). To avoid these problems, paleomagnetic sampling should be conducted only on fresh exposures of rock that have remained demonstrably stable since formation.

Lightning strikes also can affect the magnetization of a sample. These effects are very localized (centimeters to decimeters) and commonly are marked by a fused surface (Graham, 1961). Lightning strikes will usually result in a random orientation to the NRM of a sample (Tarling, 1983), which usually persists through demagnetization procedures. The effects of lightning strikes can be mitigated through collecting at least ten samples per site, and sampling several sites for each unit.

Most paleomagnetic orientations can be measured to within  $\pm 0.5$  degree, with the uncertainty in the declination exceeding the uncertainty in the inclination by around a factor of 2 (Geyh and Schleicher, 1990). The variation in paleomagnetic orientation observed for most samples at a site commonly exceeds this analytical uncertainty, and the  $K$  and  $\alpha_{95}$  statistics better represent the uncertainty in a unit's paleomagnetic orientation.

#### 4.2.3 Material Dated

Any unit that has been heated above the Curie temperature for the magnetic minerals present and quickly cooled can be measured for paleomagnetic orientation. Lava flows provide excellent paleomagnetic samples, due to the relatively uniform distribution of equigranular magnetic iron-oxides and rapid quenching below a Curie temperature of around 580 °C. Large bombs or agglutinated scoria also can be sampled for paleomagnetic orientation, provided the unit has remained stable since formation. Fine-grained lacustrine sediments, which may occur in young volcanic terranes, also can provide paleomagnetic orientation data (e.g., Negrini et al., 1988).

#### 4.2.4 Application to the Yucca Mountain Region

Paleomagnetic studies in the YMR have focused on the Lathrop Wells eruptive center (Champion, 1991; Turrin et al., 1991; Crowe et al., 1992b, 1993). Much of the controversy surrounding Lathrop Wells focuses on the detection of multiple eruptions separated by some finite, but measurable, amount of time. As was observed for direct dating studies, all paleomagnetic studies at Lathrop Wells to date have failed to provide sufficient analytical information to permit independent determinations of precision and accuracy. These paleomagnetic data should thus be viewed as preliminary, and no firm conclusions about these data can be reached until additional analytical information is provided.

Champion (1991) sampled 27 sites at Lathrop Wells (Figure 4-2) in units he refers to as  $Q_{s5}$  (older flows and scoria),  $Q_{l3}$  (younger flows), and  $Q_{s1}$  (main cone, equivalent to  $Q_{s2a}$  on Figure 4-2). Although paleomagnetic orientation data and statistical parameters are not provided, Champion (1991) reports an angular difference of 4.7 degrees between his units  $Q_{s5}$  and  $Q_{l3}$ , which is interpreted to indicate that these units represent paleomagnetically distinct events at a 99.98-percent confidence level. Based on an historic secular variation of about 4.5 degrees per century (Champion, 1980; Holcomb et al., 1986), Champion (1991) concludes that only 100 yr separate units  $Q_{s5}$  and  $Q_{l3}$ . Champion (1991) also reports that 40 samples from a site along the upper rim of the main Lathrop Wells scoria cone ( $Q_{s1}$ ) are indistinguishable from his unit  $Q_{s5}$ , and concludes that Lathrop Wells is a simple monogenetic volcano. The paleomagnetic data in Turrin et al. (1991) is a duplication of the data in Champion (1991).

Crowe et al. (1992b) do not present any paleomagnetic data, but state that their units  $Q_{l6}$  and  $Q_{l5}$  (Figure 4-2) have preliminary paleomagnetic orientations that do not differ significantly from Turrin et al. (1991). Samples from unit  $Q_{l4b}$  (Figure 4-2) also have preliminary paleomagnetic orientations that are similar to those reported by Turrin et al. (1991), presumably for their unit  $Q_{l3}$ . Crowe et al. (1992b) are careful to note that their data are preliminary, and that detailed demagnetization studies are required for these samples.

Some of the paleomagnetic data referred to by Crowe et al. (1992b) is presented by Crowe et al. (1993). Two sites in unit  $Q_{l6}$  (Figure 4-2) are statistically indistinguishable and have  $K = 93.2, 210.9$  and  $\alpha_{95} = 5.3, 3.5$ , respectively. Their sample sites in units  $Q_{l5}$  and  $Q_{l4b}$  (Figure 4-2) have dispersed paleomagnetic orientations and thus cannot be correlated with other units. Crowe et al. (1993) report that there are ongoing studies of paleomagnetic samples for units  $Q_{s6}$ ,  $Q_{s5}$ ,  $Q_{l4b}$ ,  $Q_{s4a}$ ,  $Q_{l4}$ ,  $Q_{l3}$ , and  $Q_{s2a}$  (Figure 4-2).

None of the paleomagnetic data presented to date disprove the polycyclic model proposed for Lathrop Wells by B.M. Crowe and coworkers (e.g., Crowe et al., 1992b). Small differences in paleomagnetic orientation apparently occur between early lavas and scoria (units  $Q_3$  to  $Q_6$ , Figure 4-2) and later deposits associated with the main cone (unit  $Q_2$ , Figure 4-2). However, the length of time required to produce the angular differences is not well constrained. Historic secular variations of about 4 degrees per century (Holcomb et al., 1986; Champion, 1991) may not accurately represent Quaternary secular variations. For example, the rate of secular variation reported by Mankinen et al. (1986) for the last 2,000 yr varies considerably. Sizeable differences in the paleomagnetic field orientation can develop in tens of years, or the orientation may remain relatively stable for hundreds of years (Mankinen et al., 1986). Holocene secular variations also are of smaller magnitude relative to the Quaternary (Mankinen et al., 1986). It is thus impossible to determine the length of time represented by the observed 4.7 degrees angular variation at Lathrop Wells (Champion, 1991; Crowe et al., 1993) without first determining, to within several hundred years, the absolute age of Lathrop Wells. Such an age resolution is impossible with currently available geochronological techniques. Thus, the paleomagnetic variations at Lathrop Wells do not refute the hypothesis of polycyclic volcanism (e.g., Crowe et al., 1992b), and may have been produced over periods of time much longer than the hundred years proposed by Champion (1991) and Turrin et al. (1991).

Champion (1991) sampled 13 sites at the Sleeping Butte volcanoes (Figure 2-1). Individual sites are not differentiated between the two volcanoes at the Sleeping Butte center; only ten data points are shown in the report, and descriptive statistics are not reported. Champion (1991) concludes that the small angular difference between Black Peak and Hidden Cone have only a 5-percent probability of being random variations in the paleomagnetic field. This conclusion suffers from the same limitations described

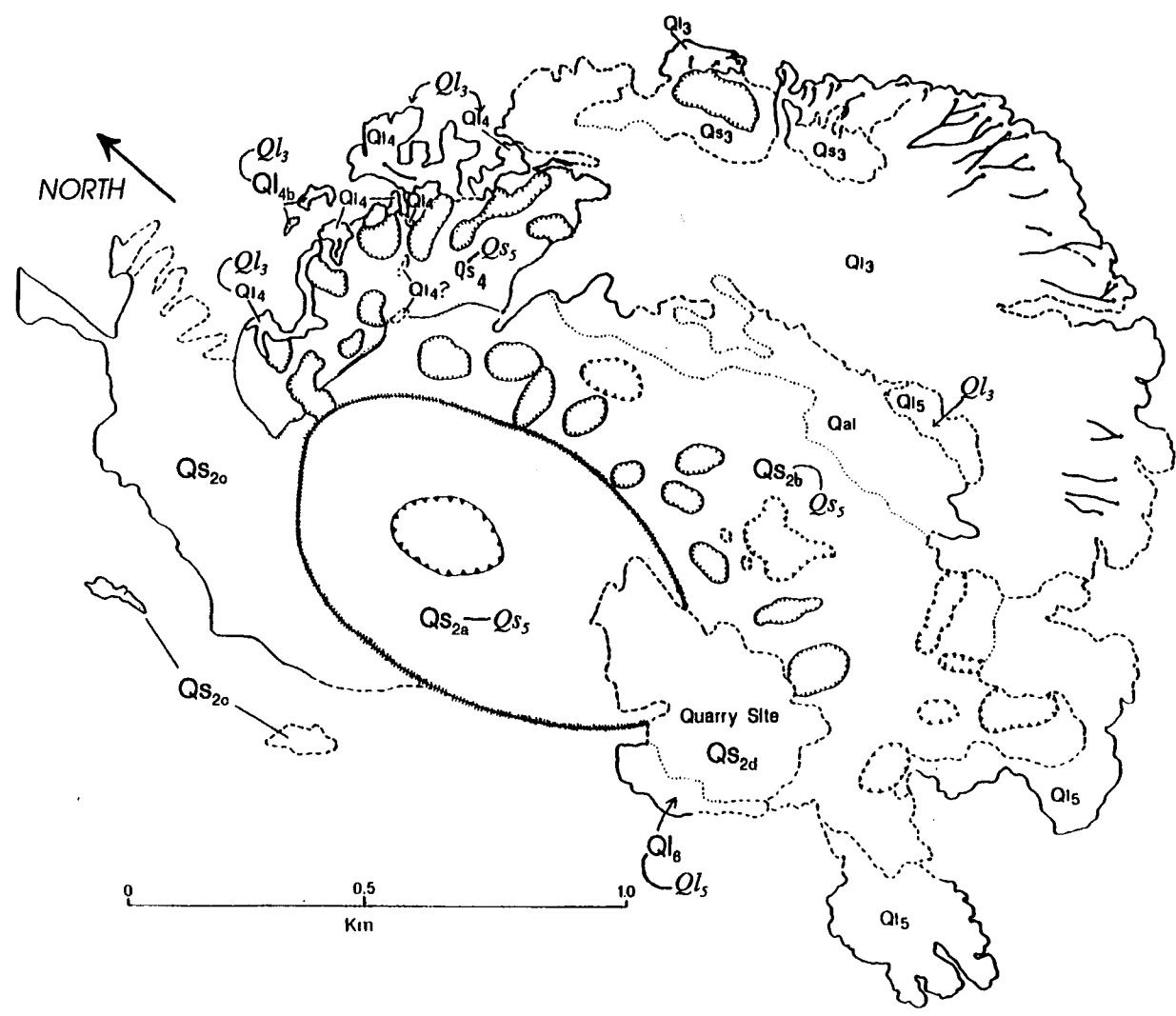


Figure 4-2. General geologic map of Lathrop Wells (Crowe et al., 1988) modified to show unit designations of Crowe et al. (1993), Champion (1991)(italics), and Turrin et al. (1991)(italics), and to indicate true north. Unit *Qs<sub>1</sub>*, of Champion (1991) is equivalent to unit *Qs<sub>2a</sub>* of Crowe et al. (1988).

for Lathrop Wells, in that small angular variations in paleomagnetic orientation are presumed to represent a small, finite, and well-constrained interval of time. Again, the paleomagnetic data for the Sleeping Butte volcanoes (Champion, 1991) fail to disprove the hypothesis of polycyclic eruptions at this center (e.g., Crowe and Perry, 1991).

Quaternary Crater Flat volcanoes also were studied by Champion (1991). Although 20 sites were reportedly sampled, only 10 sites are presented in the report. These data cannot be evaluated without first knowing sample locations, number of samples per site, number of sites per volcano, magnetic orientation data for all samples, and the descriptive statistics for each unit. The limited data presented by Champion (1991) apparently indicate that some sample sites have distinct paleomagnetic orientations at a 95-percent confidence interval, which would refute the stated conclusion that all five of the Quaternary Crater Flat volcanoes erupted within the span of 100 yr. A limited number of data also were presented by Champion (1991) for the Pliocene Crater Flat basalt. Although only a minimum of information is presented, the four sampled sites appear to have small differences in paleomagnetic orientation (Champion, 1991).

In conclusion, paleomagnetic studies can demonstrate that volcanic units are likely contemporaneous, or were formed during magnetically discrete intervals of time. However, the absolute amount of time necessary to produce resolvable differences in paleomagnetic orientation is at best poorly known for eruptions older than about 2 ka. None of the basaltic rocks sampled in the YMR have unique or diagnostic paleomagnetic orientations that can be compared to western North America secular variation curves, and thus cannot be assigned ages based on magnetic data. Available paleomagnetic data do not disprove the hypothesis of polycyclic volcanism proposed for many of the Quaternary volcanoes in the YMR.

### 4.3 GEOMORPHIC DATING

The relatively poorly consolidated character of basaltic cinder cones provides a means to determine relative ages, based on increasing degrees of erosion with time (Scott and Trask, 1971; Wood, 1980; Dohrenwend et al., 1984, 1986; Hasenaka and Carmichael, 1985; Wells et al., 1990). Geomorphic modifications associated with increasing age include decreases in cone slope and height, and increases in the thickness and length of the cone apron, crater diameter, cone diameter, and the number of gullies on the cone slope (e.g., Dohrenwend et al., 1984; Hasenaka and Carmichael, 1985). These geomorphic characteristics can be determined for cinder cones of known age and compared to cinder cones in similar climates to produce an age estimate.

A similar approach has been applied to the time-dependent geomorphic modification of lava flows in arid climates (e.g., Wells et al., 1985; McFadden et al., 1987; Farr, 1992). With increasing age, the tops of lava flows will be smoothed by erosion, topographic depressions will be filled by eolian deposition, and flows will be dissected by fluvial erosion (e.g., Dohrenwend et al., 1987). Geomorphic variations on lava flows are not as time sensitive as geomorphic variations on cinder cones (e.g., Wells et al., 1985), and, consequently, have a more limited application to geomorphic dating.

Before geomorphic characteristics can be used as a dating technique, two important assumptions must be addressed. First, the paleoclimate for the known and unknown age volcanoes must be similar. Variations in the amount of rainfall, rates of precipitation, vegetation, and eolian conditions can strongly affect the geomorphic modification of volcanic features (e.g., Wells et al., 1985; McFadden et al., 1986).

Second, the initial characteristics of the volcanic features must be similar (i.e., Porter, 1972; Wood, 1980). Although cinder cones generally have a similar initial morphology, variations in wind direction and eruption dynamics can strongly affect the form of a cinder cone (Porter, 1972; McGetchin et al., 1974; Gutmann, 1979; Settle, 1979). In addition, the degree of cinder annealing, presence of agglutinate layers, and initial breaching of the cone will strongly affect subsequent geomorphic modifications.

### **4.3.1 Analytical Methods**

The morphology of basaltic cinder cones can be described by a number of parameters that show time-dependent variations (e.g., Wood, 1980). Commonly used parameters (Porter, 1972; Dohrenwend et al., 1986) are shown on Figure 4-3A. Parameters such as cone height, cone width, and crater width are easily determined from topographic maps or aerial photographs. Other parameters are more subjective, and are largely dependent on recognition of the transition from the cinder cone slope onto the colluvial apron (Figure 4-3A).

Before volcanoes of known age can be compared to the studied volcanoes, additional work is required to demonstrate that initial morphologies and climates are similar for each volcanic system. Most geomorphic dating studies have focused on volcanoes in arid climates. The parameters used to describe cinder cone morphology are relatively insensitive to the small microclimate variations that can occur within the southwestern United States (e.g., Wells et al., 1990; McFadden et al., 1986). However, basaltic volcanoes in the southwestern United States and elsewhere may have markedly different initial morphologies (e.g., Scott and Trask, 1971). Variations in morphology can occur due to difference in the strength or direction of prevailing winds (Porter, 1972), eruption dynamics (Scott and Trask, 1971; McGetchin et al., 1974), or composition (Hasenaka and Carmichael, 1985). The internal structure of a cinder cone also can affect the rate and extent of erosion. For example, cinder cones composed primarily of agglutinated cinders will be more resistant to erosion and down-slope movement of tephra than cones composed primarily of loose, nonagglutinated tephra. Variations in magma composition, temperature, volatile content and degassing rates all can affect the initial cohesiveness of cinder cone deposits (e.g., McGetchin et al., 1974).

Once these analogous features are determined, the geomorphic criteria for the volcanoes of known age can be used to derive age-calibration curves (Figure 4-3B). Note that the ratio of crater width-to-cone width appears the most time dependent for the Cima Volcanic Field (Dohrenwend et al., 1986). Other ratios, such as cone height-to-cone width, are relatively insensitive to intervals of time less than about 100 ka (Dohrenwend et al., 1986) and trends are strongly controlled by a single young volcano. Similar relationships have been observed in the Lunar Crater Volcanic Field (Scott and Trask, 1971) and the Michoacán-Guanajuato Volcanic Field in central Mexico (Hasenaka and Carmichael, 1985).

### **4.3.2 Sources of Error**

Geomorphic parameters can be determined precisely and accurately through careful measurements on standard U.S. Geological Survey topographic maps, which have contour intervals of 6.1 m (20 ft) at scales of 1:24,000. Most basaltic cinder cones have heights in excess of 50 m and basal diameters in excess of 200 m (e.g., Wood, 1980). With conservative estimates of map resolution at around 5 m for vertical and 10 m for horizontal measurements, errors are thus around 10 percent for vertical parameters and around 5 percent for horizontal parameters.

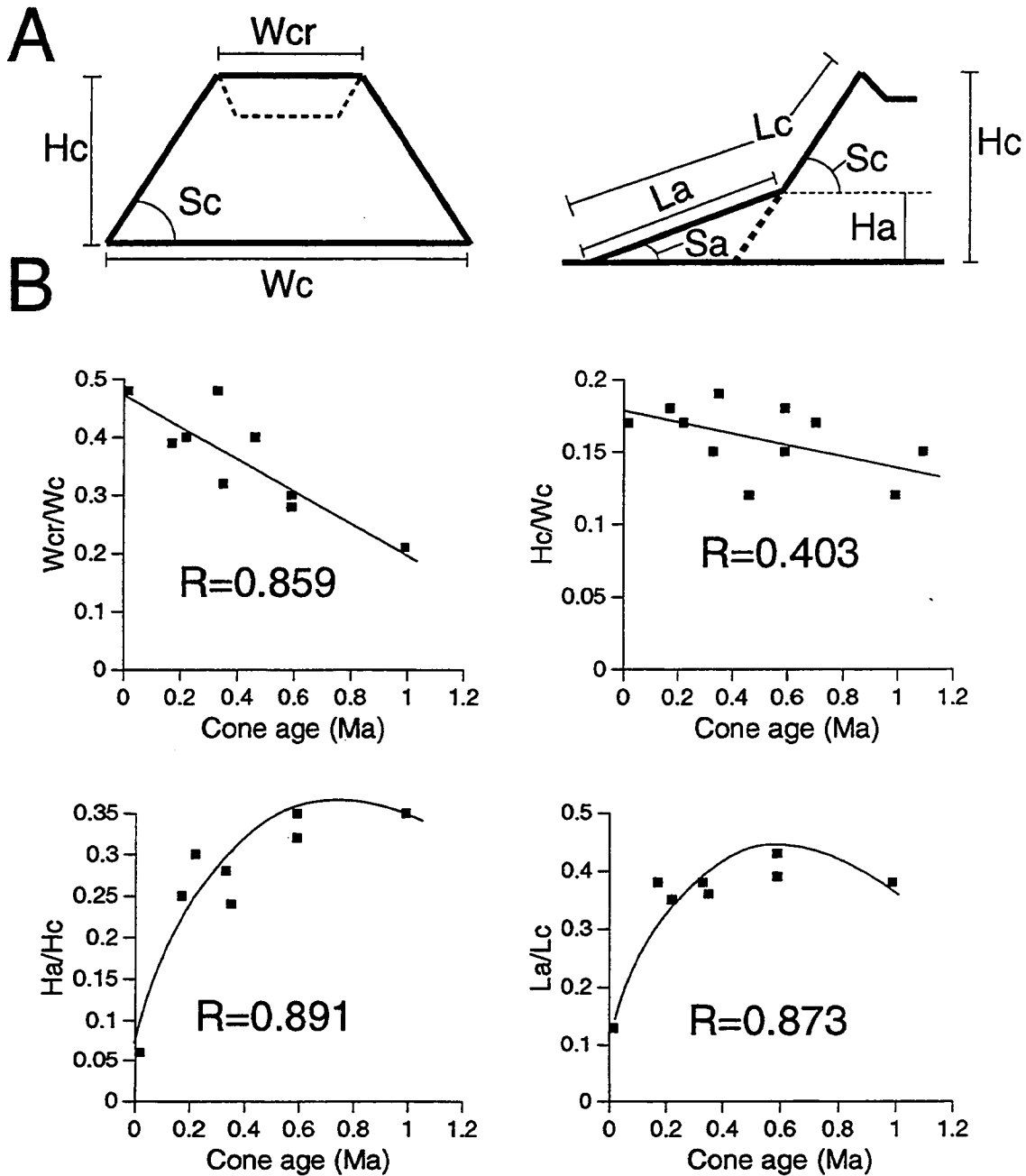


**Figure 4-3. (A) Cinder cone morphology parameters from Porter (1972) and Dohrenwend et al. (1986):  $W_{cr}$  = crater width;  $W_c$  = cone width;  $H_c$  = cone height;  $Sc$  = cone slope;  $Ha$  = apron height;  $Sa$  = mean slope of apron;  $La$  = apron-slope length;  $Lc$  = cone-slope length. (B) Geomorphic parameters for Cima cinder cones (Dohrenwend et al., 1986). Lines represent best fits to observed trends with corresponding correlation coefficients. With the apparent exception of crater-to-cone width, these parameters are relatively insensitive to age differences of less than around 100 k.y.**

The main source of error in geomorphic dating is not in measuring the actual geomorphic parameters, but in the assumption that the studied volcanoes are directly analogous to the volcanoes used in the calibration curves. For example, many of the volcanoes in the Cima Volcanic Field (Dohrenwend et al., 1986), including the ones used to construct the curves in Figure 4-3B, have multiple layers of agglutinated spatter and tephra within the cones. It would be incorrect to assume that these relatively cohesive cinder cones would erode at rates and styles identical to nonagglutinated cinder cones. A more intuitive interpretation would be that agglutinated cinder cones will be more resistant to erosion than nonagglutinated cinder cones. Geomorphic age relationships determined for agglutinated cinder cones would thus overestimate the age of nonagglutinated cinder cones. In addition, cinder cones that formed with an initial hydromagmatic phase of activity will have different morphologies than cones that formed without hydromagmatic eruptions and are thus not directly comparable (Dohrenwend et al., 1986).

### **4.3.3 Material Dated**

Geomorphic dating does not involve direct sampling of igneous material. Although several important parameters of cinder cone morphology can be directly measured from topographic maps, geologic field work and mapping are required to accurately determine parameters associated with cone aprons. Some recent applications in geomorphic dating of lava flow surfaces utilize remote sensing data to determine flow roughness or reflectance (e.g., Farr, 1992; Arvidson et al., 1993).

### **4.3.4 Application to the Yucca Mountain Region**

Wells et al. (1990) have compared the morphologies of the Lathrop Wells and Quaternary Crater Flat volcanoes with Quaternary volcanoes in the Cima Volcanic Field, California. In comparison with approximately 1-Ma Cima cinder cones, the Crater Flat volcanoes (Little, Black and Red Cones) have morphological characteristics consistent with a 1-Ma age (Wells et al., 1990). The presented geomorphic parameters lack sufficient resolution to determine if any of the Crater Flat volcanoes have relatively different degrees of erosion, which would indicate significant differences in age. However, the variations in most geomorphic parameters apparently are incapable of resolving intervals of time roughly less than about 100 ka (cf. Figure 4-3B). Relative degrees of soil development may indicate that Black Cone is younger than Red Cone (Crowe et al., 1993), and Black Cone appears somewhat less deeply incised and eroded than Red Cone.

Wells et al. (1990) concluded that the geomorphic characteristics of the main Lathrop Wells cone are indistinguishable from those of the Black Tank Cone in the Cima Volcanic Field, which has an age of only about 20-30 ka. There are, however, several problems with this widely cited (Crowe et al., 1992b; 1993) interpretation.

- Dohrenwend et al. (1986) clearly state the cinder cones associated with tephra rings (i.e., hydrovolcanic deposits) have different constructional forms than cones without tephra ring. The Lathrop Wells cone had hydrovolcanic eruptions prior to formation of the main cinder cone (e.g., Vaniman and Crowe, 1981; Crowe et al., 1988), whereas the Black Tank Cone lacks hydrovolcanic deposits (Dohrenwend et al., 1986). These two cinder cones thus have different original morphologies and cannot be directly compared for geomorphic dating.
- The internal structure of these two cinder cones is markedly different. The Black Tank Cone has at least three relatively thick (2-3 m) agglutinate layers exposed in the crater walls and

flanks. Lapilli and bombs at Black Tank Cone are highly oxidized, commonly have aerodynamic deformation features such as spindles and ribbons, and form somewhat cohesive deposits. Lathrop Wells lacks discernable, thick agglutinate layers, has relatively nonoxidized cinders, lacks abundant spindles and ribbons, and forms poorly consolidated deposits of loose, angular tephra. A logical conclusion would be that it is more difficult to erode Black Tank Cone than Lathrop Wells, due to differences in the relative cohesiveness of these two cones. Thus, the age represented by the geomorphology of Black Tank Cone will overestimate the age of Lathrop Wells, because it should take a shorter amount of time to erode a less cohesive cone.

- Lathrop Wells is morphologically younger than Black Tank Cone. Lathrop Wells lacks a cone apron and shows essentially no erosional modification of the cone flanks and crater (Wells et al., 1990). In contrast, Black Tank Cone has a well-defined cone apron and has unevenly distributed rills and gullies on the cone flanks (Wells et al., 1990).

These problems make it difficult to rigorously evaluate the 20-ka age proposed for Lathrop Wells by Wells et al. (1990). If these two relatively young cinder cones are indeed comparable, then Lathrop Wells should be significantly younger than the 20–30-ka Black Tank Cone. However, <sup>3</sup>He exposure ages at Lathrop Wells indicate a minimum age in excess of 40 ka (Crowe et al., 1992b). Lathrop Wells is undoubtedly a young volcanic center and clearly does not have the geomorphic characteristics of a 200 ka Cima volcano or the roughly 1-Ma Crater Flat volcanoes. The absolute age of Lathrop Wells, however, cannot be determined robustly by geomorphic criteria. Direct dates of lathrop Wells indicate that the age of this volcano probably is between 50 and 150 ka.

#### 4.4 MISCELLANEOUS DATING TECHNIQUES

Several additional techniques are currently available to date young basaltic volcanic rocks. These techniques provide only general or relative age information, and have had few direct applications to the YMR.

##### 4.4.1 Soil Development

The extent and character of soil development can be used to provide relative ages of Quaternary deposits. In areas of similar climate, drainage, and initial composition, soils will become thicker and show increasing degrees of development with increasing age (e.g., McFadden et al., 1986). Soil development can readily distinguish relative ages of Quaternary alluvial deposits in a given area (McFadden et al., 1989; Hardin et al., 1991). Soil development, however, is very sensitive to variations in drainage and climate (McFadden et al., 1986; Wells et al., 1987), which limits the application of this technique in geochronology.

Crowe et al. (1992b) compare degrees of soil development between Lathrop Wells and Black Tank Cone, and conclude that Lathrop Wells soils closely resemble Holocene soils in the area. They conclude that these soils "probably cannot be older than 20 ka and almost certainly cannot be older than 50 ka." It is important to note that all the soils used as calibration standards have ages of  $\leq 20$  ka or  $\geq 130$  ka (Wells et al., 1987; Hardin et al., 1991). Although pedogenic processes at Lathrop Wells are similar to those at the Cima Volcanic Field (Crowe et al., 1992b), they are not identical. From the data presented (Crowe et al., 1992b, 1993), it is not at all clear if soil development could resolve age

differences of around 20 k.y. in 50–80-ka deposits. Clearly, additional studies of soil development on 20–100-ka volcanic rocks are needed before absolute ages can be assigned to the weakly developed soils at Lathrop Wells. Based on the soil data presented to date, it appears reasonable to conclude that the main Lathrop Wells cone does not have an age in excess of about 100 ka (i.e., Crowe et al., 1993) as has been proposed by Turrin et al. (1991).

#### 4.4.2 Tephrastratigraphy

Regionally extensive ash deposits can be used as absolute age markers in local stratigraphy studies (e.g., Sarna-Wojcicki, 1976; Sarna-Wojcicki et al., 1985). The ash must have a sufficiently distinctive composition to permit identification and correlation with proximal deposits, and must have a relatively precise and accurate age that corresponds to the age of the studied stratigraphic section (Sarna-Wojcicki, 1976). Finally, the ash must be preserved in a depositional environment that does not allow reworking to occur, such as pluvial lakes (e.g., Davis, 1985).

In the YMR, regionally extensive Quaternary silicic ash deposits are scarce. Hoover et al. (1981) report isolated lenses of volcanic ash in middle-to-late Pleistocene alluvium, which is the 0.74-Ma Bishop ash bed (Izett et al., 1988). Bishop ash has not been observed in soil studies of the  $1.2 \pm 0.4$ -Ma Crater Flat volcanoes (Crowe et al., 1993), which likely indicates a lack of preservation rather than a post-0.74-Ma age of these volcanoes. However, Bishop ash beds in the YMR had original thicknesses between 30 and 100 cm (Izett et al., 1988). Summit craters and small topographic depressions in lava flows should contain Bishop ash deposits if the Quaternary Crater Flat volcanoes are indeed older than 0.74 Ma. Silicic ash beds younger than the Bishop ash (e.g., Izett et al., 1988) have not been reported in YMR alluvial or eolian deposits associated with Quaternary volcanoes.

#### 4.4.3 Cation-ratio

Cation-ratio dating is based on differences in the rates that minor elements are presumedly leached from rock varnish. For most rocks, the cations  $K^+$  and  $Ca^{2+}$  are more soluble than  $Ti^{4+}$  and thus the ratio of  $K + Ca / Ti$  (KCT) will decrease with time (e.g., Dorn, 1983). KCT ratios are measured for varnishes from rocks with known ages to create an age-calibration curve, to which samples of unknown age are compared. The cation-ratio dating technique relies on the accurate determination of K, Ca, and Ti abundances in the rock varnish, and on accurately dated varnish standards.

Application of this technique has been primarily to samples younger than about 20 ka (e.g., Dorn et al., 1986). Although older dates are possible, difficulties in determining accurate  $^{14}C$  dates hinders the application of cation-ratio dating to rocks much older than about 20 ka (e.g., Dorn, 1983). Rocks younger than about 100 ka also are difficult to date by conventional methods, which further limits cation-ratio dating for late Pleistocene rocks. In addition, the method commonly used to determine KCT ratios (proton-induced x-ray emission) may have significant errors in precision and accuracy (Bierman and Gillespie, 1991b), although the magnitude and extent of these errors are still being debated (Cahill, 1992; Bierman and Gillespie, 1992a,b; Dorn, 1992). Additional complexities include the possibility that young varnish dates reflect the amount of unaltered (i.e., high KCT) rock incorporated into the thin varnish sample (Harrington and Whitney, 1987; Reneau and Raymond, 1991) and significant differences in varnish production rates between areas of relatively similar climate and rock composition (Harrington and Whitney, 1987; Whitney and Harrington, 1993). Although the cation-ratio dating technique appears

to yield accurate dates under some conditions (e.g., Dorn et al., 1986; Whitney and Harrington, 1993), the basis for the technique is not universally accepted (Reneau and Raymond, 1991).

The cation-ratio dating technique has not been directly applied to determining the ages of young basaltic rocks in the YMR. Harrington and Whitney (1987) used varnish characteristics of Red and Black Cones to calibrate a KCT-age curve for the YMR, which has relatively large uncertainties. The varnish KCT-ratio for the roughly 1.2-Ma Red and Black Cones (Harrington and Whitney, 1987), however, is indistinguishable from the KCT-ratio of roughly 0.1-Ma basalt in the Cima Volcanic Field (Dorn et al., 1986). Although the cation ratio of rock varnish may provide accurate relative dates within the YMR, the determination of absolute ages in the YMR may not be possible due to poorly constrained calibration curves.

## 5 EFFECTS OF AGE UNCERTAINTY ON PROBABILITY MODELS

### 5.1 INTRODUCTION

Accurate and precise geochronological data are critical to the development of geologically reasonable probability models of volcanic disruption of the candidate repository. All probability models proposed to date (e.g., Ho, 1991; Ho et al., 1991; Crowe et al., 1992a, Margulies et al., 1992; Connor and Hill, 1993) rely on estimates of the recurrence rate of volcanism in the YMR in order to calculate the probability of disruptive volcanic activity. Assuming that the probability of future cinder cones forming in the YMR is Poissonian (Ho et al., 1991; Crowe et al., 1983), the probability of a new volcano forming within the region during a given interval of time (such as the 10,000 yr isolation period of regulatory interest for a repository) is dependent only on the expected recurrence rate of new cinder cone formation. Most previous estimates of recurrence rate for basaltic volcanism during the late Quaternary in the YMR vary from about 1 to 12 volcanoes per million years (v/m.y.) (e.g., Ho, 1991; Ho et al., 1991; Crowe et al., 1992a; Margulies et al., 1992). This range in estimated recurrence rate is a result of the application of various averaging techniques and statistical estimators, and of the uncertainty in the ages of Quaternary volcanoes in the YMR. Over periods of time of 10,000 to 50,000 yr, this variation in estimated recurrence rate creates a large uncertainty in the probability of a new volcano forming in the region (Figure 5-1). For example, the probability of a new volcano forming within the YMR within the next 10,000 yr is between about 1 percent and 11 percent, for recurrence rates of between 1 and 12 v/m.y. During the next 50,000 yr, the probability of a new volcano forming increases to almost 40 percent, given a recurrence rate of 10 v/m.y., but remains less than 10 percent for recurrence rates of less than 2 v/m.y. Given this effect on probability calculations, it is important to reduce uncertainty in recurrence rate estimates as much as possible. It is the purpose of this section to illustrate how a reduction in volcano age uncertainty also may reduce uncertainty in expected recurrence rate estimates, and, therefore, improve probability models for potential magmatic disruption of the candidate repository site.

### 5.2 EFFECT OF AGE UNCERTAINTY ON AVERAGE RECURRENCE RATE ESTIMATES

Ho et al. (1991) used several methods to estimate the expected recurrence rate of new volcano formation. The simplest approach is to average the number of events that have occurred during some arbitrary period of time. For instance, Ho et al. (1991) average the number of volcanoes that have formed during the Quaternary (i.e., 1.6 m.y.) to calculate the recurrence rate. Through this approach they estimate an expected recurrence rate of 5 v/m.y. Crowe et al. (1982) averaged the number of new volcanoes over a 1.8 m.y. period. Crowe et al. (1992a) consider the two Little Cones to represent a single magmatic event, and therefore conclude that there are seven Quaternary centers in the YMR. This lowers the estimated recurrence rate to approximately 4 v/m.y. In this approach, the precision with which the age of the volcano is known does not matter as long as the ages of the volcanoes fall within the arbitrary period of time with a high degree of certainty. Crater Flat volcanoes almost certainly formed within the last 1.6 m.y., based on current age estimates (Table 2-2) and, therefore, estimates of expected recurrence rates made using this approach likely will not be improved upon with further refinement of age estimates. Assuming a recurrence rate of between 4 and 5 v/m.y., the probability of a new volcano forming in the YMR during the next 10,000 yr thus is between 4 and 5 percent.

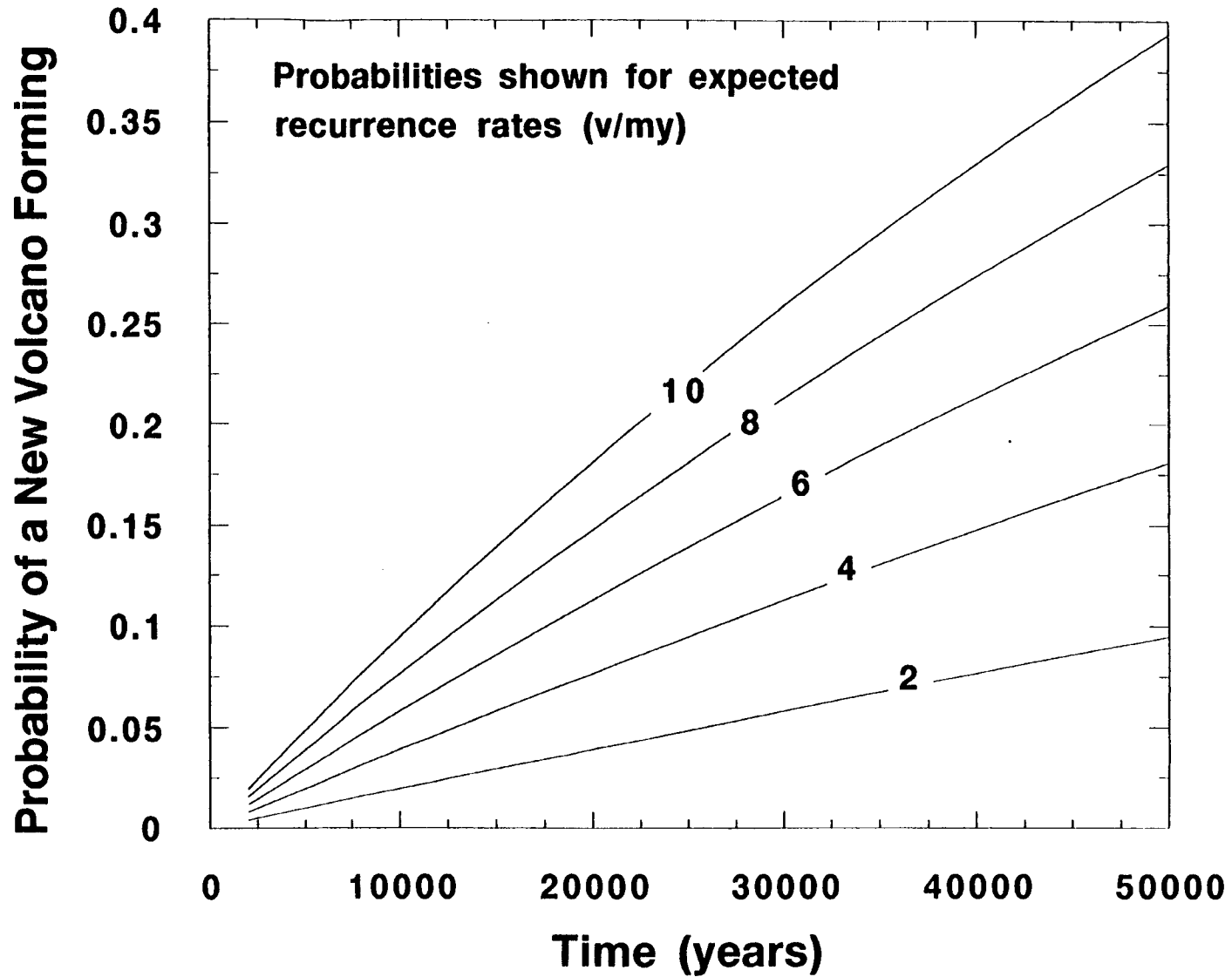


Figure 5-1. The probability of a new volcano forming within the YMR during the next 10,000 to 50,000 yr is strongly dependent on the expected recurrence rate.

An alternative approach is the repose-time method (Ho et al., 1991). In this method, a recurrence rate is defined using a maximum likelihood estimator (Hogg and Tanis, 1988) that averages events over a specific period of volcanic activity

$$\hat{\lambda} = \frac{(E-1)}{(T_o - T_y)} \quad (5-1)$$

where  $E$  is the number of events,  $T_o$  is the age of the first event,  $T_y$  is the age of the most recent event, and  $\hat{\lambda}$  is the estimated recurrence rate. Using eight Quaternary volcanoes as the number of events,  $E$ , and 0.1 Ma for the formation of Lathrop Wells, the estimated recurrence rate depends on the age of the first Quaternary volcanic eruption in Crater Flat. Using a mean age of 1.2 Ma yields an expected recurrence rate of approximately 7 v/m.y. However, the ages of Crater Flat volcanoes are currently estimated at  $1.2 \pm 0.4$  Ma. Therefore, the expected recurrence rate is between approximately 4.5 and 10 v/m.y.

The repose-time method has distinct advantages over techniques that average over an arbitrary period of time because it restricts the analysis to a time period that is meaningful in terms of volcanic activity. In this sense, it is similar to methods applied previously to estimate time-dependent relationships in active volcanic fields (e.g., Kurtz et al., 1986). However, because the method depends on the age of the oldest event, geochronological uncertainty has a greater effect. In this case, the result is that the recurrence rate is known only to within approximately  $7 \pm 2$  v/m.y. Using this range of recurrence rates, the probability of a new volcano forming within the YMR within the next 10,000 yr is between 5 percent and 10 percent. Application of more precise dating techniques would likely reduce uncertainty in expected recurrence rate based on the repose time method.

### 5.3 EFFECT ON WEIBULL-POISSON MODELS

Ho (1991) applied a Weibull-Poisson technique (Crow, 1982) to estimate the recurrence rate of new volcano formation in the YMR as a function of time. A Weibull process is a nonhomogeneous Poisson process in which the estimated recurrence rate is a function of time. There are several ways to estimate  $\hat{\lambda}(t)$ . Ho (1991) uses

$$\hat{\lambda}(t) = \left( \frac{\hat{\beta}}{\hat{\theta}} \right) \left( \frac{t}{\hat{\theta}} \right)^{\hat{\beta}-1} \quad (5-2)$$

where  $t$  is the total time interval under consideration (such as the Quaternary), and  $\hat{\beta}$  and  $\hat{\theta}$  are intensity parameters in the Weibull distribution that depend on the frequency of new volcano formation within the time period,  $t$ , and the change in frequency during  $t$ . In a time-truncated series,  $\hat{\beta}$  and  $\hat{\theta}$  are estimated from the distribution of past events. In this case, there are  $n = 8$  new volcanoes formed in the YMR during the Quaternary.  $\hat{\beta}$  and  $\hat{\theta}$  are given by

$$\hat{\beta} = \frac{n}{\sum_{i=1}^n \ln \left( \frac{t}{t_i} \right)} \quad (5-3)$$

and

$$\hat{\theta} = \frac{t}{n^{1/\hat{\beta}}} \quad (5-4)$$

where  $t_i$  refers to the time of formation of the  $i^{\text{th}}$  volcano. If  $\hat{\beta}$  is approximately equal to unity, there is little or no change in the recurrence rate as a function of time and a homogeneous Poisson model would provide an estimate of regional recurrence rate quite similar to the nonhomogeneous Weibull-Poisson model. If  $\hat{\beta} > 1$  then a time trend exists in the recurrence rate and events tend to occur more frequently with time, which may indicate a waxing magma system. If  $\hat{\beta} < 1$ , new volcanoes form less frequently over time and the magmatic system may be waning.

Where few data are available, such as for volcanism in the YMR, the value of  $\hat{\beta}$  can be strongly dependent on the period  $t$  and the timing of individual eruptions. Ho (1991) analyzed volcanism from 6 Ma, 3.7 Ma, and 1.6 Ma to the present. Ho (1991) discovered that volcanism is waxing in the YMR on time scales of  $t=6$  Ma and 3.7 Ma, and has been relatively steady ( $\hat{\beta} = 1.1$ ) during the Quaternary.

Uncertainty in the ages of Quaternary volcanoes has a strong impact on recurrence rate estimates calculated using a Weibull-Poisson model. For example, if mean ages of Quaternary volcanoes are used (Figure 2-1) and  $t=1.6$  Ma, then, as Ho (1991) calculated,  $\hat{\beta} = 1.1$  and the probability of a new volcano forming in the YMR within the next 10,000 yr is approximately 5 percent. This agrees well with recurrence rate calculations based on simply averaging the number of new volcanoes that have formed since 1.6 Ma. However, if the older ages derived from uncertainty in the dates are used (i.e., Crater Flat volcanoes are 1.6 Ma) then  $\hat{\beta} = 0.3$  and the magmatic system appears to be waning. Using these parameters, the probability of a new volcano forming during 10,000 yr is approximately 1.5 percent (Table 5-1). Conversely, using the younger volcano ages derived from uncertainty in the dates (i.e., 0.8 Ma),  $\hat{\beta} = 2.2$  and the magmatic system appears to be waxing. The probability of a new volcano forming within 10,000 yr then is approximately 10 percent. Therefore, given the degree of uncertainty in the ages of Quaternary volcanoes in the YMR, it currently is not possible to differentiate between waxing and waning models for the frequency of new volcano formation, using the Weibull-Poisson method within a constant time period,  $t=1.6$  Ma.

Crowe et al. (1993) have pointed out that the Weibull-Poisson model is strongly dependent on the value of  $t$ , and suggest that  $t$  should be limited to the time since the initiation of a particular episode of volcanic activity. This has an important effect on Weibull-Poisson probability models. If mean ages

of Quaternary volcanoes are used and  $t = 1.2$  Ma, then the probability of a new volcano forming in the next 10,000 years drops from 5 percent to 2 percent and  $\hat{\beta} < 1$ , indicating waning activity (Table 5-1).

**Table 5-1. Dependence of the Weibull-Poisson model of recurrence rate of volcano formation on age.**

Volcano Age Estimates	t(m.y.)	$\hat{\beta}$	$\hat{\theta}$	$\hat{\lambda}$ (v/my) (90% Confidence Interval)	P[10,000 yr]
mean ages <sup>1</sup>	1.6	1.1	0.2	5.4 (1.8, 12.4)	5%
oldest ages <sup>2</sup>	1.6	0.3	0.001	1.5 (0.5, 3.44)	1.5%
youngest ages <sup>3</sup>	1.6	2.2	0.6	11.0 (3.7, 25.3)	10%
mean ages <sup>1</sup>	1.2	0.3	0.002	2.1 (0.7, 4.8)	2%
varying ages <sup>4</sup>	1.2	0.7	0.2	4.8 (1.6, 11.0)	5%

<sup>1</sup> Volcanoes are assumed to have the mean ages reported in Figure 2-1. For example, an age of 1.2 m.y. is used for Black Cone.

<sup>2</sup> Volcanoes are assumed to have the oldest ages reported in Figure 2-1. For example, an age of 1.6 m.y. is assumed for Black Cone.

<sup>3</sup> Volcanoes are assumed to have the youngest ages reported in Figure 2-1. For example, an age of 0.8 m.y. is assumed for Black Cone.

<sup>4</sup> Crater Flat volcanoes are assumed to vary in age between 1.2 and 0.8 m.y.

In this model, it might be inferred that the Quaternary episode of volcanism began with comparatively widespread activity within the Crater Flat volcano alignment. Subsequent activity was limited to Sleeping Buttes and Lathrop Wells. Probability models thus would need to account for fewer volcanic events that affect a large area, such as the formation of cinder cone alignments, rather than many smaller events. Alternatively, volcanism along the Crater Flat volcano alignment may have occurred over a period of several hundred thousand years. If volcanism was initiated along the alignment approximately 1.2 Ma, but continued through 0.8 Ma, then the recurrence rate is again close to 5 v/m.y. and the probability of

new volcanism in the YMR within the next 10,000 yr is about 5 percent ( $t=1.2$  Ma, Table 5-1). Uncertainty in the ages of Quaternary volcanoes has a dramatic effect on recurrence rate estimates when confidence intervals also are taken into account. The confidence intervals calculated on  $\hat{\lambda}(t)$  are quite large due to the few events ( $n=8$ ) on which the calculations are based. Using the youngest volcano ages, for example, the recurrence rate is less than 25 v/m.y. with 90-percent confidence. Using mean ages, the recurrence rate is less than 12 v/m.y. with 90-percent confidence (Table 5-1).

These calculations indicate that the Weibull-Poisson method may provide important insight into the recurrence rate of volcanism, and the probability of a new volcano forming, within the YMR during the next 10,000 yr. However, the results of Weibull-Poisson probability estimates are quite sensitive to uncertainty in the ages of volcanoes. More precise geochronological data than are currently available for Quaternary YMR volcanoes are necessary to fully evaluate Weibull-Poisson models.

#### 5.4 EFFECT ON SPATIALLY AND TEMPORALLY NONHOMOGENEOUS POISSON MODELS

Connor and Hill (1993) provide an example of how uncertainty in the ages of YMR volcanoes can be propagated through a spatially and temporally nonhomogeneous Poisson probability model. In a spatially and temporally nonhomogeneous Poisson model, the recurrence rate is allowed to vary across a region based on the distance from points in that region to volcanoes of various ages. Probability estimates that result from these calculations will be comparatively high at a point close to young volcanoes, and will be comparatively low far from young volcanoes. Because of this dependence on spatial and temporal aspects of volcano distribution, this type of nonhomogeneous Poisson model can take into account several features of volcanism the homogeneous models cannot. For example, cinder cones in the YMR are not randomly distributed, rather, they form clusters in a manner similar to what is observed at other cinder cone fields (Connor and Hill, 1993). Uncertainty in the ages of volcanoes will affect the estimates of repository disruption because the nonhomogeneous Poisson model strongly depends on the ages of volcanoes.

Connor and Hill (1993) estimated expected recurrence rate per unit area at an arbitrary point,  $\hat{\lambda}_r$ , using varying numbers of near neighbors

$$\hat{\lambda}_r = \frac{m}{\sum_{i=1}^m u_i t_i} \quad (5-5)$$

where near-neighbor volcanoes are determined as the minimum of  $u_i t_i$ , and  $t_i$  is the time elapsed since the formation of the  $i^{\text{th}}$  near-neighbor volcano and  $u_i$  is an area term dependent on the distance from the point to the  $m^{\text{th}}$  near-neighbor, with  $u_i \geq 1 \text{ km}^2$ .

It is possible to differentiate between various near-neighbor nonhomogeneous Poisson models by comparing the observed recurrence rate for the region with the expected regional recurrence rate calculated using near-neighbor methods determined by integrating the estimated recurrence rates [Eq. (5-5)] over the YMR

$$\hat{\lambda}_r = \iint_{X Y} \hat{\lambda}_r(x,y) dy dx \quad (5-6)$$

where  $\hat{\lambda}_r$  is the estimated YMR recurrence rate, based on the nonhomogeneous model. In practice, recurrence rates,  $\hat{\lambda}_r$ , are calculated on a grid and these values are summed over the region of interest

$$\hat{\lambda}_r = \sum_{i=0}^m \sum_{j=0}^n \hat{\lambda}_r(i,j) \Delta x \Delta y \quad (5-7)$$

where  $\Delta x$  and  $\Delta y$  are each 2000 m, which is the grid spacing used in the calculations, and  $m$  and  $n$  are the number of grid points used in the  $X$  and  $Y$  directions, respectively. The dependence of expected regional recurrence rate,  $\hat{\lambda}_r$ , on the number of near-neighbor volcanoes,  $m$ , used in the calculation is illustrated in Figure 5-2. The relationship between the number of near-neighbor volcanoes and regional recurrence rate depends on the ages of the volcanoes [Eq. (5-5)], which are known with varying precision. Consequently, Eq. (5-7) is used to calculate regional recurrence rates using mean volcano ages, and the youngest and oldest ages for each volcano (Table 2-2) based on reported uncertainties. Nonhomogeneous Poisson models using six to seven near-neighbor volcanoes give regional recurrence rates that are close to those calculated for the late Quaternary in the YMR, for mean, oldest, and youngest volcano ages (Figure 5-2), if the regional recurrence rate is assumed to be  $7 \pm 2$  v/m.y. Ten to thirteen near-neighbor volcanoes are required to model recurrence rates similar to the estimated post-caldera recurrence rate of  $\approx 3$  v/m.y. (e.g., Crowe et al, 1983).

The probability of volcanic disruption of the candidate repository site can be estimated assuming a nonhomogeneous Poisson distribution

$$P [N \geq 1] = 1 - \exp \left[ -t \iint_{x y} \hat{\lambda}_r(x,y) dy dx \right] \quad (5-8)$$

where the limits of integration define the area of the repository. This relation is closely approximated by

$$P[N \geq 1] = 1 - \exp \left[ -t \sum_a \hat{\lambda}_r \Delta x \Delta y \right] \quad (5-9)$$

where  $\Delta_x$  and  $\Delta_y$  are one kilometer and  $a$  is the approximate total area of the repository. These probabilities are very close to the probability of one volcanic event because the probability of two or more events is vanishingly small ( $\approx 1 \times 10^{-9}$ ). Calculations of the probability of volcanic disruption of the repository using a range of near-neighbor models are given in Figure 5-3. Using  $a=8 \text{ km}^2$ , the probability of disruption during a 10,000 yr confining period is between  $1.4 \times 10^{-4}$  and  $1.7 \times 10^{-4}$  for a mean late-Quaternary recurrence rate (six to seven near neighbors), and  $6.9 \times 10^{-5}$  to  $9.2 \times 10^{-5}$  for a post-caldera basalt recurrence rate ( $m=10$  to 13 near neighbors). Using a range of late Quaternary rates and an  $8 \text{ km}^2$  area, the probability of disruption is between  $1.1 \times 10^{-4}$  and  $2.7 \times 10^{-4}$ . Based on the nonhomogeneous Poisson models for various Quaternary recurrence rates and areas, most estimates of

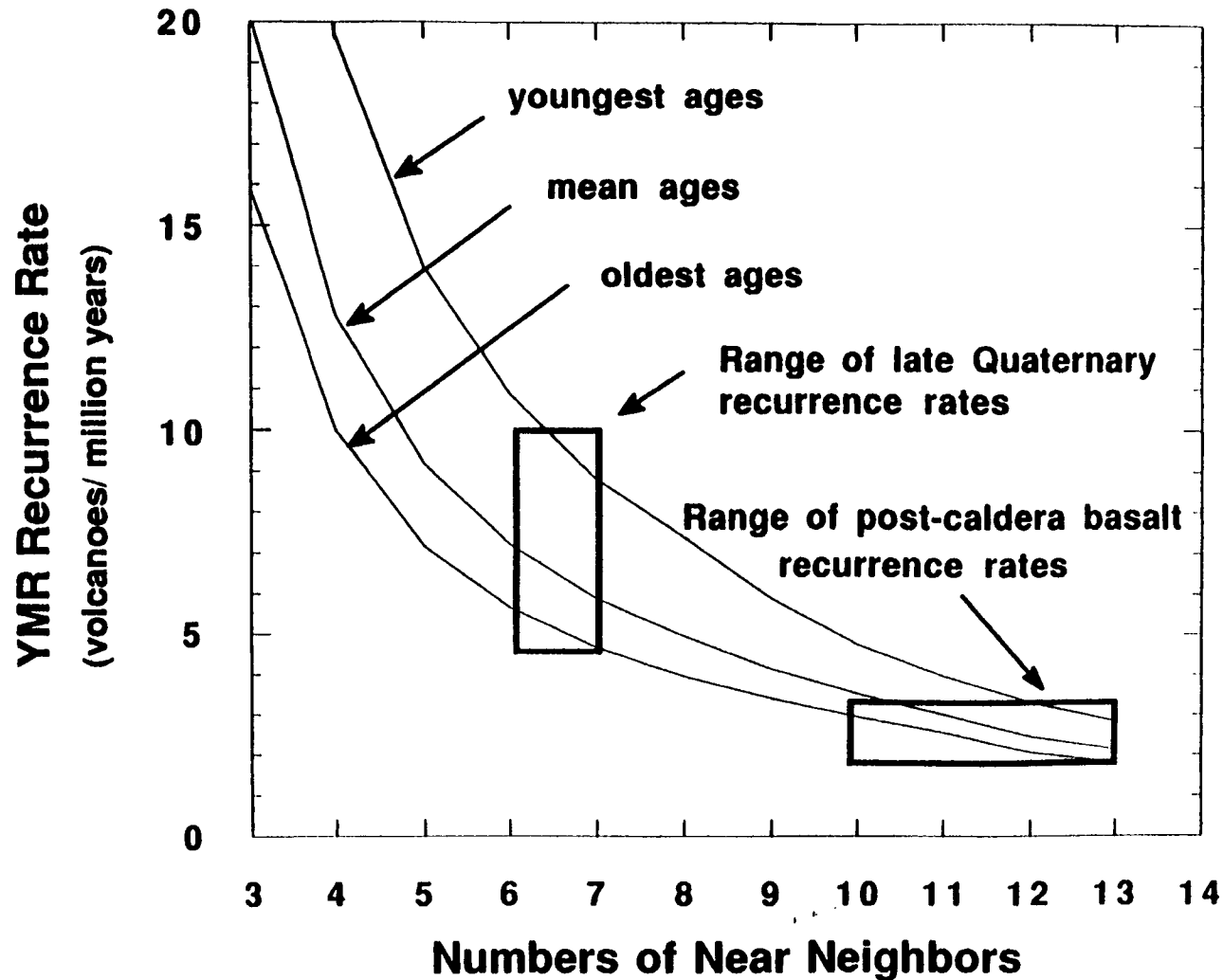


Figure 5-2. Recurrence rate for the formation of new volcanoes in the YMR is estimated using a number of near-neighbor nonhomogeneous Poisson models. Curves are calculated using mean volcano ages, oldest estimated ages, and youngest estimated ages (Table 2-2) to illustrate the effect of uncertainty in volcano age on the models. Calculated recurrence rates decrease with increasing numbers of near neighbors because near-neighbor volcanoes are young. Comparison with recurrence rates estimated directly from geochronological data indicates that six and seven near-neighbor models most closely approximate late Quaternary recurrence rates; ten to thirteen near-neighbor models most closely approximate post-caldera basalt recurrence rates.

the probability of repository disruption are between  $1 \times 10^{-4}$  and  $3 \times 10^{-4}$  for the next 10,000 years (Connor and Hill, 1993).

In this type of model, uncertainty in volcano ages affects the probability calculation in two related ways. First, error is introduced into the near-neighbor model because of uncertainty in the values of  $t_i$  in Eq. (5-5). Second, error is introduced into the model because of uncertainty in estimating the regional recurrence rate. If comparatively high regional recurrence rates are considered, uncertainty in the values of  $t_i$  becomes more important. For instance, at low recurrence rates ( $m = 11$  to 13 near neighbors), uncertainty in the ages of late Quaternary volcanoes makes little difference and the probability of volcanic disruption varies from approximately  $5 \times 10^{-5}$  to  $1 \times 10^{-4}$  (Figure 5-3). In contrast, if recurrence rates are comparatively high ( $m=6$  near neighbors) then the probability of disruption is between  $1 \times 10^{-4}$  and  $3 \times 10^{-4}$  in 10,000 yr. By comparison, this is a broad range of probabilities which can be better constrained through more precise age determinations.

Uncertainty in the age of Lathrop Wells is small compared to other volcanoes in the YMR and has little effect on probability calculations, except at very high, possibly unreasonable, recurrence rates (Figure 5-4). The uncertainty in the ages of Crater Flat volcanoes is more important, because these volcanoes are more numerous and their ages are currently less certain.

## 5.5 SUMMARY OF EFFECTS ON PROBABILITY MODELS

Geologically reasonable probability models are strongly dependent on the ages of Quaternary volcanoes in the YMR. Current uncertainty in volcano ages adversely affects these probability models. Uncertainty in the age of Quaternary volcanoes, for example, makes it impossible to distinguish between waxing, waning, or steady-state magmatism using Weibull-Poisson methods. Reduction of uncertainty in volcano ages through improved dating techniques can improve probability models significantly. This is particularly important for the youngest, late Quaternary volcanoes in the YMR.

Furthermore, identification of the duration of activity at individual volcanoes will open a broad range of probability models that currently cannot be applied. These include time-dependent survival models (Cressie, 1991), Poisson cluster models, and related models.

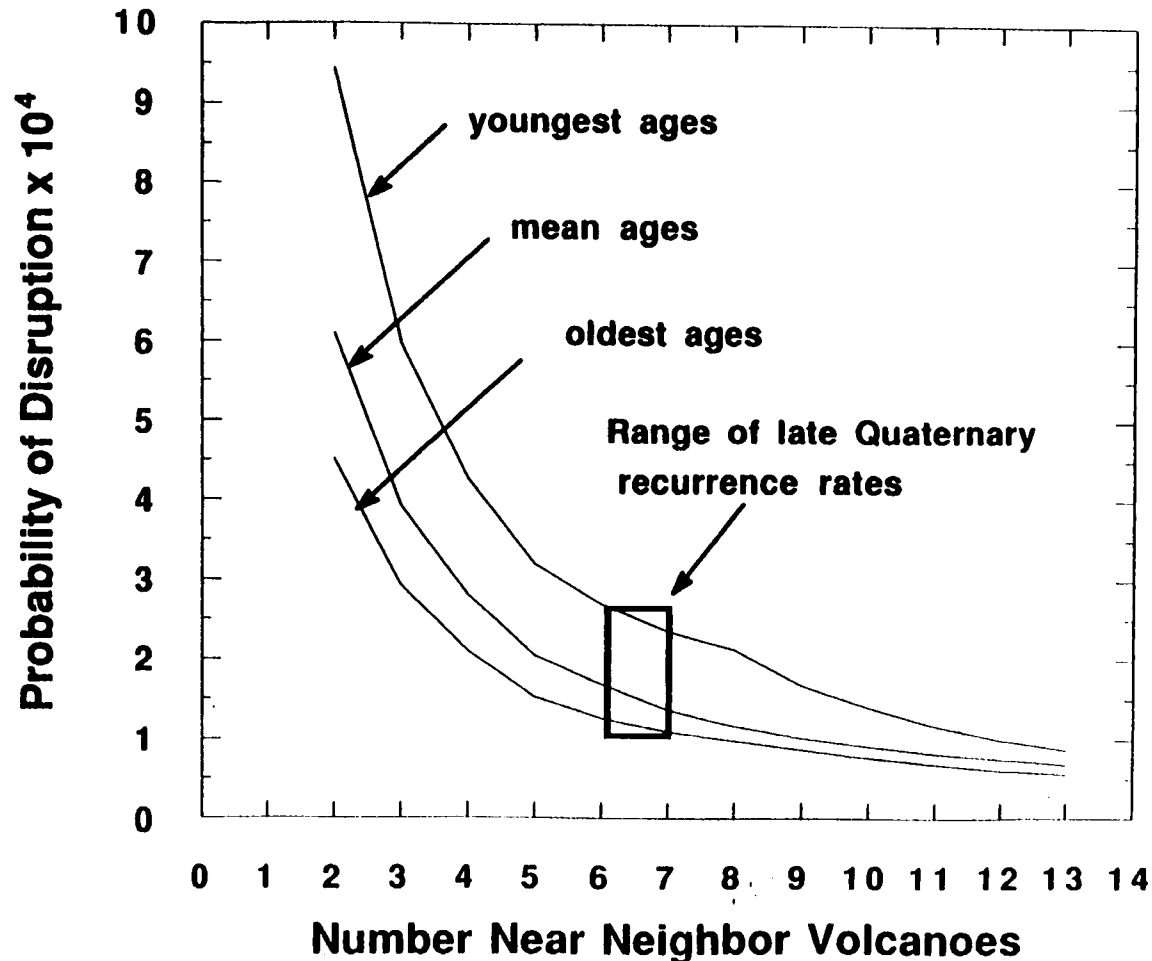


Figure 5-3. Estimated probability of disruption of the candidate HLW repository varies with the number of near neighbors used in nonhomogeneous Poisson models and because of uncertainty in the ages of Quaternary YMR cinder cones (Table 2-2). Calculations are made for the probability of a volcano forming within an 8 km<sup>2</sup> block at the Yucca Mountain repository site (Figure 2-1), during the next 10,000 years. Six to seven near-neighbor models most closely approximate the late Quaternary recurrence rate. Ten to thirteen near-neighbor models most closely approximate the post-caldera basalt recurrence rate.

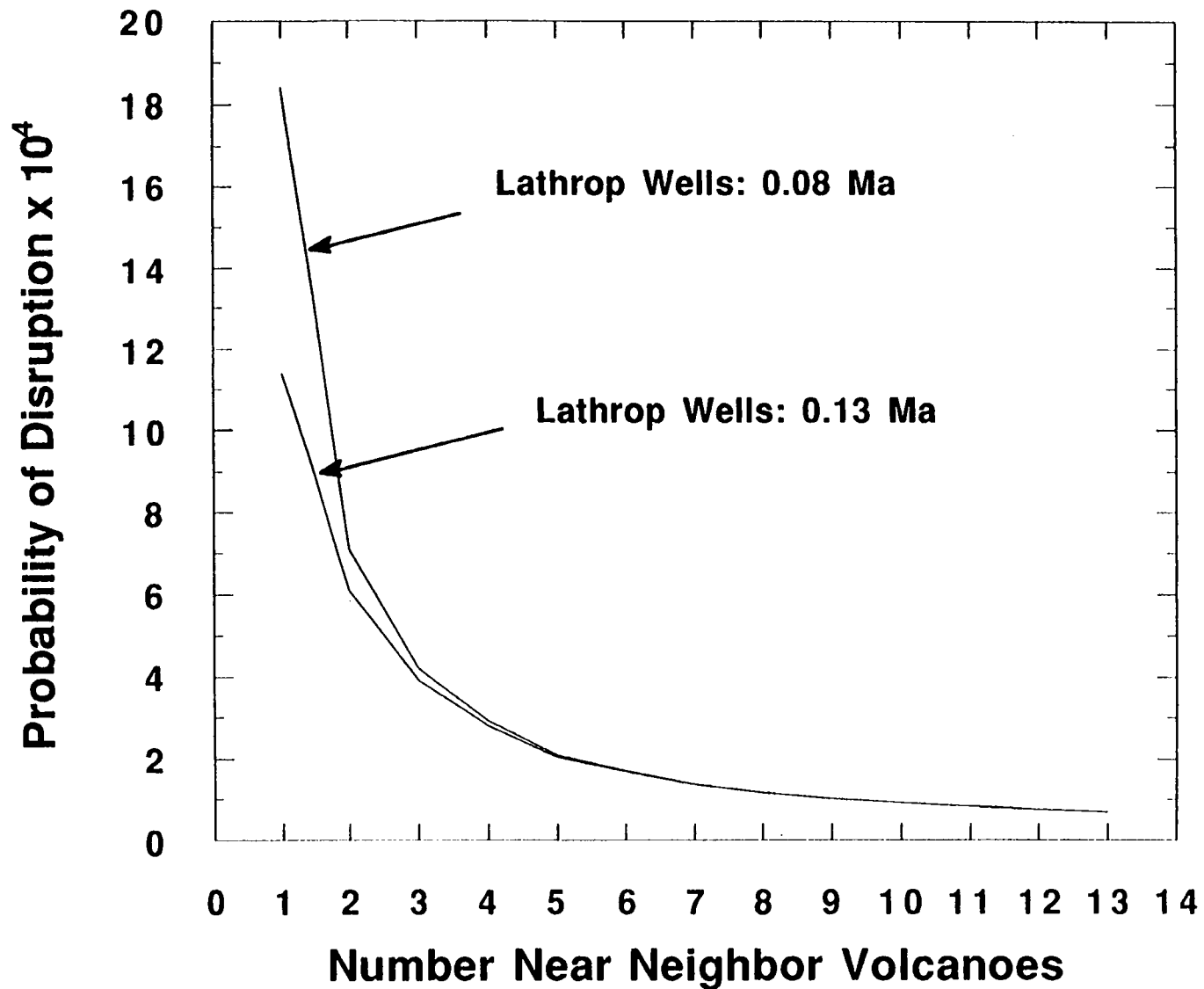


Figure 5-4. The probability of disruption is not strongly affected by uncertainty in the age of Lathrop Wells, unless four or fewer near-neighbor volcanoes (i.e., very high recurrence rates) are considered.

## 6 CONCLUSIONS

The ages of post-10 Ma basaltic volcanoes in the YMR are poorly constrained. Most geochronologic studies to date have focused on the ages of eruptions at the Lathrop Wells volcanic center and have failed to improve the precision and accuracy of decade-old analyses on other eruptive centers. In addition, few dates have presented sufficient analytical information to independently calculate the dates or evaluate analytical errors. There is often only a cursory explanation provided for dating methods reported in the available literature, and dated samples are inadequately characterized by petrographic or geochemical analyses. Average dates reported in the literature fail to propagate analytical error through statistical calculations, or incorrectly apply weighted-mean statistics to techniques with nongaussian distributions of analytical error. Uncertainties in the precision and accuracy of dates produced with the most widely used techniques increase with decreasing age, such that Quaternary volcanoes have age errors that are large enough to significantly affect probability calculations. All the post-caldera basaltic volcanoes have relatively large age-uncertainties, which must be reported and propagated through all calculations.

K/Ar ages for the oldest post-caldera basalts reflect the relative precision of conventional K/Ar analyses. Pahute Mesa has three dates that range from  $8.8 \pm 0.1$  to  $10.4 \pm 0.4$  Ma, Scarp Canyon has one date of  $8.7 \pm 0.3$  Ma, Paiute Ridge has one date of  $8.5 \pm 0.3$  Ma, Rocket Wash has one date of  $8 \pm 0.2$  Ma, and the Nye Canyon basalt has three dates that average  $6.8 \pm 0.3$  Ma. Pliocene basalts in Crater Flat have multiple K/Ar age determinations, which average at  $4.0 \pm 0.5$  Ma. No dates have been published for presumed Pliocene Basalt at Thirsty Mesa or the buried lavas in Amargosa Valley. The Buckboard Mesa center has two K/Ar dates, which average at  $2.8 \pm 0.1$  Ma.

Quaternary Crater Flat volcanoes have numerous K/Ar dates, which show wide ranges in precision and apparent accuracy. Propagation of reported analytical error results in an average age of  $1.2 \pm 0.4$  Ma for the Quaternary Crater Flat volcanoes. Although different volcanoes in the Crater Flat system have different degrees of erosional modification and soil development, which may indicate significant differences in age, available dates cannot resolve age distinctions between these volcanoes. Large analytical uncertainties at the Sleeping Butte volcanoes result in an average age of  $0.3 \pm 0.2$  Ma for this eruptive center.

Lathrop Wells has been the focus of many dating studies that utilize numerous analytical techniques. Because Lathrop Wells basalt has a low potassium content and the volcanic center is relatively young, conventional K/Ar studies yield an average date of  $0.5 \pm 0.5$  Ma. This relatively large uncertainty reflects the lower detection limits of this technique. Ar/Ar studies have large analytical errors and also are limited by the young age of Lathrop Wells. When analytical errors are propagated through statistical calculations, Lathrop Wells has an average Ar/Ar date of  $0.2 \pm 0.3$  Ma. It is interesting to note that these dates are indistinguishable from the  $0.3 \pm 0.2$  Ma Sleeping Butte eruptive center. U/Th disequilibrium studies indicate that older units at Lathrop Wells may be  $150 \pm 50$  ka, although little U/Th fractionation has occurred between the sparse number of phases at this volcano. U/Th dates on caliche deposits above and below the Lathrop Wells lavas are  $25 \pm 10$  ka and around  $350 \pm 100$  ka, which is well within the age range determined by other analytical techniques. TL dates on the stratigraphically youngest deposits at Lathrop Wells are  $< 10$  ka. However, there is insufficient information presented to evaluate the accuracy of these TL dates. Consequently, these TL dates could merely represent the mean lifetime of low-temperature electron traps. Cosmogenic  $^3\text{He}$  exposure ages are around 40 ka for the Lathrop Wells cinder cone and extend to  $73 \pm 9$  ka for associated lava flows. However,  $^{36}\text{Cl}$  exposure ages extend to  $83 \pm 9$  ka for the main Lathrop Wells cone and to  $96 \pm 5$  ka for associated lava flows. Given the large variations present

in the precision and accuracy of these dating studies, an age of  $100 \pm 50$  ka encompasses many of the reported dates for Lathrop Wells and provides a reasonable average age for this eruptive center.

Field relationships at Lathrop Wells indicate that multiple eruptions have occurred at this volcano. However, the lengths of time between these eruptions are poorly constrained. None of the direct dating techniques yet applied to Lathrop Wells have sufficient precision to resolve age differences of less than about 10,000 yr. However, cosmogenic isotopic methods may be able to provide 10 Ka resolution if analytical precision can be increased slightly. Indirect methods, such as paleomagnetic orientation, cone and flow morphology, and soil development, fail to provide robust constraints on the absolute period of time represented by these eruptions. Current estimates for the lengths of time between eruptions range from about 100 yr to several thousands of years.

Uncertainty in the age of Lathrop Wells is relatively small compared to other volcanoes in the YMR. This uncertainty has little effect on probability calculations except at unreasonably high eruption recurrence rates. However, the uncertainty in the ages of the Crater Flat volcanoes significantly affects probability calculations, because these volcanoes are more numerous and their ages are currently less certain.

In order to resolve current uncertainties in the ages of most 10-Ma and younger basaltic volcanoes in the YMR, these data are needed.

- Descriptions of analytical methods used and sufficient analytical information to allow independent calculation of dates, evaluation of analytical error, and evaluation of reported uncertainties.
- Sample location maps, petrographic, and geochemical data for dated samples.
- More precise and accurate dates for Quaternary Crater Flat volcanoes. Currently it cannot be resolved if these eruptions are contemporaneous, or may have occurred more than 100 k.y. apart.
- More precise and accurate dates for the Sleeping Butte volcanoes. Currently it cannot be resolved if these eruptions are contemporaneous with Lathrop Wells or may have occurred more than 100 k.y. apart.
- More complete descriptions of analytical methods and results for dating techniques used at Lathrop Wells. With the currently available data, it is not possible to independently determine the precision and accuracy of most of the dates reported for Lathrop Wells. Although many of these dates are produced in some of the leading research laboratories in the country, the techniques used are neither standardized or universally accepted.

Precise and accurate dates are required for robust probability calculations, and for modeling the potential effects of volcanism on repository performance. Dates for basaltic volcanoes in the YMR currently presented in the geologic literature are inadequate to meet these needs.

## 7 REFERENCES

- Aitken, M.J. 1967. Thermoluminescence. *Science Journal* 1: 32-38.
- Aitken, M.J. 1978. Archaeological involvements of physics. *Physics Reports (Section C of Physics Letters)* 40-5: 277-351.
- Albarède, F. 1978. The recovery of spatial isotope distributions from stepwise degassing data. *Earth and Planetary Science Letters* 39: 387-397.
- Alexander, E.C., Jr., M.R. Coscio, Jr., J.C. Dragon, R.O. Pepin and K. Saito. 1977. K/Ar dating of lunar soils: III. Comparison of  $^{40}\text{Ar}/^{39}\text{Ar}$  and conventional techniques, 12032 and the age of Copernicus. *Proceedings of the 8<sup>th</sup> Lunar and Planetary Science Conference Supplement to Geochimica et Cosmochimica Acta* 3: 2725-2740.
- Anderson, E.C., W.F. Libby, S. Weinhouse, A.F. Reid, A.D. Kirshenbaun, and A.V. Grosse. 1947. Natural radiocarbon from cosmic radiation. *Physics Review* 72: 931-936.
- Anthony, E.Y. 1993. Dating techniques for Quaternary lavas. *EOS* 74: 350.
- Anthony, E.Y., and J. Poths. 1992.  $^3\text{He}$  surface exposure dating and its implication for magma evolution in the Potrillo Volcanic Field, Rio Grande Rift, New Mexico, USA. *Geochimica et Cosmochimica Acta* 56: 4,105-4,108.
- Arvidson, R.E., M.K. Shepard, E.A. Guinness, S.B. Petroy, J.J. Plaut, D.L. Evand, T.G. Farr, R. Greeley, N. Lancaster, and L.R. Gaddis. 1993. Characterization of lava-flow degradation in the Pisgah and Cima volcanic fields, California, using Landsat Thematic Mapper and AIRSAR data. *Geological Society of America Bulletin* 105: 175-188.
- Bacon, C.R. 1989. Crystallization of accessory phases in magmas by local saturation adjacent to phenocrysts. *Geochimica et Cosmochimica Acta* 53: 1,055-1,066.
- Bard, E., B. Hamelin, R.G. Fairbanks, and A. Zindler. 1990. Calibration of the  $^{14}\text{C}$  timescale over the past 30,000 years using mass spectrometric U-Th ages from Barbados corals. *Nature* 345: 405-408.
- Bell, W.T. 1979. Thermoluminescence dating: revised dose-rate data. *Archaeometry* 21: 243-245.
- Bennett, C.L. 1979. Radiocarbon dating with accelerators. *American Scientist* 67: 450-457.
- Bennett, C.L., R.P. Beukens, M.R. Clover, H.E. Gove, R.B. Liebert, A.E. Litherland, K.H. Purser, and W.E. Sondheim. 1977. Radiocarbon dating using electrostatic accelerators: Negative ions provide the key. *Science* 198: 508-510.
- Berger, G.W. 1985. Thermoluminescence dating of volcanic ash. *Journal of Volcanology and Geothermal Research* 25: 333-347.

- Berger, G.W. 1986. Dating Quaternary deposits by luminescence—recent advances. *Geoscience Canada* 13: 15-21.
- Berger, G.W. 1991. The use of glass for dating volcanic ash by thermoluminescence. *Journal of Geophysical Research* 96: 19,705–19,720.
- Bierman, P.R., and A.R. Gillespie. 1992a. Reply to comment by T.A. Cahill on "Accuracy of rock-varnish chemical analyses: Implications for cation-ratio dating." *Geology* 20: 470.
- Bierman, P.R., and A.R. Gillespie. 1992b. Reply to comment by R.I. Dorn on "Accuracy of rock-varnish chemical analyses: Implications for cation-ratio dating." *Geology* 20: 471-472.
- Bierman, P.R., and A.R. Gillespie. 1991a. The evolution of granitic landforms—field observations and cosmogenic insights. *Geological Society of America Abstracts with Programs* 23: A89.
- Bierman, P.R., and A.R. Gillespie. 1991b. Accuracy of rock-varnish chemical analyses: Implications for cation-ratio dating. *Geology* 19: 196-199.
- Bischoff, J.L., and J.A. Fitzpatrick. 1991. U-series dating of impure carbonates: an isochron technique using total-sample dissolution. *Geochimica et Cosmochimica Acta* 55: 543-554.
- Bogaard, P. v.d., C.M. Hall, H-U. Schmincke, and D. York. 1987.  $^{40}\text{Ar}/^{39}\text{Ar}$  laser dating of single grains: Ages of Quaternary tephra from the East Eifel Volcanic Field, FRG. *Geophysical Research Letters* 14: 1,211-1,214.
- Bogue, S.W., and R.S. Coe. 1981. Paleomagnetic correlation of Columbia River Basalt flows using secular variation. *Journal of Geophysical Research* 86: 11,883-11,897.
- Brereton, N.R. 1970. Corrections for interfering isotopes in the  $^{40}\text{Ar}/^{39}\text{Ar}$  dating method. *Earth and Planetary Science Letters* 8: 427-433.
- Byers, F.M., Jr., W.J. Carr, and P.P. Orkild. 1989. Volcanic centers of southwestern Nevada: Evolution of understanding, 1960-1988. *Journal of Geophysical Research* 94: 5,908-5,924.
- Byers, F.M. Jr., W.J. Carr, P.P. Orkild, W.D. Quinlivan, and K.A. Sargent. 1976. *Volcanic Suites and Related Cauldrons of the Timber Mountain-Oasis Valley Caldera Complex*. U.S. Geological Survey Professional Paper 919: Washington, DC: U.S. Government Printing Office.
- Cahill, T.A. 1992. Comment on "Accuracy of rock-varnish chemical analyses: Implications for cation-ratio dating." *Geology* 20: 469.
- Calk, L.C., and C.W. Naeser. 1973. The thermal effect of a basalt intrusion onto fission tracks in quartz monzonite. *Journal of Geology* 81: 189–198.
- Cassignol, C., and P-Y. Gillot. 1982. Range and effectiveness of unspiked potassium-argon dating: Experimental groundwork and applications. *Numerical Dating in Stratigraphy*. G.S. Odin, ed. New York, NY: John Wiley and Sons: 159-179.

- Cerling, T. E. 1990. Dating geomorphologic surfaces using cosmogenic  $^3\text{He}$ . *Quaternary Research* 33: 148-156.
- Champion, D.E. 1991. Volcanic episodes near Yucca Mountain as determined by paleomagnetic studies at Lathrop Wells, Crater Flat, and Sleeping Butte, Nevada. *Proceedings of the Second International High Level Radioactive Waste Management Conference*. La Grange Park, IL: American Nuclear Society: 61-67.
- Champion, D.E. 1980. *Holocene Geomagnetic Secular Variation in the Western United States: Implications for the Global Geomagnetic Field*. U.S. Geological Survey Open-File Report 80-824. Washington, DC: U.S. Government Printing Office.
- Chen, J.H., R.L. Edwards, and G.J. Wasserburg. 1992. Mass spectrometry and applications to uranium-series disequilibrium. *Uranium Series Disequilibrium: Applications to Earth, Marine, and Environmental Sciences 2nd ed.* M. Ivanovich, and R.S. Harmon, eds. Oxford: Clarendon Press: 174-206.
- Cohen, A.S., and R.K. O'Nions. 1991. Precise determination of femtogram quantities of radium by thermal ionization mass spectrometry. *Analytical Chemistry* 63: 2,705-2,708.
- Colman, S.M. 1982. *Chemical Weathering of Basalts and Andesites: Evidence from Weathering Rinds*. U.S. Geological Survey Professional Paper 1246. Washington, DC: U.S. Government Printing Office.
- Colman, S.M., K.L. Pierce, and P.W. Birkeland. 1987. Suggested terminology for Quaternary dating methods. *Quaternary Research* 28: 314-319.
- Connor, C.B., and B.E. Hill. 1993. Volcanism Research. *NRC High-Level Radioactive Waste Research at CNWRA, July 1 Through December 31, 1992*. Nuclear Regulatory Commission Contract NRC-02-88-005, 10-1-10-31.
- Cox, A. 1969. Geomagnetic reversals. *Science* 163: 237-245.
- Creer, K.M. 1981. Long-period geomagnetic secular variations since 12,000 yr BP. *Nature* 292: 208-212.
- Crow, L.H. 1982. Confidence interval procedures for the Weibull process with applications to reliability growth. *Technometrics* 24: 67-71.
- Crowe, B.M. 1990. Basaltic volcanic episodes of the Yucca Mountain region. *Proceedings of the First International High Level Radioactive Waste Management Conference*. La Grange Park, IL: American Nuclear Society: 65-73.
- Crowe, B.M., and F.V. Perry. 1989. Volcanic probability calculations for the Yucca Mountain site: estimation of volcanic rates. *Proceedings Nuclear Waste Isolation in the Unsaturated Zone, Focus '89*. La Grange Park, IL: American Nuclear Society: 326-334.

- Crowe, B., and F. Perry. 1991. *Preliminary geologic map of the Sleeping Butte Volcanic Centers*. Los Alamos National Laboratory Report LA-12101-MS. Los Alamos, NM: Los Alamos National Laboratory.
- Crowe, B.M., M.E. Johnson, and R.J. Beckman. 1982. Calculation of the probability of volcanic disruption of a high-level nuclear waste repository within southern Nevada, USA. *Radioactive Waste Management and the Nuclear Fuel Cycle* 3: 167-190.
- Crowe, B.M., D.T. Vaniman, and W.J. Carr. 1983. *Status of Volcanic Hazard Studies for the Nevada Nuclear Waste Storage Investigations*. Los Alamos National Laboratory Report LA-9325-MS. Los Alamos, NM: Los Alamos National Laboratory.
- Crowe, B.M., K.H. Wohletz, D.T. Vaniman, E. Gladney, and N. Bower. 1986. *Status of Volcanic Hazard Studies for the Nevada Nuclear Waste Storage Investigations*. Los Alamos National Laboratory Report LA-9325-MS, Vol. II. Los Alamos, NM: Los Alamos National Laboratory.
- Crowe, B., C. Harrington, L. McFadden, F. Perry, S. Wells, B. Turrin, and D. Champion. 1988. *Preliminary Geologic Map of the Lathrop Wells Volcanic Center*. Los Alamos National Laboratory Report LA-UR-88-4155. Los Alamos, NM: Los Alamos National Laboratory.
- Crowe, B.M., R. Picard, G. Valentine, and F.V. Perry. 1992a. Recurrence Models for Volcanic Events: Applications to Volcanic Risk Assessment. *Proceedings of the Third International High Level Radioactive Waste Management Conference*. La Grange Park, IL: American Nuclear Society. 2,344-2,355.
- Crowe, B., R. Morley, S. Wells, J. Geissman, E. McDonald, L. McFadden, F. Perry, M. Murrell, J. Poths, and S. Forman. 1992b. The Lathrop Wells volcanic center: Status of field and geochronology studies. *Proceedings of the Third International High Level Radioactive Waste Management Conference*. La Grange Park, IL: American Nuclear Society. 1,997-2,013.
- Crowe, B.M., F.V. Perry, and G.A. Valentine. 1993. *Preliminary Draft: Status of Volcanic Hazard Studies for the Yucca Mountain Site Characterization Project*. Los Alamos National Laboratory Report: Los Alamos, NM: Los Alamos National Laboratory.
- Dalrymple, G.B. 1964. Argon retention in a granitic xenolith from a Pleistocene basalt, Sierra Nevada, California. *Nature* 201: 282.
- Dalrymple, G.B., and M.A. Lanphere. 1969. *Potassium-argon dating*. San Francisco, CA: W.H. Freeman and Co.
- Dalrymple, G.B., and M.A. Lanphere. 1971.  $^{40}\text{Ar}/^{39}\text{Ar}$  technique of K-Ar dating: A comparison with the conventional technique. *Earth and Planetary Science Letters* 12: 300-308.
- Dalrymple, G.B., and M.A. Lanphere. 1974.  $^{40}\text{Ar}/^{39}\text{Ar}$  age spectra of some undisturbed terrestrial samples. *Geochimica et Cosmochimica Acta* 38: 715-738.

- Dalrymple, G.B., E.C. Alexander, Jr., M.A. Lanphere, and G.P. Kraker. 1981. *Irradiation of Samples for  $^{40}\text{Ar}/^{39}\text{Ar}$  Dating Using the Geological Survey TRIGA Reactor*. U.S. Geological Survey Professional Paper 1176. Washington, DC: U.S. Government Printing Office.
- Daniels, F., C.A. Boyd, and D.F. Saunders. 1953. Thermoluminescence as a research tool. *Science* 117: 343-349.
- Davis, J.O. 1985. Correlation of late Quaternary tephra layers in a long pluvial sequence near Summer Lake, Oregon. *Quaternary Research* 23: 38-53.
- Dohrenwend, J.C., L.D. McFadden, B.D. Turrin, and S.G. Wells. 1984. K-Ar dating of the Cima Volcanic Field, eastern Mojave Desert, California: Late Cenozoic volcanic history and landscape evolution. *Geology* 12: 163-167.
- Dohrenwend, J.C., S.G. Wells, and B.D. Turrin. 1986. Degradation of Quaternary cinder cones in the Cima Volcanic Field, Mojave Desert, California. *Geological Society of America Bulletin* 97: 421-427.
- Dohrenwend, J.C., A.D. Abrahams, and B.D. Turrin. 1987. Drainage development on basaltic lava flows, Cima Volcanic Field, southeast California, and Lunar Crater volcanic field, south-central Nevada. *Geological Society of America Bulletin* 99: 405-413.
- Dorn, R.I. 1983. Cation-ratio dating: A new rock varnish age-determination technique. *Quaternary Research* 20: 49-73.
- Dorn, R.I. 1992. Comment on "Accuracy of rock-varnish chemical analyses: Implications for cation-ratio dating." *Geology* 20: 470-471.
- Dorn, R. I., and F. M. Phillips. 1991. Surface exposure dating: review and critical evaluation. *Physical Geography* 12: 303-333.
- Dorn, R.I., J.B. Bamforth, T.A. Cahill, J.C. Dohrenwend, B.D. Turrin, D.J. Donahue, A.J.T. Jull, A. Long, M.E. Macko, E.B. Weil, D.S. Whitley, and T.H. Zabel. 1986. Cation-ratio and accelerator radiocarbon dating of rock varnish on Mojave artifacts and landforms. *Science* 231: 830-833.
- Dorn, R.I., A.J.T. Jull, D.J. Donahue, T.W. Linick, and L.J. Toolin. 1989. Accelerator mass spectrometry radiocarbon dating of rock varnish. *Geological Society of America Bulletin* 101: 1,363-1,372.
- Elmore, D., and F.M. Phillips. 1987. Accelerator mass spectrometry for measurement of long-lived radioisotopes. *Science* 236: 543-550.
- Engles, J.C., and C.O. Ingamells. 1970. Effect of sample inhomogeneity in K-Ar dating. *Geochimica et Cosmochimica Acta* 34: 1,007-1,017.

- Farr, T.G. 1992. Microtopographic evolution of lava flows at Cima Volcanic Field, Mojave Desert, California. *Journal of Geophysical Research* 97: 15,171-15,179.
- Féraud, G., P. LoBello, C.M. Hall, J.-M. Cantagrel, D. York, and M. Bernat. 1990. Direct dating of Plio-Quaternary pumices by  $^{40}\text{Ar}/^{39}\text{Ar}$  step-heating and single-grain laser fusion methods: The example of the Monts-Dore massif (Massif Central, France). *Journal of Volcanology and Geothermal Research* 40: 39-53.
- Fisher, R.A. 1953. Dispersion on a sphere. *Proceedings of the Royal Society A* 217: 295-305.
- Fleck, R.J., J.F. Sutter, and D.H. Elliot. 1977. Interpretation of discordant  $^{40}\text{Ar}/^{39}\text{Ar}$  age-spectra of Mesozoic tholeiites from Antarctica. *Geochimica et Cosmochimica Acta* 41: 15-32.
- Fleischer, R.L., P.B. Price, and R.M. Walker. 1965. Effects of temperature, pressure, and ionization on the formation and stability of fission tracks in minerals and glasses. *Journal of Geophysical Research* 70: 1,497-1,502.
- Foland, K.A., T.H. Fleming, A. Heimann, and D.H. Elliot. 1993. Potassium-argon dating of fine-grained basalts with massive Ar loss: Application of the  $^{40}\text{Ar}/^{39}\text{Ar}$  technique to plagioclase and glass from the Kirkpatrick Basalt, Antarctica. *Chemical Geology* 107: 173-190.
- Forman, S.L. 1989. Applications and limitations of thermoluminescence to date Quaternary sediments. *Quaternary International* 1: 47-59.
- Geyh, M.A., and H. Schleicher. 1990. *Absolute Age Determination*. New York, NY: Springer Verlag.
- Gill, J.B., D.M. Pyle, and R.W. Williams. 1992. Igneous rocks. *Uranium Series Disequilibrium: Applications to Earth, Marine, and Environmental Sciences 2nd ed.* M. Ivanovich, and R.S. Harmon, eds. Oxford: Clarendon Press: 207-258.
- Gillespie, A.R., J.C. Huneke, and G.J. Wasserburg. 1982. An assessment of  $^{40}\text{Ar}-^{39}\text{Ar}$  dating of incompletely degassed xenoliths. *Journal of Geophysical Research* 87: 9,247-9,257.
- Gillespie, A.R., J.C. Huneke, and G.J. Wasserburg. 1983. Eruption age of a Pleistocene basalt from  $^{40}\text{Ar}-^{39}\text{Ar}$  analysis of partially degassed xenoliths. *Journal of Geophysical Research* 88: 4,997-5,008.
- Gillespie, A.R., J.C. Huneke, and G.J. Wasserburg. 1984. Eruption age of a ~100,000-year-old basalt from  $^{40}\text{Ar}-^{39}\text{Ar}$  analysis of partially degassed xenoliths. *Journal of Geophysical Research* 89: 1,033-1,048.
- Gillot, P.-Y., and Y. Cornette. 1986. The Cassinot technique for potassium-argon dating, precision and accuracy: Examples from the late Pleistocene to Recent volcanics from southern Italy. *Chemical Geology (Isotope Geoscience Section)* 59: 205-222.

- Goldstein, S.J., M.T. Murrell, and D.R. Janecky. 1989. Th and U isotopic systematics of basalts from the Juan de Fuca and Gorda Ridges by mass spectrometry. *Earth and Planetary Science Letters* 96: 134-146.
- Graham, K.W.T. 1961. The remagnetization of a surface outcrop by lightning currents. *Geophysical Journal of the Royal Astronomical Society* 6:85-102.
- Green, T.H., and E.B. Watson. 1982. Crystallization of apatite in natural magmas under high pressure, hydrous conditions, with particular reference to 'orogenic' rocks series. *Contributions to Mineralogy and Petrology* 79: 96-105.
- Green, P.F. I.R. Duddy, A.J.W. Gleadow, P.R. Tingate, and G.M. Laslett. 1986. Thermal annealing of fission tracks in apatite. I. A qualitative description. *Chemical Geology* 59: 237-253.
- Gutmann, J.T. 1979. Structure and eruptive cycle of cinder cones in the Pinacate Volcanic Field and the controls of strombolian activity. *Journal of Geology* 87: 448-454.
- Hardin, J.W., E.M. Taylor, C. Hill, R.K. Mark, L.D. McFadden, M.C. Reheis, J.M. Sowers, and S.G. Wells. 1991. Rates of soil development from four soil chronosequences in the southern Great Basin. *Quaternary Research* 35: 383-399.
- Harland, W.B., A.V. Cox, P.G. Llewellyn, C.A.G. Pickton, A.G. Smith, and R. Walters. 1982. *A Geologic Time Scale*. Cambridge: Cambridge University Press.
- Harrington, C.D., and J.W. Whitney. 1987. Scanning electron microscope method for rock-varnish dating. *Geology* 15: 967-970.
- Harrison, T.M. 1983. Some observations on the interpretation of  $^{40}\text{Ar}/^{39}\text{Ar}$  age spectra. *Isotope Geoscience* 1: 319-338.
- Hasenaka, T., and I.S.E. Carmichael. 1985. The cinder cones of Michoacán-Guanajuato, central Mexico: Their age, volume and distribution, and magma discharge rate. *Journal of Volcanology and Geothermal Research* 25: 105-124.
- Ho, C.-H. 1991. Time trend analysis of basaltic volcanism for the Yucca Mountain site. *Journal of Volcanology and Geothermal Research* 46: 61-72.
- Ho, C.-H., E.I. Smith, D.L. Feurbach, and T.R. Naumann. 1991. Eruptive probability calculation for the Yucca Mountain site, USA: statistical estimation of recurrence rates. *Bulletin of Volcanology* 54: 50-56.
- Hogg, R.V., and E.A. Tanis. 1988. *Probability and Statistical Inference*, Third Edition. Macmillan: New York.
- Holcomb, R., D. Champion, and M. McWilliams. 1986. Dating recent Hawaiian lava flows using paleomagnetic secular variation. *Geological Society of America Bulletin* 97: 829-839.

- Hoover, D.L., W.C. Swadley, and A.J. Gordon. 1981. *Correlation Characteristics of Surficial Deposits with a Description of Surficial Stratigraphy in the Nevada Test Site Region*. U.S. Geological Survey Open-File Report 81-512. Washington, DC: U.S. Government Printing Office.
- Izett, G.A., J.D. Obradovich, and H.A. Mehnert. 1988. *The Bishop Ash Bed (Middle Pleistocene) and Some Older (Pliocene and Pleistocene) Chemically and Mineralogically Similar Ash Beds in California, Nevada, and Utah*. U.S. Geological Survey Bulletin 1675. Washington, DC: U.S. Government Printing Office.
- Kaneoka, I. 1972. The effect of hydration on the K/Ar ages of volcanic rocks. *Earth and Planetary Science Letters* 14: 216-220.
- Kaufman, A. 1993. An evaluation of several methods for determining  $^{230}\text{Th}/\text{U}$  ages in impure carbonates. *Geochimica et Cosmochimica Acta* 57: 2,303-2,317.
- Kurz, M.D. 1986a. Cosmogenic helium in a terrestrial igneous rock. *Nature* 320: 435-439.
- Kurz, M.D. 1986b. *In situ* production of terrestrial cosmogenic helium and some applications to geochronology. *Geochimica et Cosmochimica Acta* 50: 2,855-2,862.
- Kurtz, M.A., D.E. Champion, E.C. Spiker, and R.H. Lefebvre. 1986. Contrasting magmas types and steady-state, volume-predictable, basaltic volcanism along the Great Rift, Idaho. *Geological Society of America, Bulletin* 97: 579-594.
- Kurz, M.D., D. Colodner, T.W. Trull, R.B. Moore, and K. O'Brien. 1990. Cosmic ray exposure dating with *in situ* produced cosmogenic  $^3\text{He}$ : results from young Hawaiian lava flows. *Earth and Planetary Science Letters* 97: 177-189.
- Lal, D. 1987. Cosmogenic nuclides produced in situ in terrestrial solids. *Nuclear Instruments and Methods in Physics Research* B29: 238-243.
- Lal, D. 1988. In situ-produced cosmogenic isotopes in terrestrial rocks. *Annual Review of Earth and Planetary Science* 16: 355-388.
- Lal, D. 1991. Cosmic ray labeling of erosion surfaces: in situ nuclide production rates and erosion models. *Earth and Planetary Science Letters* 104: 424-439.
- Lally, A. E. 1992. Chemical procedures. *Uranium Series Disequilibrium: Applications to Earth, Marine, and Environmental Sciences 2nd ed.* M. Ivanovich, and R.S. Harmon, eds., Oxford: Clarendon Press: 95-126.
- Lanphere, M.A., and G.B. Dalrymple. 1976. Identification of excess  $^{40}\text{Ar}$  by the  $^{40}\text{Ar}/^{39}\text{Ar}$  age spectrum technique. *Earth and Planetary Science Letters* 32: 141-148.
- Libby, W.F. 1946. Atmospheric helium-three and radiocarbon from cosmic radiation. *Physics Review* 69: 671-672.

- Lo Bello, P., G. Féraud, C.M. Hall, D. York, P. Lavina, and M. Bernat. 1987.  $^{40}\text{Ar}/^{39}\text{Ar}$  step-heating and laser fusion dating of a Quaternary pumice from Neschers, Massif Central, France: The defeat of xenocrystic contamination. *Chemical Geology (Isotope Geosciences Section)* 66: 61-71.
- Lutton, R.J. 1969. Internal structure of the Buckboard Mesa basalt. *Bulletin of Volcanology* 33: 579-593.
- Luo, S., and T.-L. Ku. 1991. U-series isochron dating: a generalized method employing total-sample dissolution. *Geochimica et Cosmochimica Acta* 55: 555-564.
- Mankinen, E.A., and G.B. Dalrymple. 1979. Revised geomagnetic polarity time scale for the interval 0-5 m.y. B.P. *Journal of Geophysical Research* 84: 615-626.
- Mankinen, E.A., C.S. Grommé, G.B. Dalrymple, M.A. Lanphere, and R.A. Bailey. 1986. Paleomagnetism and K-Ar ages of volcanic rocks from Long Valley Caldera, California. *Journal of Geophysical Research* 91: 633-652.
- Margulies, T., L. Lancaster, N. Eisenberg, and L. Abramson. 1992. Probabilistic analysis of magma scenarios for assessing geologic waste repository performance. *American Society of Mechanical Engineers, Winter Annual Meeting*. New York, NY: American Society of Mechanical Engineers.
- Marti, K., and H. Craig. 1987. Cosmic-ray produced neon and helium in the summit lavas of Maui. *Nature* 325: 335-337.
- May, R. J. 1979. *Thermoluminescence Dating of Hawaiian basalt*. U.S. Geological Survey Professional Paper 1095. Washington, DC: U.S. Government Printing Office.
- McDermott, F., T.R. Elliot, P. van Calsteren, and C.J. Hakesworth. 1993. Measurement of  $^{230}\text{Th}/^{232}\text{Th}$  ratios in young volcanic rocks by single-sector thermal ionization mass spectrometry. *Chemical Geology* 103: 283-29.
- McDougall, I., and T.M. Harrison. 1988. *Geochronology and Thermochronology by the  $^{40}\text{Ar}/^{39}\text{Ar}$  Method*. New York, NY: Oxford University Press.
- McFadden, L.D., S.G. Wells, and J.C. Dohrenwend. 1986. Influences of Quaternary climatic changes on processes of soil development on desert loess deposits of the Cima Volcanic Field, California. *Catena* 13: 361-389.
- McFadden, L.D., S.G. Wells, and M.J. Jercinovich. 1987. Influences of eolian and pedogenic processes on the origin and evolution of desert pavements. *Geology* 15: 504-508.
- McFadden, L.D., J.B. Ritter, and S.G. Wells. 1989. Use of multiparameter relative-age methods for age estimation and correlation of alluvial fan surfaces on a desert piedmont, eastern Mojave Desert, California. *Quaternary Research* 32: 276-290.

- Megrue, G.H. 1971. Distribution and origin of helium, neon, and argon isotopes in Apollo 12 samples measured by in situ analysis with laser-probe mass spectrometer. *Journal of Geophysical Research* 76: 4,956-4,968.
- Merrihue, C., and G. Turner. 1966. Potassium-argon dating by activation with fast neutrons. *Journal of Geophysical Research* 71: 2,852-2,857.
- Negrini, R.M., K.L. Verosub, and J.O. Davis. 1988. The middle to late Pleistocene geomagnetic field recorded in fine-grained sediments from Summer Lake, Oregon and Double Hot Spring, Nevada, U.S.A. *Earth and Planetary Science Letters* 87: 173-192.
- Nishiizumi, K., C.P. Kohl, E.M. Shoemaker, J.R. Arnold, J. Klein, D. Fink, and R. Middleton. 1991. In situ  $^{10}\text{Be}$ - $^{26}\text{Al}$  exposure ages at Meteor Crater, Arizona. *Geochimica et Cosmochimica Acta* 55: 2,699-2,703.
- Paces, J.B., E.M. Taylor, and C. Bush. 1993. Late Quaternary history and uranium isotopic compositions of ground water discharge deposits, Crater Flat, Nevada. *Proceedings of the Fourth Annual International High-Level Radioactive Waste Management Conference*. La Grange Park, IL: American Nuclear Society. 1,573-1,580.
- Palmer, A.R. 1983. The Decade of North American Geology 1983 Geologic Time Scale. *Geology* 11: 503-504.
- Phillips, F.M., M.G. Zreda, S.S. Smith, D. Elmore, P.W. Kubik, R.I. Dorn, and D.J. Roddy. 1991. Age and geomorphic history of Meteor Crater, Arizona, from cosmogenic  $^{36}\text{Cl}$  and  $^{14}\text{C}$  in rock varnish. *Geochimica et Cosmochimica Acta* 55: 2,695-2,698.
- Porter, S.C. 1972. Distribution, morphology, and size frequency of cinder cones on Mauna Kea Volcano, Hawaii. *Geological Society of America Bulletin* 83: 3,607-3,612.
- Poeths, J., and B.M. Crowe. 1992. Surface exposure ages and noble gas components of volcanic units at the Lathrop Wells volcanic center, Nevada. *EOS, Transactions of the American Geophysical Union* 73-43: 610.
- Price, P.B., and R.M. Walker. 1963. Fossil tracks of charged particles in mica and the age of minerals. *Journal of Geophysical Research* 68: 4,847-4,862.
- Ralph, E.K. 1971. Carbon-14 dating. *Dating Techniques for the Archaeologist*. N. Michael and E.K. Ralph, eds. Cambridge, MA: Massachusetts Institute of Technology Press: 1-48.
- Reneau, S.L., and R. Raymond, Jr. 1991. Cation-ratio dating of rock varnish: Why does it work? *Geology* 19: 937-940.
- Sabels, B.E. 1963. Age studies on basaltic lava using natural alpha activity and thermoluminescence. *Radioactive Dating*. Vienna, Austria: International Atomic Energy Agency: 87-104.

- Sarna-Wojcicki, A.M. 1976. *Correlation of Late Cenozoic Tuffs in the Central Coast Ranges of California by Means of Trace- and Minor-Element Chemistry*. U.S. Geological Survey Professional Paper 972. Washington, DC: U.S. Government Printing Office.
- Sarna-Wojcicki, A.M., C.E. Meyer, H.R. Bowman, N.T. Hall, P.C. Russell, M.J. Woodward, and J.L. Slate. 1985. Correlation of the Rockland Ash Bed, a 400,000-year-old stratigraphic marker in northern California and western Nevada, and implications for middle Pleistocene paleogeography of central California. *Quaternary Research* 23: 236-257.
- Scott, D.H., and N.J. Trask. 1971. *Geology of the Lunar Crater Volcanic Field, Nye County, Nevada*. U.S. Geological Survey Professional Paper 599-I. Washington, DC: U.S. Government Printing Office.
- Settle, M. 1979. The structure and emplacement of cinder cone fields. *American Journal of Science* 279: 1,089-1,107.
- Sharma, P.V. 1986. *Geophysical Methods in Geology*. New York, NY: Elsevier.
- Simonsen, A. 1983. Procedures for sampling, sorting and pretreatment of charcoal for  $^{14}\text{C}$  dating.  *$^{14}\text{C}$  Dating and Archaeology*. W.G. Mook and H.T. Waterbolk, eds. Brussels: PACT-8: 313-318.
- Singhvi, A.K., and V. Mejdahl. 1985. Thermoluminescence dating of sediments. *Nuclear Tracks* 10: 137-161.
- Sinnock, S., and R.G. Easterling. 1983. *Empirically Determined Uncertainty in Potassium-Argon Ages for Plio-Pleistocene Basalts from Crater Flat, Nye County, Nevada*. Sandia National Laboratory Report SAND 82-2441. Albuquerque, NM: Sandia National Laboratory.
- Smith, E.I., T.R. Feuerbach, and J.E. Faulds. 1990. The area of most recent volcanism near Yucca Mountain, Nevada: implications for volcanic risk assessment. *Proceedings of the First International High Level Radioactive Waste Management Conference*. La Grange Park, IL: American Nuclear Society: 81-90.
- Spell, T.L., and I. McDougall. 1992. Revisions to the age of the Brunhes-Matuyama boundary and the Pleistocene geomagnetic polarity timescale. *Geophysical Research Letters* 19: 1,181-1,184.
- Stuiver, M., 1978. Radiocarbon timescale tested against magnetic and other dating methods. *Nature* 273: 271-274.
- Stuiver, M., and Kra, R. 1986. Calibration Issues. *Radiocarbon* 28-2B: 805-1030.
- Stuiver, M., and Polach, H.A. 1977. Discussion on reporting of  $^{14}\text{C}$  data. *Radiocarbon* 19-3: 355-363.
- Steiger, R.H., and E. Jäger. 1977. Subcommittee on geochronology: Convention on the use of decay constants in geo- and cosmochronology. *Earth and Planetary Science Letters* 36: 359-362.

- Steiger, R.H., and E. Jäger. 1977. Subcommission on geochronology: Convention on the use of decay constants in geo- and cosmochronology. *Earth and Planetary Science Letters* 36: 359-362.
- Szabo, B. J., W. J. Carr, and W. C. Gottschall. 1981. *Uranium-Thorium Dating of Quaternary Carbonate Accumulations in the Nevada Test Site Region, Southern Nevada*. U.S. Geological Survey Open-File Report. 81-19. Washington, DC: U.S. Government Printing Office.
- Tarling, D.H. 1983. *Paleomagnetism—Principles and Application in Geology, Geophysics, and Archaeology*. New York, NY: Chapman and Hall.
- Taylor, J.K. 1990. *Statistical Techniques for Data Analysis*. Boca Raton, FL: CRC Press.
- Trapp, J.S., and P.S. Justus. 1992. Regulatory requirements to address issues related to volcanism and magmatism: Code of Federal Regulations, Title 10, Part 60, disposal of high-level radioactive wastes in geologic repositories. *Proceedings of the Third International High-Level Radioactive Waste Management Conference*. La Grange Park, IL: American Nuclear Society: 2,039-2,046.
- Turner, G. 1971.  $^{40}\text{Ar}/^{39}\text{Ar}$  ages from the lunar maria. *Earth and Planetary Sciences Letters* 11: 169-191.
- Turner, G., and P.H. Cadogan. 1974. Possible effects of  $^{39}\text{Ar}$  recoil in  $^{40}\text{Ar}$ - $^{39}\text{Ar}$  dating. *Geochimica et Cosmochimica Acta Supplement 5, Proceedings of the 5<sup>th</sup> Lunar Science Conference*: 1,601-1,615.
- Turrin, B.D., and D.E. Champion. 1991.  $^{40}\text{Ar}/^{39}\text{Ar}$  laser fusion and K-Ar ages from Lathrop Wells, Nevada, and Cima, California: The age of the latest volcanic activity in the Yucca Mountain area. *Proceedings of the Second International High Level Radioactive Waste Management Conference*. La Grange Park, IL: American Nuclear Society: 68-75.
- Turrin, B.D., D. Champion, and R.J. Fleck. 1991.  $^{40}\text{Ar}/^{39}\text{Ar}$  age of the Lathrop Wells Volcanic Center, Yucca Mountain, Nevada. *Science* 253: 654-657.
- Turrin, B.D., D. Champion, and R.J. Fleck. 1992. Measuring the age of the Lathrop Wells volcanic center at Yucca Mountain: Response. *Science* 257: 556-558.
- Vaniman, D., and B. Crowe. 1981. *Geology and Petrology of the Basalts of Crater Flat: Applications to Volcanic Risk Assessment for the Nevada Nuclear Waste Storage Investigations*. Los Alamos National Laboratory Report LA-8845-MS. Los Alamos, NM: Los Alamos National Laboratory.
- Vaniman, D.T., B.M. Crowe, and E.S. Gladney. 1982. Petrology and geochemistry of Hawaiite lavas from Crater Flat, Nevada. *Contributions to Mineralogy and Petrology* 80: 341-357.
- Villa, I.M., J.C. Huneke, and G.J. Wasserburg. 1983.  $^{39}\text{Ar}$  recoil losses and presolar ages in Allende inclusions. *Earth and Planetary Science Letters* 63: 1-12.
- Vogel, J.C. 1983. 14-C variations during the upper Pleistocene. *Radiocarbon* 25: 213-218.

- Watson, E.B., and T.M. Harrison, 1983. Zircon saturation revisited: temperature and composition effects in a variety of crustal magma types. *Earth and Planetary Science Letters* 64: 295-304.
- Watson, E.B., and T.M. Harrison, 1984. Accessory minerals and the geochemical evolution of crustal magma systems: a summary and prospectus of experimental approaches. *Physics of the Earth and Planetary Interiors* 35: 19-30.
- Wells, S.G., J.C. Dohrenwend, L.D. McFadden, B.D. Turrin, and K.D. Mahrer. 1985. Late Cenozoic landscape evolution on lava flow surfaces of the Cima volcanic field, Mojave Desert, California. *Geological Society of America Bulletin* 96: 1,518-1,529.
- Wells, S.G., L.D. McFadden, and J.C. Dohrenwend. 1987. Influence of late Quaternary climatic changes on geomorphic and pedogenic processes on a desert piedmont, eastern Mojave Desert, California. *Quaternary Research* 27: 134-146.
- Wells, S.G., L.D. McFadden, C.E. Renault, and B.M. Crowe. 1990. Geomorphic assessment of late Quaternary volcanism in the Yucca Mountain area, southern Nevada: Implications for the proposed high-level radioactive waste repository. *Geology* 18: 549-553.
- Wells, S.G., B.M. Crowe, and L.D. McFadden. 1992. Measuring the age of the Lathrop Wells volcanic center at Yucca Mountain: Comment. *Science* 257: 555-556.
- Westgate, J.A. 1989. Isothermal plateau fission-track ages of hydrated glass shards from silicic tephra beds. *Earth and Planetary Science Letters* 95: 226-234.
- Whitney, J.W., and C.D. Harrington. 1993. Relict colluvial boulder deposits as paleoclimatic indicators in the Yucca Mountain region, southern Nevada. *Geological Society of America Bulletin* 105:1,008-1,018.
- Wintle, A.G. 1982. Thermoluminescence properties of fine-grain minerals in loess. *Soil Science* 134: 164-170.
- Wood, C.A. 1980. Morphometric evolution of cinder cones. *Journal of Volcanology and Geothermal Research* 7: 387-413.
- Zreda, M.G., F.M. Phillips, D. Elmore, P.W. Kubik, P. Sharma, and R.I. Dorn. 1991. Cosmogenic chlorine-36 production rates in terrestrial rocks. *Earth and Planetary Science Letters* 105: 94-109.
- Zreda, M.G., F.M. Phillips, P.W. Kubik, P. Sharma, and D. Elmore. 1993. Cosmogenic  $^{36}\text{Cl}$  dating of a young basaltic eruption complex, Lathrop Wells, Nevada. *Geology* 21: 57-60.